EXPERIMENTAL INVESTIGATION ON FREEZING OF A FALLING FILM

HANI H.W.SAIT

FACULTY OF ENGINEERING

KING ABDULAZIZ UNIVERSITY, JEDDAH

Dhu Al Qada, 1419H-February, 1999G

بسم الله الرحمن الرحيم

قال الله تعالى

صدق الله العظيم

التوبة (١٠٥)

EXPERIMENTAL INVESTIGATION ON FREEZING OF A FALLING FILM

By

Hani H.W.Sait

A thesis submitted in partial fulfillment of the requirements for the degree of Master of Science in Mechanical Engineering (Thermal Engineering and Desalination Technology)

FACULTY OF ENGINEERING

KING ABDULAZIZUNIVERSITY

JEDDAH-SAUDI ARABIA

Dhu Al Qada, 1419H-February, 1999G

EXPERIMENTAL INVESTIGATION ON FREEZING OF A FALLING FILM

By

Hani H.W.Sait

We certify that we have read this thesis and that in our opinion is fully adequate in scope and quality as a thesis for the degree of Master of Science

Thesis Supervisors

Prof.Kadry A. Fathalah

Dr.Ramzy.G.Abdel-Gayed

Dr.Abdulzaher M.Selim

EXPERIMENTAL INVESTIGATION ON FREEZING OF A FALLING FILM

By

Hani H.W.Sait

This thesis has been approved and accepted in partial fulfillment of the requirements for the degree of Master of Science

Examiners:

_____

Dr.Mahmoud A.A. Shahin ,External Examiner

_____

Prof.Dr.Samir E.Aly ,Internal Examiner

_____

Prof.Kadry A. Fathalah ,Examinar/Supervisor

_____

Dr.Ramzy.G.Abdel-Gayed ,Examiner/Co-Supervisor

_____

Dr.Abdulzaher M.Selim ,Examiner/Co-Supervisor

ACKNOWLEDGMENT

Thanks to Allah who helped and guided me during this work. I ask him to write every single minute I spent in this project in my good work. I hope that the present work be of benefit to all nations, especially Muslim's ones. I would like to offer my sincere gratitude and appreciation to Prof.Dr.Kadry A.Fathalah,Dr.Abdulzaher M.Selim,and Dr.Ramzy.G.Abdel-Gayed for their great guidance,helpful advises and their important comments. I would like also to express my gratitude to my father, mother and wife for their encouragement, patience and support. Thanks for every body who helped me to complete this work.

EXPERIMENTAL INVESTIGATION ON FREEZING OF A FALLING FILM

By

Hani Hussain Sait

ABSTRACT

There are two methods to form ice on tubes. The first is to use immersed tubes, while the second is to freeze a falling film on horizontal tubes. Falling film heat exchangers have a lot of uses in industries, refrigeration, desalination, etc, because they provide high heat transfer coefficient and operate with small inventories than flooded or immersed heat exchangers. The heat exchanger considered here, is a horizontal-tube falling film one. When a falling liquid film flows from one horizontal tube to another below it, the flow may take the form of discrete droplets, jets or a continuous sheet depending on the flow rate.

In this research, the cooled liquid falling film falls down over a set of seven in-line tubes arranged in parallel or series. The liquid falling film is then freezes outside the test tubes, which is internally cooled by a controlled temperature cooling machine. Pure water and water with 2%

aceton are used as a falling film liquid .A solution of 40% ethylene glycol is used as a coolant. The quantity of ice formed on the test tubes is measured at different run times. The heat transfer coefficient is also calculated.

The coolant flow rate and the falling film flow rate are the two main parameters, which are varied, in the present study. As the coolant flow rate increases the formed ice increases due to an increase in the inside heat transfer coefficient. When the falling film flow rate gradually increases, the flow changes from droplet to jet and finally to sheet mode which produces the largest quantity of ice. Series arrangement gives more ice than parallel one at the same flow rate interring test section, due to an increase of the coolant temperature difference and the coolant velocity inside the test tubes.

It has been found that the ice formed outside the test tubes dramatically affected the convective heat transfer rate of the test tubes. This leads to the reduction of the coolant temperature difference between the inlet and outlet of the test section as the formation of ice increases. Ice layers acts as insulation to the heat transfer from the liquid falling film to the coolant. Adding 2% aceton to water reduces the ice formed on the test tubes, but no slurry ice is formed as expected.

The outcome of the experimental setup is hopped to be a practical technique for the comparative studies of a cold thermal storage system.

TABLE OF CONTENTS

LIST OF TABLES

LIST OF FIGURES

LIST OF SYMBOLS

A	area, m^2
Ar	Archimedes number based on tube diameter = d^3g/ν^2
C_{pc}	specific heat of the coolant, kJ/kg.K
C_{pl}	specific heat of water falling film , kJ/kg.K
C_{pice}	specific heat of ice , kJ/kg.K
d	diameter, m
D_h	hydraulic diameter of the concentric tube,m
$D_{o,i}$	outer diameter of the inner tube, m
$D_{i,o}$	inner diameter of the outer tube, m
$D_{o,o}$	outer diameter of the outer tube, m
Ga	modified Galileo number = $\rho\sigma^3/\mu^4 g$
g	gravitational acceleration, m/s^2
h	heat transfer coefficient, $W/m^2.K$
h_i	heat transfer coefficient inside the tube, $W/m^2.K$
h_o	heat transfer coefficient outside the tube, $W/m^2.K$
h_{ov}	Experimental overall heat transfer coefficient, $W/m^2.K$
k	thermal conductivity, W/m.K
k_c	thermal conductivity of copper, W/m.K
L	latent heat of fusion of ice = 335 kJ/kg

l	length of the test tube,m
M_{ice}	mass of the frozen ice, kg
$\dot{m}_c$	mass flow rate of coolant, kg/s
$\dot{m}_f$	mass flow rate of falling film, kg/s
Nu	Nusselt number
Pr	Prandtle number = $C_p \mu/k$
$\dot{Q}_c$	rate of heat transfer from the test tubes to the coolant, W
$\dot{Q}_{c,ave}$	average rate of heat transfer from the test tubes to the coolant, W
$\dot{Q}_{c,cal}$	Calculated rate of heat transfer from the test tubes to the coolant, W
$\dot{Q}_{s,f}$	sensible cooling rate of the falling film, W
$\dot{Q}_{fr}$	rate of heat transfer which contributes to freezing , W
$\dot{Q}_{s,s}$	sensible average subcooling rate of ice, W
$\dot{Q}_{ls}$	loses in the test section, W
$\dot{Q}_{ls,c}$	loses from the test tubes due to convection,W
$\dot{Q}_{a,f}$	the absorbed heat from the falling film to the coolant,W
R	thermal resistance, K/W
Re_f	film Reynolds number = $2\Gamma/\mu$
Re_c	coolant Reynolds number inside tubes = $\rho u_m D_h/\mu$
s	tube spacing, m

T temperature, ^0C

T_{ci} temperature of coolant inlet to the test section, ^0C

T_{co} temperature of coolant outlet from the test section, ^0C

T_{li} temperature of the liquid falling film inlet to the test section, ^0C

T_{lo} temperature of the liquid falling film outlet from the test section, ^0C

T_c average temperature of coolant at the test section, ^0C

T_l average temperature of liquid falling film at the test section, ^0C

T_f freezing temperature of the liquid falling film , ^0C

U overall heat transfer coefficient, $W/m^2.K$

u_m mean fluid velocity over the cross section, m/s

V volume, m^3

w width of the supporting box, m

Greek Letters

Γ falling liquid mass flow rate per unit length of tube, kg/s.m

μ dynamic viscosity, $N.s/m^2$

ν kinematic viscosity, m^2/s

ρ_c density of the coolant, kg/m^3

ρ_w density of water, kg/m^3

ρ_{ice} **density of ice, kg/m^3**

σ **surface tension at gas / liquid interface**

CHAPTER-I

LITERATURE REVIEW

1.1 Introduction

The use of electric energy for air conditioning increases drastically during summer time. Unlike other building electric users, cooling incurs a peak demand for only a few hours per day or months per year. The consumption of electrical energy for air conditioning may reach to 75% of total electrical energy production by the Saudi Electrical Companies during summer season. The annual rate of this increase was about 21% during the period 1975-1988[1]. The use of electric energy causes an excessive load on electric utilities demand. One of the solutions to meet this problem is the use of cold thermal storage. Cold storage technology has improved significantly since 1980 when electric utility companies recognized the need to reduce the peak demand on their generation and distribution systems [2].

The increasing demand for advanced building cooling systems that are both economical and environmentally friendly has led to the development of various new types of thermal energy storage devices. Some of them operate on the

principle of utilizing either sensible heat or latent heat of phase change materials. Chilled water, ice or eutectic phase change materials are cold storage mediums. Chilled water uses sensible heat while ice and eutectic phase change use latent heat. System which function based upon phase change materials can generally be categorized into three different hardware storage configurations: ice-on-tube design, ice harvesters, and encapsulated ice systems. The ice storage method most widely utilized today is of the first kind: it essentially consists of pipes, submersed in a cross flow of cold water or exposed to a falling film, that are refrigerated sufficiently to cause ice formation to be deposited upon the tubes' exteriors [3].

The phenomenon of forced convective freezing of ice in a tube bank geometry has only recently received the attention of research workers, primarily due to the increased interest in commercially viable phase change thermal storage systems. Studies of fluid flow and heat transfer to tube banks without phase change, and research into melting and freezing heat transfer in general, have been reported by the research community. The simultaneous occurrence of both phenomena has recently been explored by a small group of investigators.[4]

Horizontal-tube, falling film heat exchangers have the advantages of providing higher heat transfer coefficient and operate with small liquid inventories than flooded heat exchanger. In this study a horizontal-tube falling film heat exchanger is used to form ice on the tubes' exteriors.

1.2 Types of cold storage mediums

Cold storage systems remove heat from a thermal storage medium during periods of low cooling demand. The stored cooling potential is later used to meet an air-conditioning or process cooling load. The cold storage medium can be chilled water, ice or eutectic phase change material [2].

1.2.1 Chilled water storage systems

Chilled water storage systems use the sensible heat capacity of water to store cooling potential. Water is cooled by chiller and stored in a tank for later use in meeting cooling needs. The amount of stored cooling potential depends on the temperature difference between the chilled water stored in the tank and the warm return water from the load. Chilled water system with multiple tanks can also store warm and chilled water. Figure (1.1) shows basic stratified chilled water configuration. Moreover, the tanks

can be used as water reservoir for fire protection. The space requirements for chilled water storage systems are very large. When space is available, chilled water storage can be an economical way of storing large amount of cooling capacity.[2]

1.2.2 Ice storage systems

Ice harvesting, external and internal melt ice -on-coil and encapsulated ice are different types of ice storage systems. These systems store latent heat of a phase changing material. The latent heat storage system can scale down the pipe size due to augment the transported heat [5]. The space requirements for ice storage are one third to one seventh that of chilled water storage systems [2]. It can also increase the heat transfer coefficient by the churning effect and by the high thermal conductivity of the dispersion material [5].

In ice harvesting, water is pumped out of the storage tank and is distributed over the low temperature surfaces, where it is chilled or frozen depending on: the temperature of the water as it enters the evaporator and temperature of the evaporator (Figure 1.2).

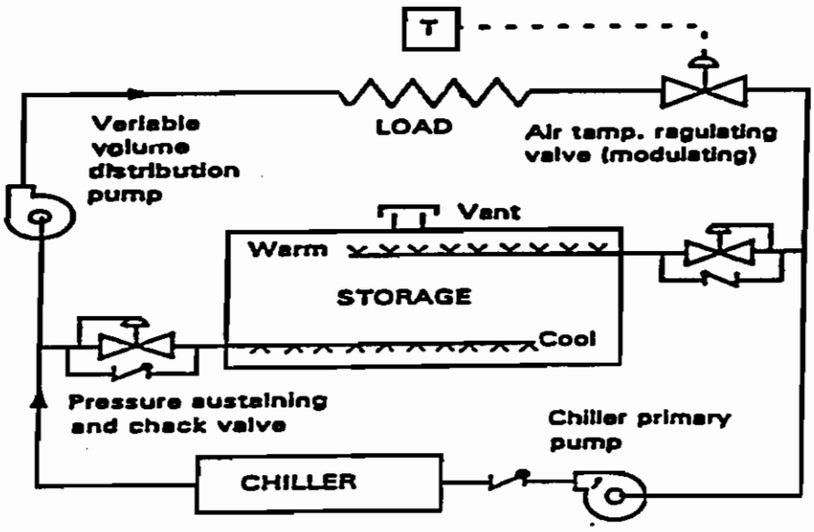

Figure 1.1:Basic Stratified Chilled Water Configuration [2].

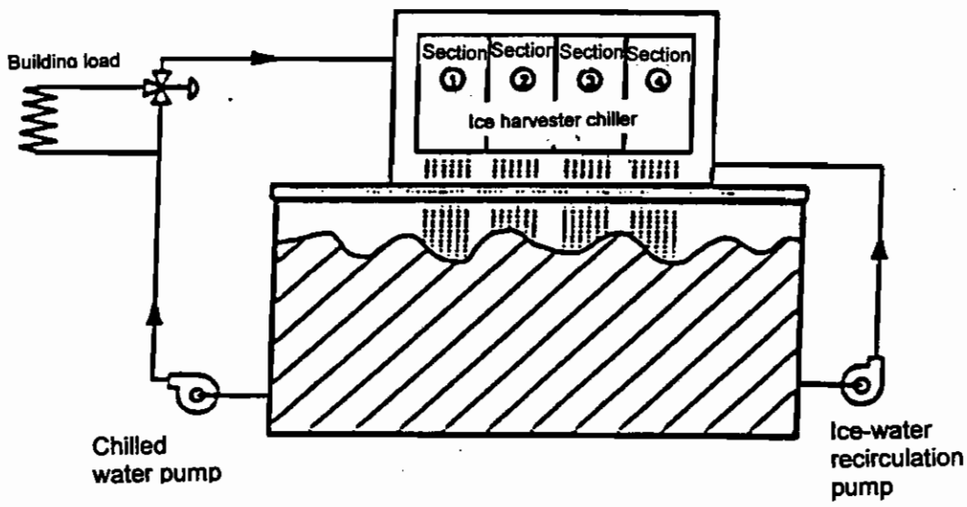

Figure 1.2: Ice Harvesting System [2]

This is denoted as charging cycle. The solidified layers are periodically dropped into the storage tank below by activating defrost cycle (discharging cycle) at a suitable intervals. The formed ice is used for cooling in a discharge cycle, in which, iced water is taken from the bottom of the storage tank and circulated to the load. The discharge temperature remains approximately constant during discharge until the last ice has melted.

1.2.3 Types of eutectic systems

There are two types of eutectic materials: salt and oil. An eutectic salt is a chemical mixture which changes phase from liquid to solid at a specific temperature. Just as water, it stores a large amount of cooling as it changes from a liquid to solid. Eutectic salts are used in air-conditioning application to store cooling at their phase change temperatures. Conventional chilling equipment at standard temperatures; can therefore be used with such systems. This makes this medium attractive for retrofits of existing systems. [2]

Salt material is encapsulated in rectangular cross section plastic containers, which are stacked within a storage tank. Water circulates through the tank among the eutectic

salt containers carrying heat to or from the storage medium. The plastic containers decrease heat transfer between the salt and circulated water [6].

Eutectic oil is dispersed into water forming an emulsion with the help of a special surfactant. Phase change emulsion has the advantage of using the conventional available water chillers. Only a storage tank (nearly of the same size as of ice storage tank) is needed. There are various materials with different latent heat at different freezing temperatures (4-13^{0}C) [7], e.g. tetradecan ($C_{14}H_{30}$) as the phase change material with water as the continuous phase emulsion. Tetradecan has the following properties[5]:

* Freezing point 278.9 K (5.75 ^{0}C) which is the same as A/C chillers working temperature.

* Latent heat L=229 kJ/kg which is ≈ 68.3% of latent heat of water (L=335 kJ/kg [7]).

Inaba [5] studied tetradecan properties and found that, the pressure loss of the emulsion in the coiled tube heat exchanger increases with an increase in the concentration of the dispersion phase change material. In addition, Nusselt number increases with an increase in the concentration of the phase change materials as it flows in

a coiled tube heat exchanger. On the other hand, some of the phase change emulsion is expensive and toxic.

1.3 Types of ice formation on tubes

Two methods are used to form ice on tubes. One is to use flooded tubes, the second is to freeze a falling film on tubes. Intemann [4] has carried out an experiment on cold tube banks subject to a cross flow of water. The tubes were internally cooled below the freezing temperature to form ice. In order to study and photograph the growth of ice on the tubes, coolant entry into and exit out of the tubes were located on one end of the tubes as shown in figure (1.3). It was found that the ice formation dramatically affected the convective heat transfer rate of the tube banks (when compared to nonicing tube banks at the same Reynolds number). Ice layers acts as an insulation between the tube surface and the cross flow of water. The ice formation at the rear side of the tubes is thicker than that at the front side, with respect to the flow direction.

Horizontal-tube falling film heat exchangers are used in chemical, refrigeration, petroleum refining, desalination and food industries because they provide higher heat transfer coefficient and operate with smaller liquid

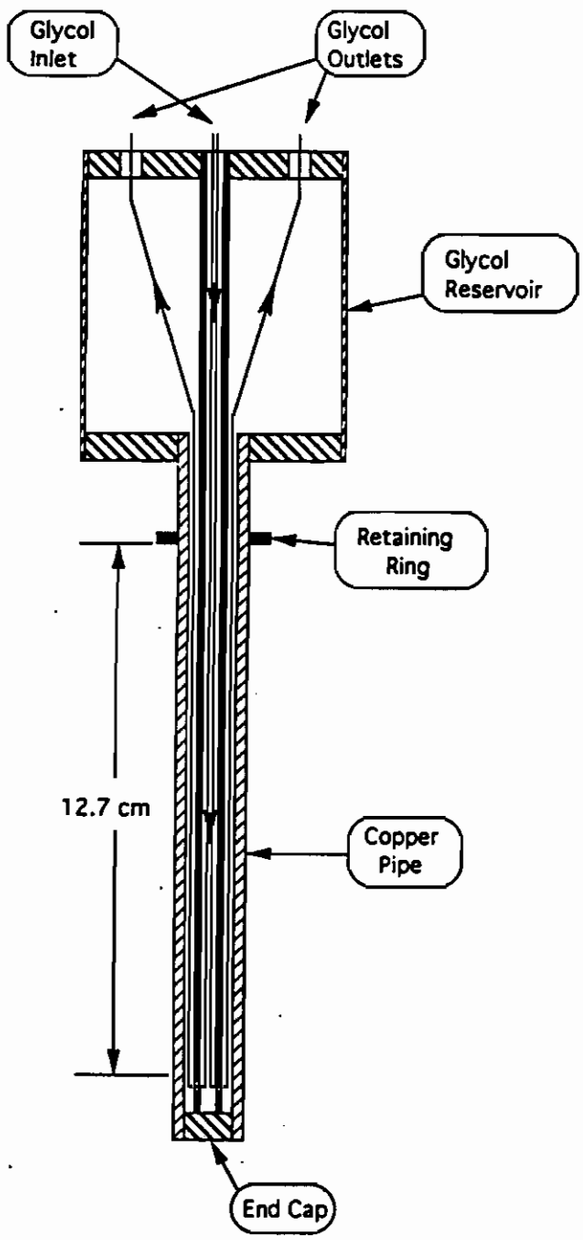

Figure 1.3: Tube section in Intemann's experiment [4]

inventories than flooded heat exchangers. In addition, they offer advantages in dealing with liquid distribution, fouling and other problems. [8]

When a falling liquid film flows from one horizontal tube to another below it, the flow may take the form of discrete droplets, jets or a continuous sheet depending on the flow rate .If the flow rate is low, the liquid leaves the tube in the droplet mode .If the flow rate is increased, the flow pattern changes to continuous circular jets. With a further increase in the flow rate, the jets merge and form a continuous liquid sheet. The opposite will happen when reducing the flow rate (see figure 1.4). A regime map showing the boundaries of different flow regimes is given by Hu [8] as a function of Reynolds number and Galilio number in figure (1.5).

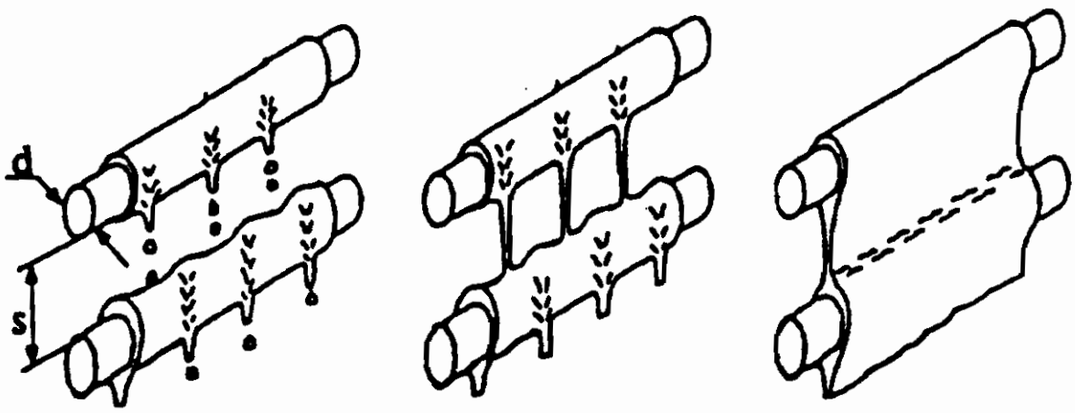

(a) (b) (c)

Figure 1.4: The idealized intertube falling film modes: (a) the droplete mode, (b) the jet mode, and (c) the sheet mode, Hu[8]

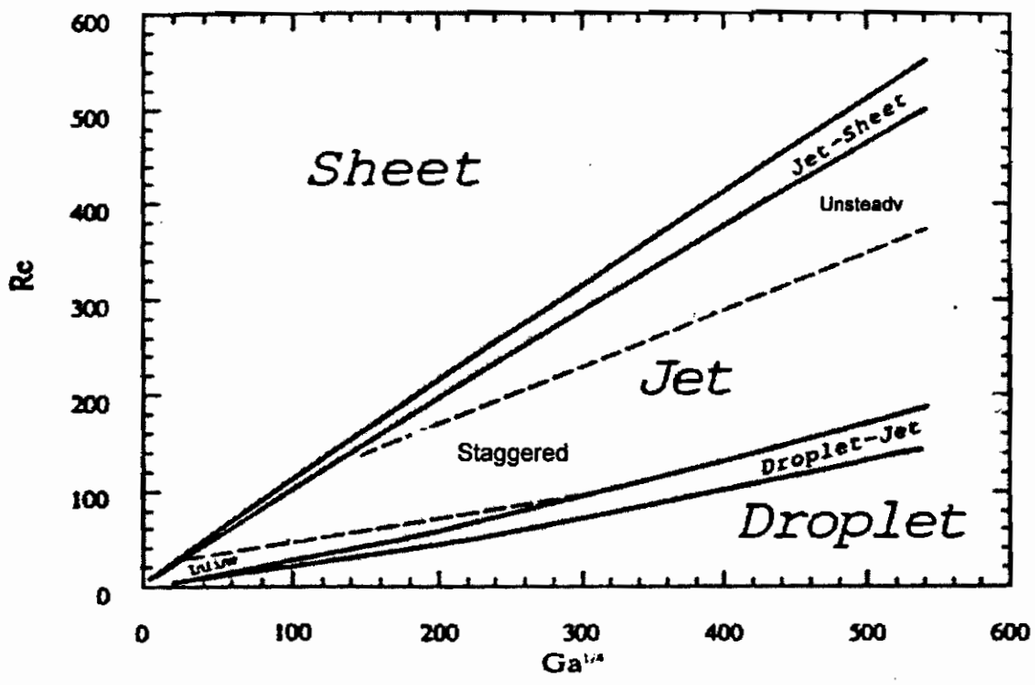

Figure 1.5: A simplified flow regime map for the falling - film mode transitions,Hu[8]

1.4 Theoretical background

Considering cooled fluid is used inside tube to cool and freeze another fluid outside the tube, the thermal resistance's for the heat transfer consists mainly of: inside convective heat transfer, freezing layer conductive heat transfer and outside convective heat transfer.

Consider a hollow cylinder (figure 1.6), with inner and outer surfaces are being exposed to fluids at different temperatures. The heat transfer rate, in radial direction and neglecting axial and peripheral conduction, using Fourier's low of heat conduction is:

$$\dot{Q} = \frac{2\pi / k (T_{s,1} - T_{s,2})}{\ln(r_2/r_1)} \qquad (1.1)$$

From this equation it is evident that for radial conduction in hollow cylinders, the thermal resistance would be,

$$R_{t,cond} = \frac{\ln(r_2/r_1)}{2\pi / k} \qquad (1.2)$$

1.4.1 Heat transfer through ice layer

In this case the heat transfer is carried out as that of composite cylinder. The heat transfer rate may be expressed as:

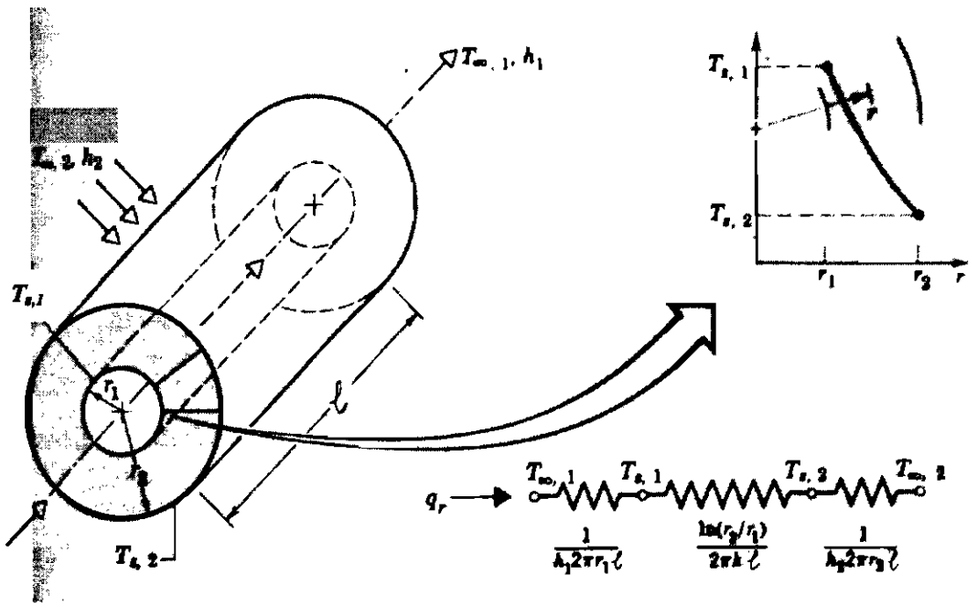

Figure 1.6:Hollow cylinder with convective surface conditions.

1.4.2 Inside heat transfer coefficient

The flow in a circular tube is either laminar or turbulent depending on the value of Reynolds number. The Reynolds number for flow in a circular tube is defined as

$$Re \equiv \frac{\rho u_m D}{\mu} \qquad (1.8)$$

Where u_m is the mean fluid velocity over the cross section and D is the wetted perimeter. In a fully developed flow, the critical Reynolds number corresponding to the onset of turbulence [9] is

$$Re_{D,c} \approx 2300 \qquad (1.9)$$

The mean fluid velocity is defined such that, when multiplied by the fluid density and the cross sectional area of the tube A_c, it provide the mass flow through the tube, $\dot{m}$

$$\dot{m} = \rho u_m A_c \qquad (1.10)$$

For constant surface temperature condition, average convection coefficient is given by many researchers, one is given by Incorpora,[9]as:

For laminar flow, Re ≤ 2300

$$Nu = 1.86 \left(\frac{Re\ Pr}{l/D} \right)^{1/3} \left(\frac{\mu}{\mu_s} \right)^{0.14} \qquad (1.11)$$

Where this equation can be applied for the following condition:

T_s(surface temperature) = constant

$0.48 < Pr < 16{,}700$

$0.0044 < (\mu/\mu_s) < 9.75$

For turbulent flow,

$$Nu = 0.023\ Re^{0.8}\ Pr^{0.3} \qquad (1.12)$$

Where the ranges are

$0.7 \leq Pr \leq 160$

$Re \geq 10{,}000$

$l/D \geq 10$

All properties except μ_s should be evaluated at the average value of the inlet and outlet temperature, T

$$T = (T_i + T_o)/2 \qquad (1.13)$$

Then,

$$h = \frac{Nu\ k}{D} \qquad (1.14)$$

Noting that equation (1.12) can be used as a first approximation at a smaller Reynolds number than 10,000.

1.4.3 Outside heat transfer coefficient

Due to lack of information in the literature, equations of Hu[10],for sensible heat transfer in a falling film are

used to approximate the Outside heat transfer coefficient. These equations are:

For sheet mode:

$$Nu=2.194\ Re_f^{\ 0.28}\ Pr^{\ 0.14}\ Ar^{(-0.20)}\ (s/d)^{0.07} \quad (1.15)$$

For jet mode:

$$Nu=1.378\ Re_f^{\ 0.42}\ Pr^{\ 0.26}\ Ar^{(-0.23)}\ (s/d)^{0.08} \quad (1.16)$$

For droplet mode:

$$Nu=0.113\ Re_f^{\ 0.85}\ Pr^{\ 0.85}\ Ar^{(-0.27)}\ (s/d)^{0.04} \quad (1.17)$$

The liquid properties were evaluated at film temperature T_f.

Where

Nu modified Nusselt number = $(\nu^2/g)^{1/3}\ h/k$ (1.18)

Re_f film Reynolds number = $2\Gamma/\mu$ (1.19)

Pr Prandtle number = $C_p\ \mu/k$ (1.20)

Ar Archimedes number based on tube diameter = d^3g/ν^2 (1.21)

d diameter,m

s tube spacing,m

g gravitational acceleration,m/s^2

μ dynamic viscosity, $N.s/m^2$

ν kinematics viscosity, m^2/s

Γ liquid mass flow rate per unit length of tube, kg/s.m

h heat transfer coefficient, $W/m^2.K$

k thermal conductivity,W/m.K

C_p specific heat of liquid falling film = 4.180 kJ/kg.K

1.5 Summary of literature review

From the previous review, one may conclude that:

1) The cold storage system is important for energy saving specially at the peak time.
2) Chilled water system needs a huge tank compared with other systems[2].
3) Eutectic phase change system needs special material and sometimes special surfactant [7].
4) Ice system uses only water, high latent heat and direct contact with circulated load water. Ice formation on immersed tubes is studied by Inteman [4]. Falling film sensible heat transfer of heating process is carried out by Hu.[8,10]
5) Falling film ice formation and heat transfer study is needed.

The main objective of the present work is to study the ice formation and the heat transfer coefficient of the freezing falling film. Test rig model is designed and constructed. In this model, water or solution of 2% aceton in water is used as phase change material. They fall down from an upper tube to the colder underneath tubes. Liquid freezes outside

these tubes. Ice formation is observed and photographed for droplet, jet and sheet modes of the falling film at different coolant flow rate. Heat transfer coefficient is calculated. The results can be used for cold thermal storage designs.

CHAPTER-II

EXPERIMENTAL TEST RIG AND MEASURING TECHNIQUES

2.1 Introduction

The test rig is designed and fabricated to form ice outside cooled tubes. Three fluid loops are used: falling film, cooling and defrosting loops. A constant head precooler tank with pipe connections and valves are used to distribute the falling film on the test tubes. A re-circulating pump is used to lift the remained water to the tank. A cooled antifreeze (ethylene glycol 40% solution) is passed though the test tubes during the cooling mode, while warm glycol is used, to defrost ice to measure its quantity. The temperature and flowrates required are measured and recorded.

The main part of the test rig is the internally cooled pipes on which the falling film is freezing. The internal cooling of the test section is carried out through a controlled temperature-cooling machine TD30 "manufactured by Tecquipment Company and available in thermal engineering

laboratories, see appendix A". The capacity of this machine is variable according to the condensing and the required cooling temperatures. For example, at condensing temperature of 30^0C and cooling temperature of -10^0C, the expected capacity is 6.74 kW.[11]

2.2 Test rig description

The test rig (figure 2.1) consists of three loops, the falling film loop, the cooling loop including TD30 and the defrosting loop. Details of different parts of the test rig are explained below.

2.2.1 The falling film loop

The falling film loop consists of a constant head and precooler tank with an overflow, a drain, a ball valve, a flow meter and a recirculation water pump(figure 2.1). From the precooler tank, the chilled water flows through the ball valve and the flow meter to the upper feed tube in the test section. Then, it is distributed on the set of the test tubes forming a falling film. The remained collected chilled water in the bottom of the test section is pumped to the constant head precooler tank.

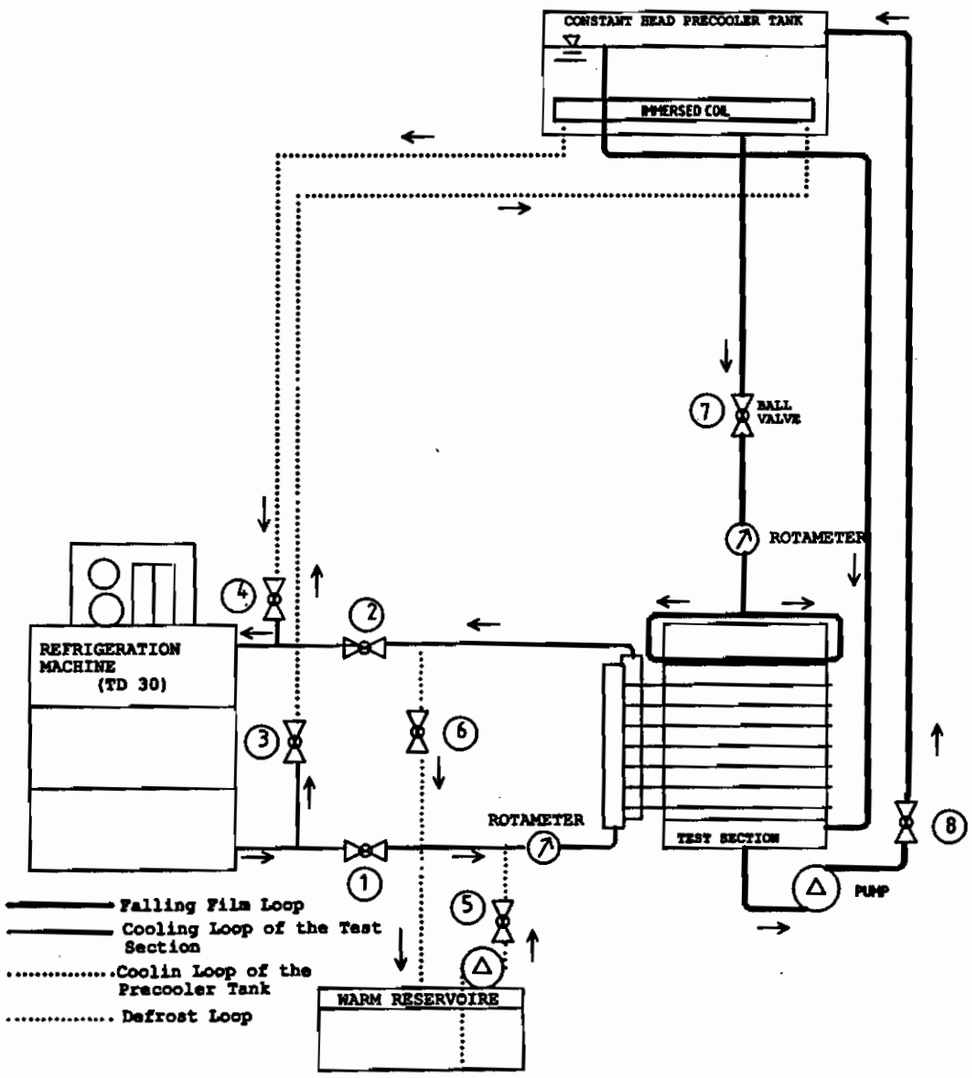

Figure 2.1:A schematic of the experimental apparatus

2.2.2 The coolant liquid circulation loop

The coolant liquid circulation loop consists of a refrigeration machine (TD 30) which pumps the coolant through the flow meter to the test section tubes or the constant head precooler tank, then back to the refrigeration machine.

2.2.3 The defrost loop

To release ice from the test section and to determine the quantity of the formed ice, a defrost loop is activated. The liquid is pumped from a heated reservoir to the test section, back to the same point. Ice will fall down into the bottom of the supporting box. The quantity of ice is calculated by measuring the change of the water level.

2.3 Test section

The test section (figure 2.1) consists of a supporting box and test tubes arrangement.

2.3.1 The supporting box

The supporting box is made of clear Perspex sheets (for falling film flow and ice observation and photographing) of 8-mm thickness with inside dimensions 273x235x550 mm (figure2.2). Every sheet is

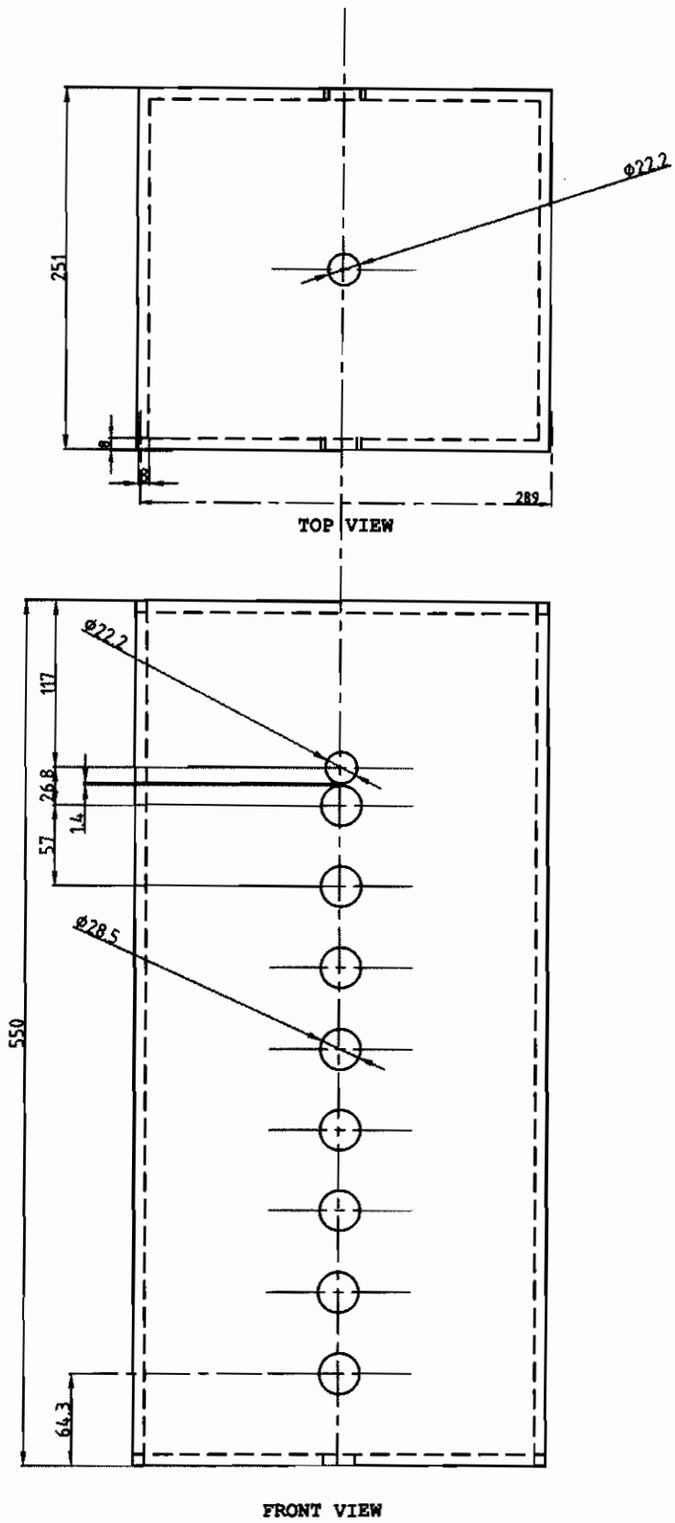

Figure 2.2:A Sketch of the supporting box

machined carefully to minimize misalignment. Nine holes with same diameter of the test tubes and the feeding tubes are drilled carefully on two counter sheets. At the bottom of the drilled sheets 6 cm is left under the last hole to act as a water pool for collecting the remained falling liquid and the quantity of ice that drops in the pool. The chilled water goes to the pump through 22 mm hole drilled at the bottom of the box. The supporting box is well insulated and covered to minimize thermal losses.

2.3.2 The tubes arrangements

To guarantee an adequate falling film, the arrangement used by Hu [8] is followed. This comprises a top feed tube, which has inside and outside diameters of 19 and 22 mm respectively. The tube is perforated with diameter of 2 mm at a pitch of 2.5 mm along 229 mm length. A second feed tube with diameter of 28.5 mm is placed 1.4 mm edge to edge from the distributing tube. Seven in-line test tubes bank configuration with diameter of 28.5 mm are placed at a pitch of 57 mm under the feed tube as shown in figure (2.3). This is to get a large contact surface area in order to hold the high latent heat of water (335 kJ/kg). The test tubes are made of copper, which has high thermal conductivity.

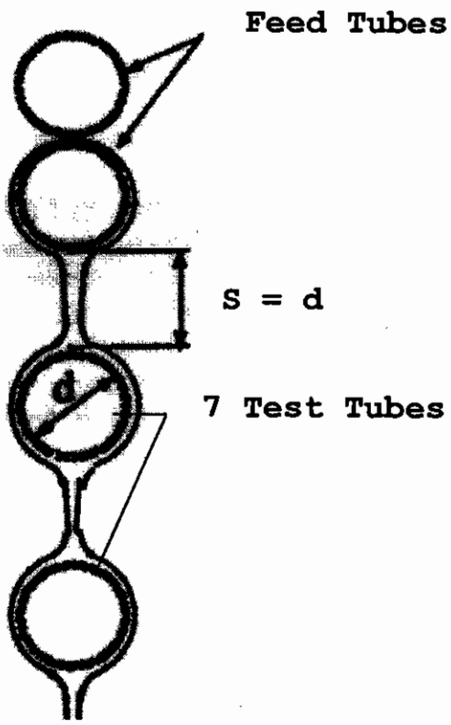

Figure 2.3: A schematic of the tubes within the test section.

Parallel and series arrangements of the test tubes are exported. Parallel connection allows the flow to enter each test tube at the same temperature. However, It reduces the mass flow rate of the flow. On the other hand the series arrangement allows higher mass flow rate but different inlet temperatures to each test tube.

In parallel arrangement (figure 2.4) two manifolds of diameter of 50.8 mm and length of 410 mm are used. The flow enters from the bottom of the first manifold to the test tubes through seven 15.8 mm diameter inner tubes fixed at the center of the test tubes as Intemen's apparatus [4]. The test tubes have a pitch of 57 mm and they are connected to the T-reducer of 28.5x15.8x15.8 mm with unions from one side and caps to close the other side. The coolant then flows to the second manifold and exits from the top of it.

On the other hand, in series arrangement the coolant enters the test tubes directly through the inner tube starting with the last tube .The coolant is then flows to the next upper tube through a 15.8 mm elbow figure (2.5).

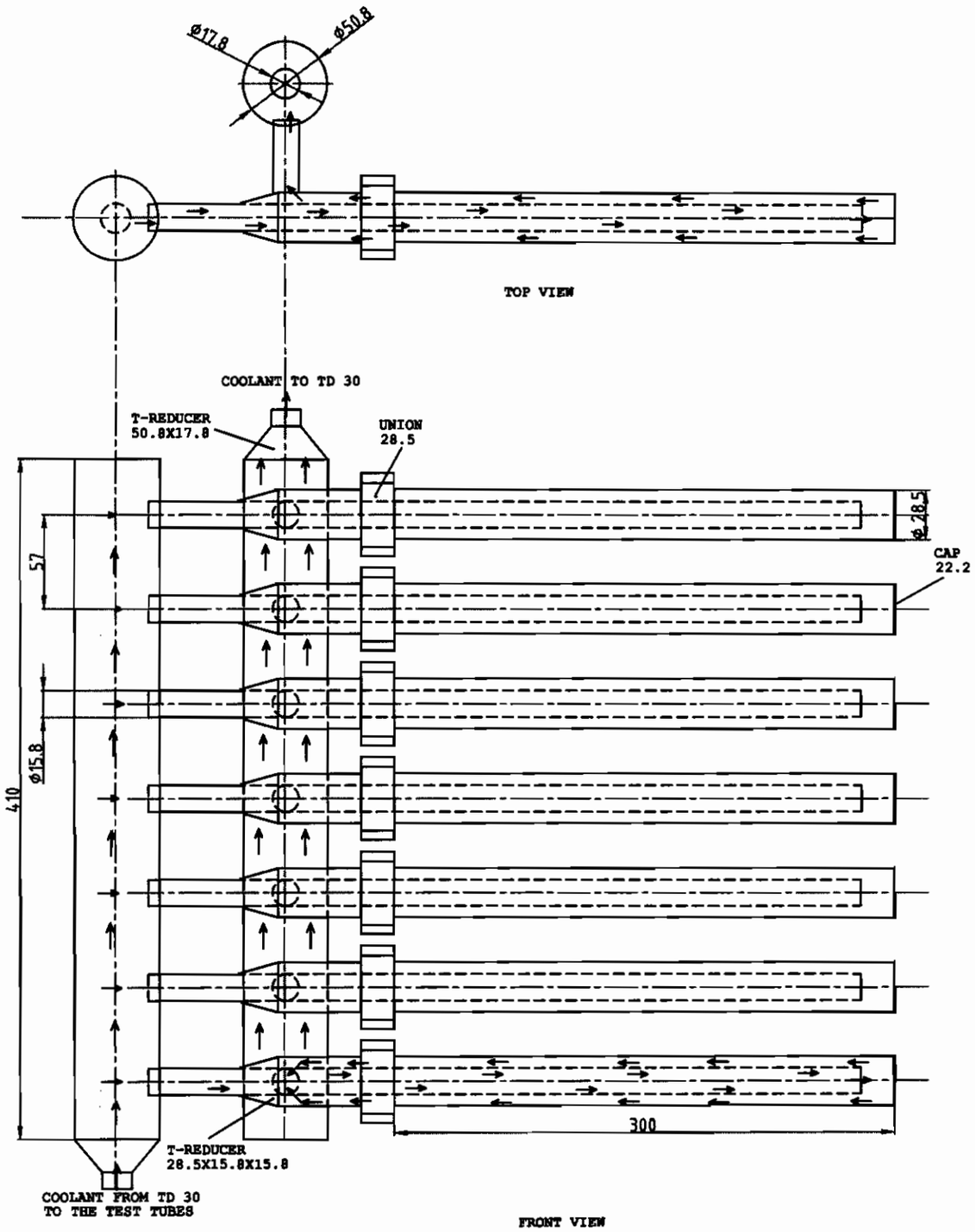

Figure 2.4:A schematic of the parallel arrangement of the test tubes

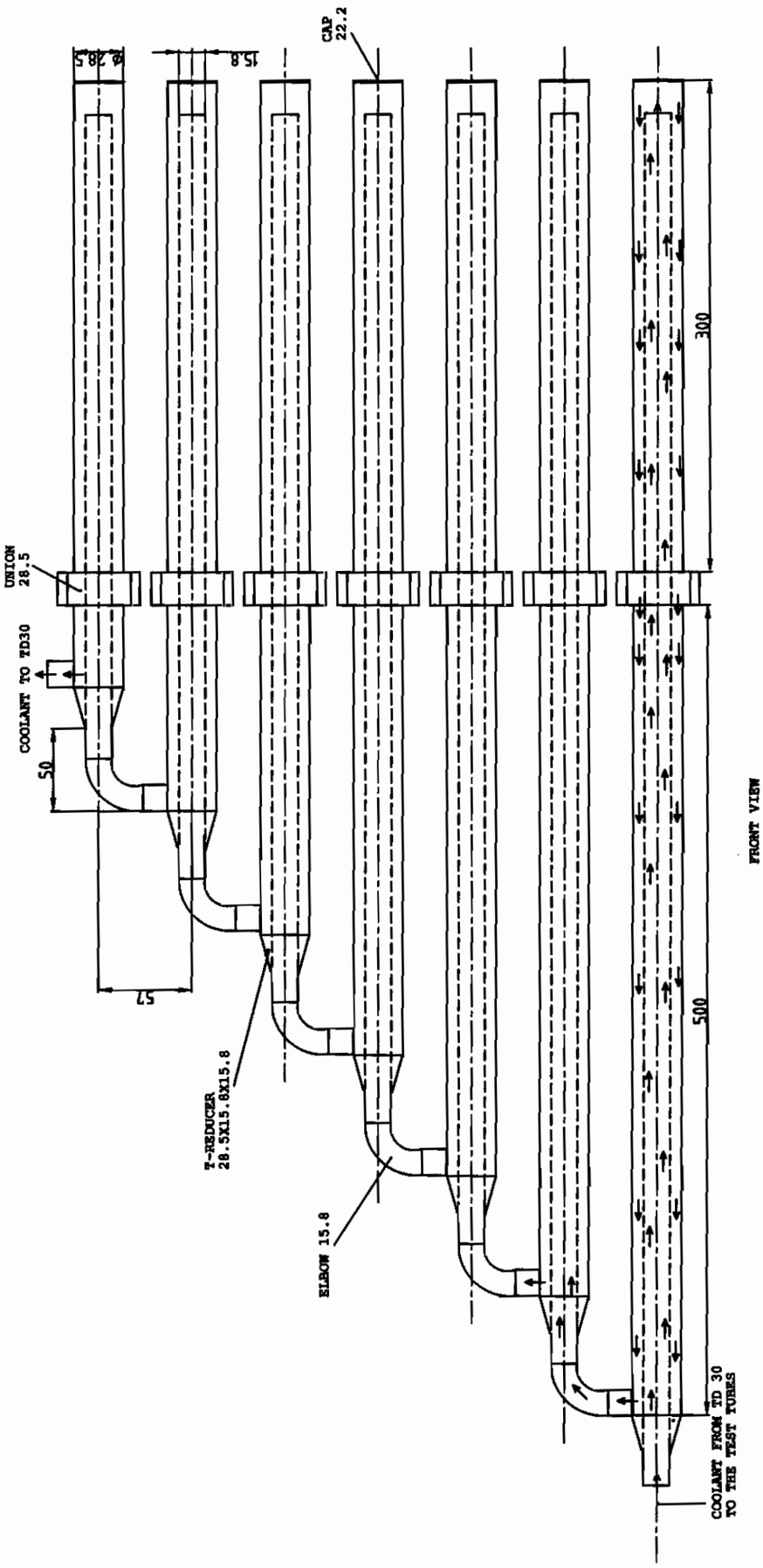

Figure 2.5 A schematic of the series arrangement of the test tubes

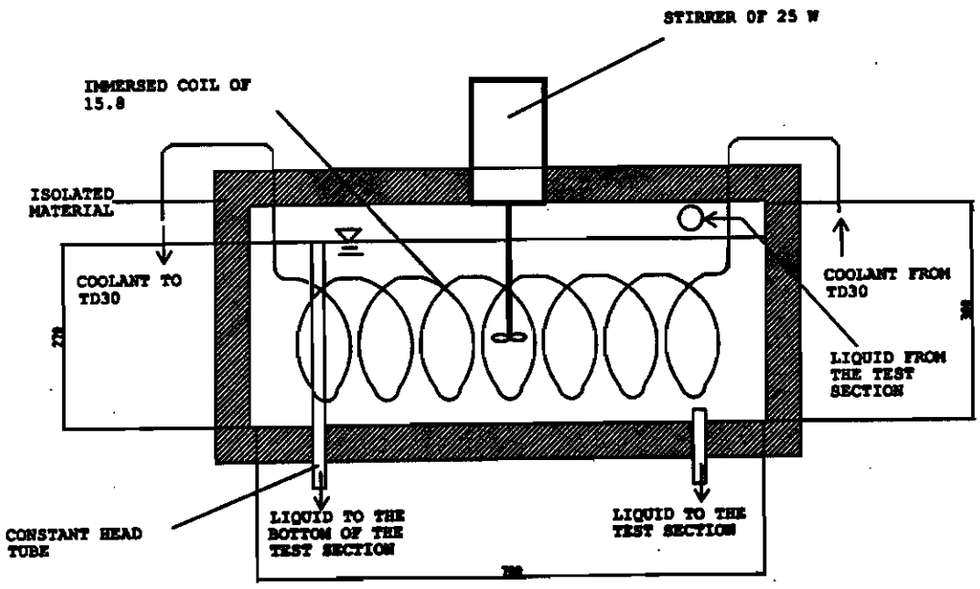

Figure 2.6: A schematic of the constant head precooler tank

2.5 Measuring techniques

Specimen surface temperatures are measured using calibrated 36-gage, copper -Constantan thermocouples. On each test tube 6 thermocouples are embedded in axial grooves at 60-degree circumferential increments as shown in figure (2.7). Using thermally conductive epoxy, each thermocouple junction is fixed to the specimen surface at the end of the groove such that the bead is barely visible at the surface. The thermocouple wires are placed in the axial grooves, and the grooves are filled with thermally conductive and electrically resistive epoxy. About 50% of the groove volume is occupied by the thermocouples and the rest is epoxy. Approximately 16.7% of the test surface area are occupied by the grooves. After the epoxy is dried, the tubes are polished with fine emery cloth to remove any excess epoxy at the exposed portions of thermocouple junctions. On the other hand, the temperature of the coolant and the cold water is measured using T-type immersed thermocouple. They are fixed in a well welded through tubes (figure 2.8). Calibrations of thermocouples are shown in figures 2.9 to 2.11. The flow rate of the coolant and the cold water is measured by using calibrated rotameters (1-15 gpm, for a Specific gravity =1), and (0.5-5 gpm, for a Specific gravity = 1) for the coolant and for

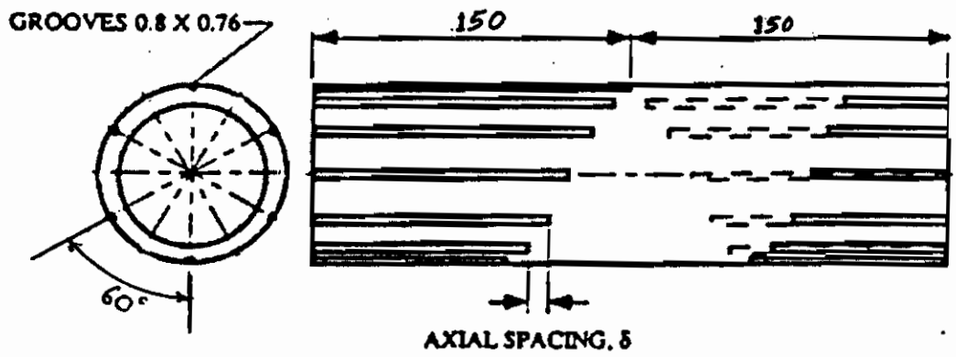

(a)

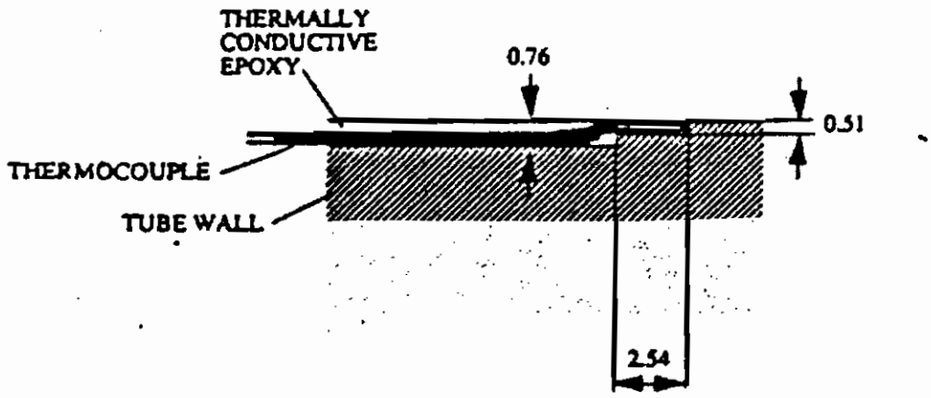

(b)

Figure 2.7: Thermocouples placement on the test specimen tube, all dimensions in mm: (a) Grooves on the tube surface and (b) location in the groove wall.

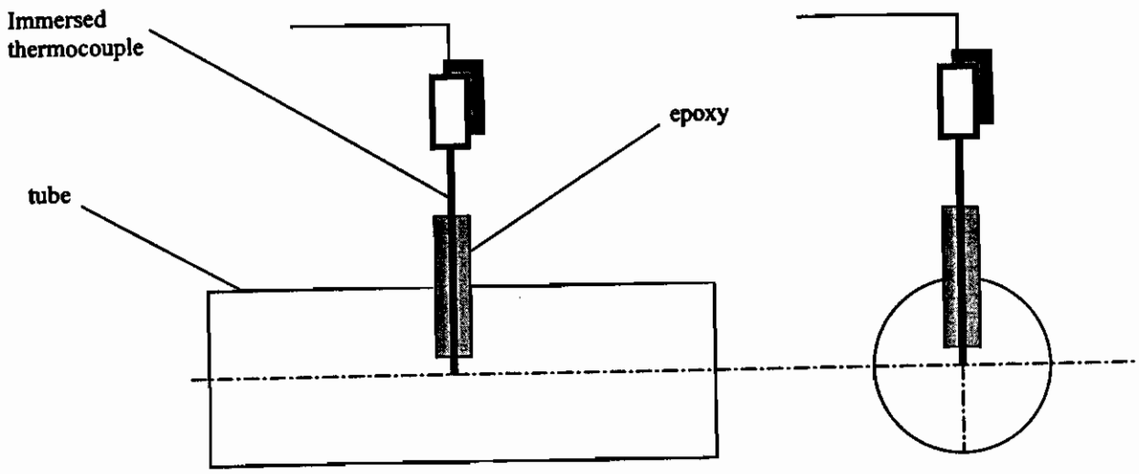

Figure 2.8: The mounting of the immersed thermocouples in the tubes.

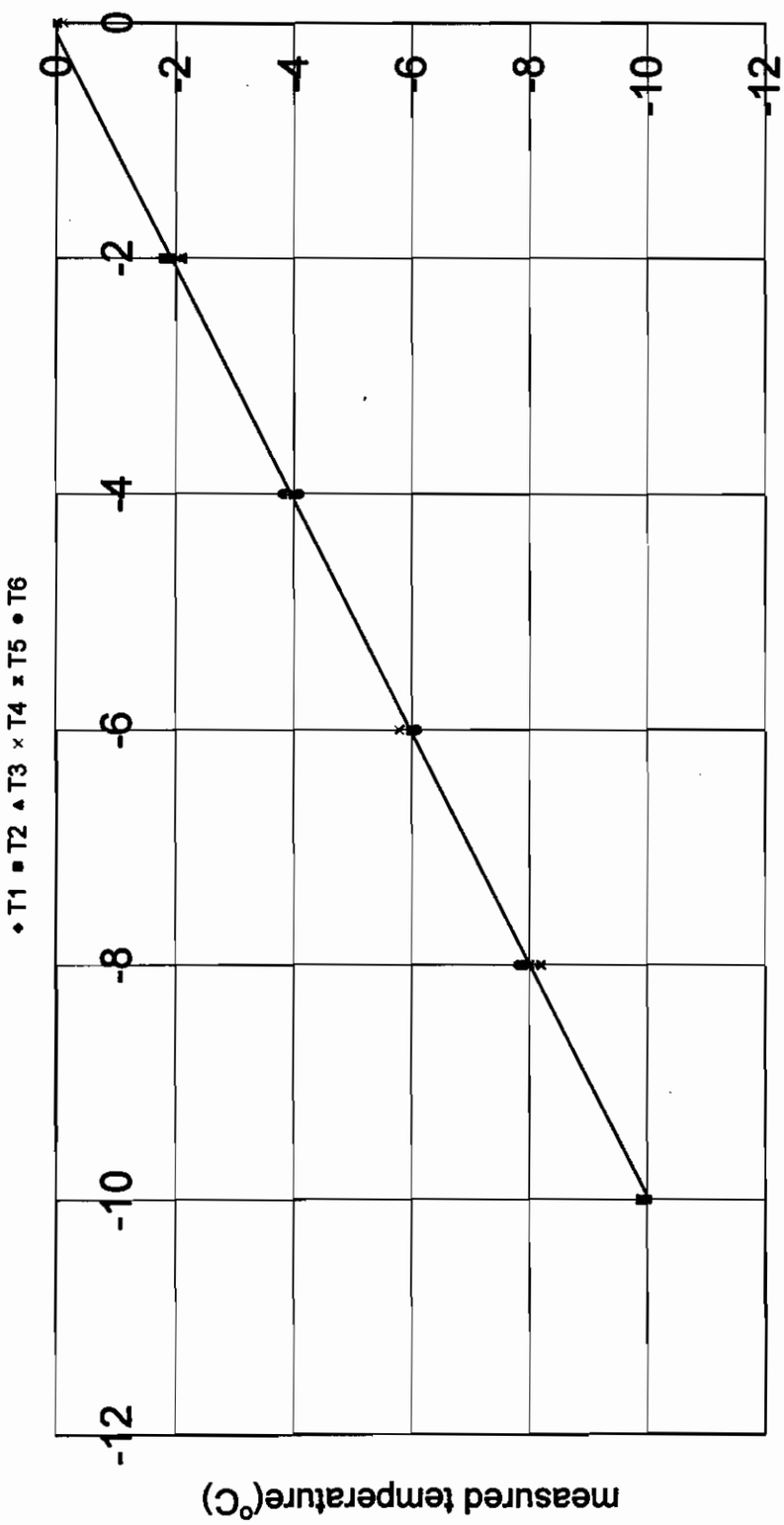

Figure 2.9 : Calibration of thermocouples at the test tube surface

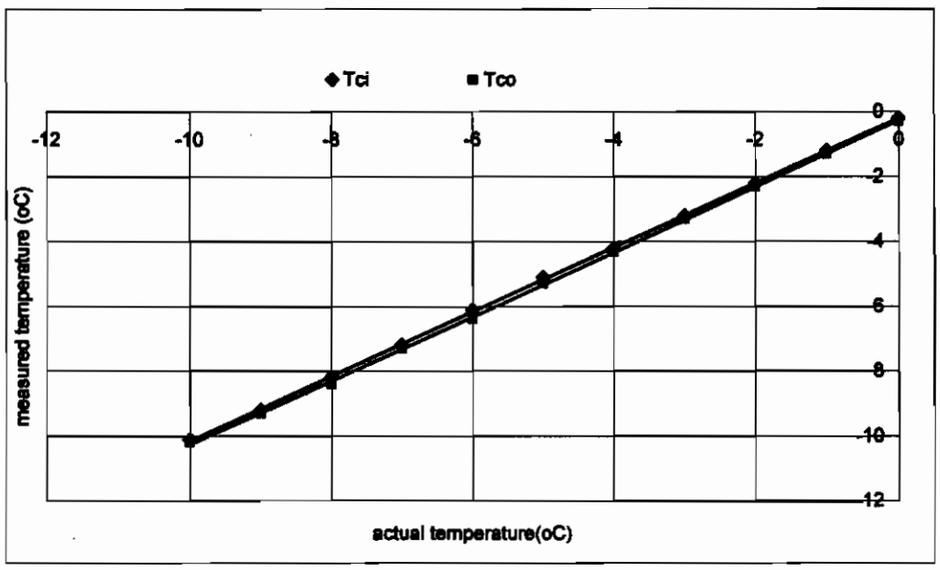

Figure 2.10: Calibration of the coolant immersed thermocouples.

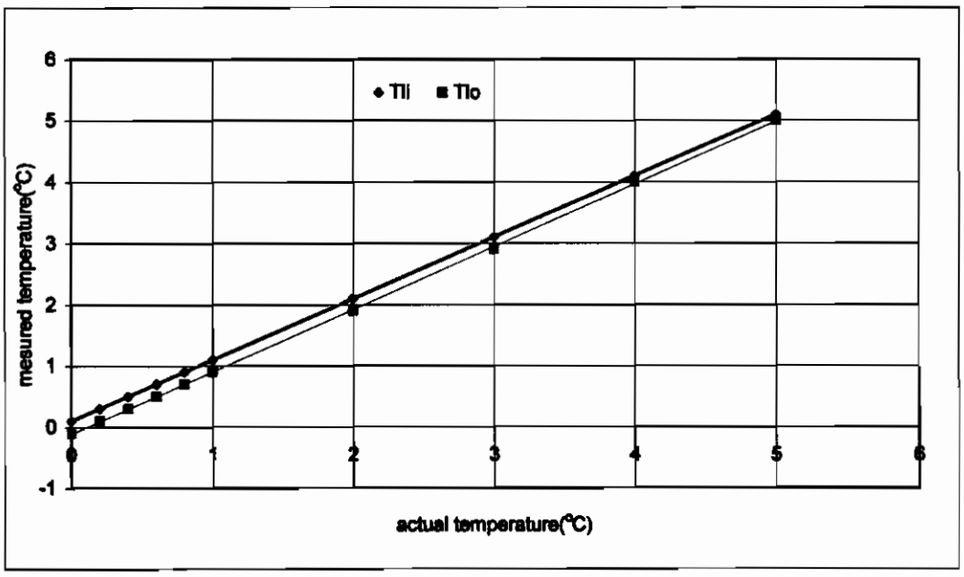

Figure 2.11: Calibration of the falling film immersed thermocouples.

the cold water respectively. Calibrations of rotameters are shown in figures 2.12 and 2.13.

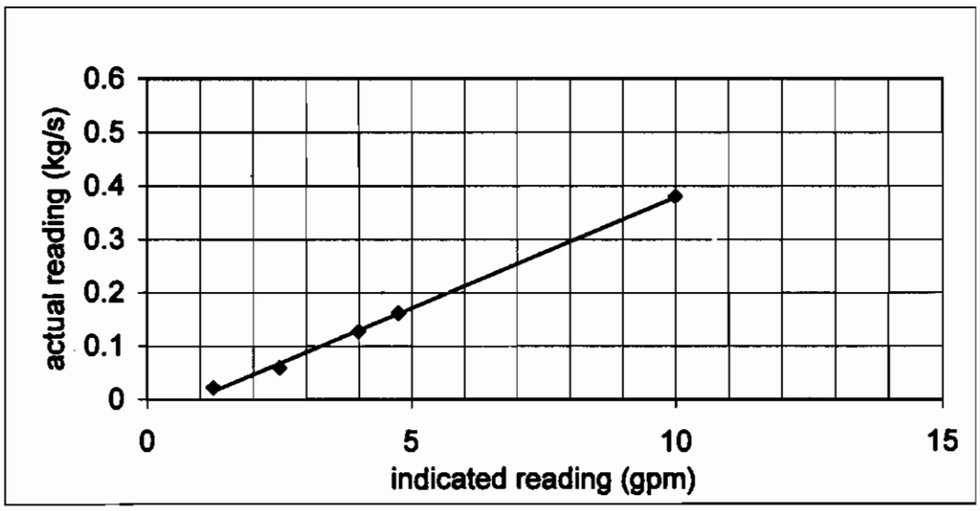

Figure 2.12: Calibration of the coolant rotameter.

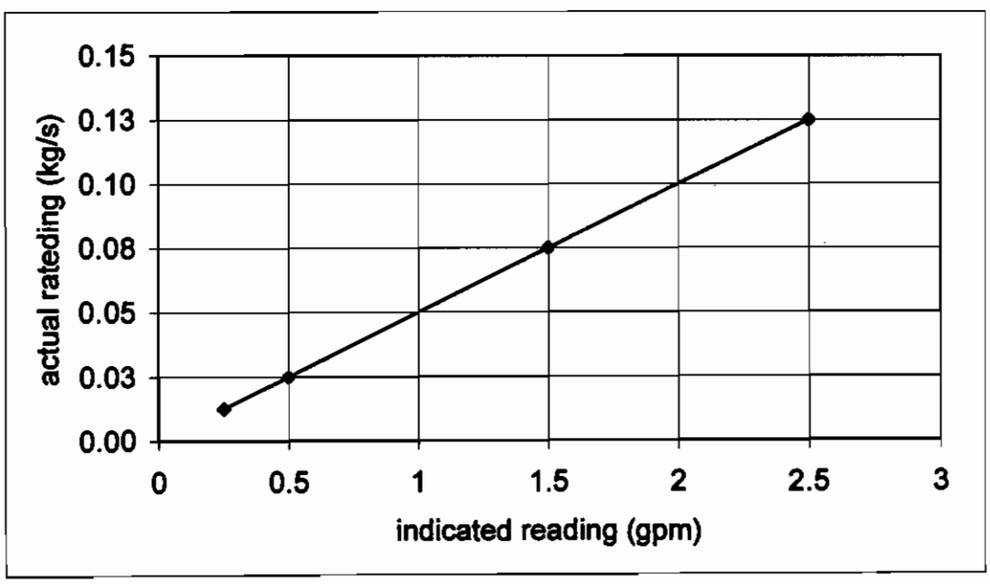

Figure 2.13: Calibration of the falling film rotameter.

CHAPTER-III

RESULTS AND DISCUSSION

3.1 Introduction

The experimental apparatus (figure 3.1) is comprised, as explained in chapter 2, of three loops, namely, the cooling loop including TD30, the falling film loop, and the defrost loop. The quantity of ice formed on the test section tubes is estimated at different run times. The coolant flow rate inside the test tubes and liquid falling film flow rate are changed. Different tube arrangements (parallel & series) are used. Employing some additive (acetone) to the water is tried. The effect of each of the previous parameters on the quantity of the formed ice, and the heat transfer rate are investigated.

The coolant flow rate m_c (kg/s), and its inlet and outlet temperature T_{ci}&T_{co} (°C) are measured. The rate of heat transfer from the test tubes to the coolant, $\dot{Q}_c$ (W), is estimated by using the following equation

$$\dot{Q}_c = \dot{m}_c C_{pc}(T_{co} - T_{ci}) \qquad (3.1)$$

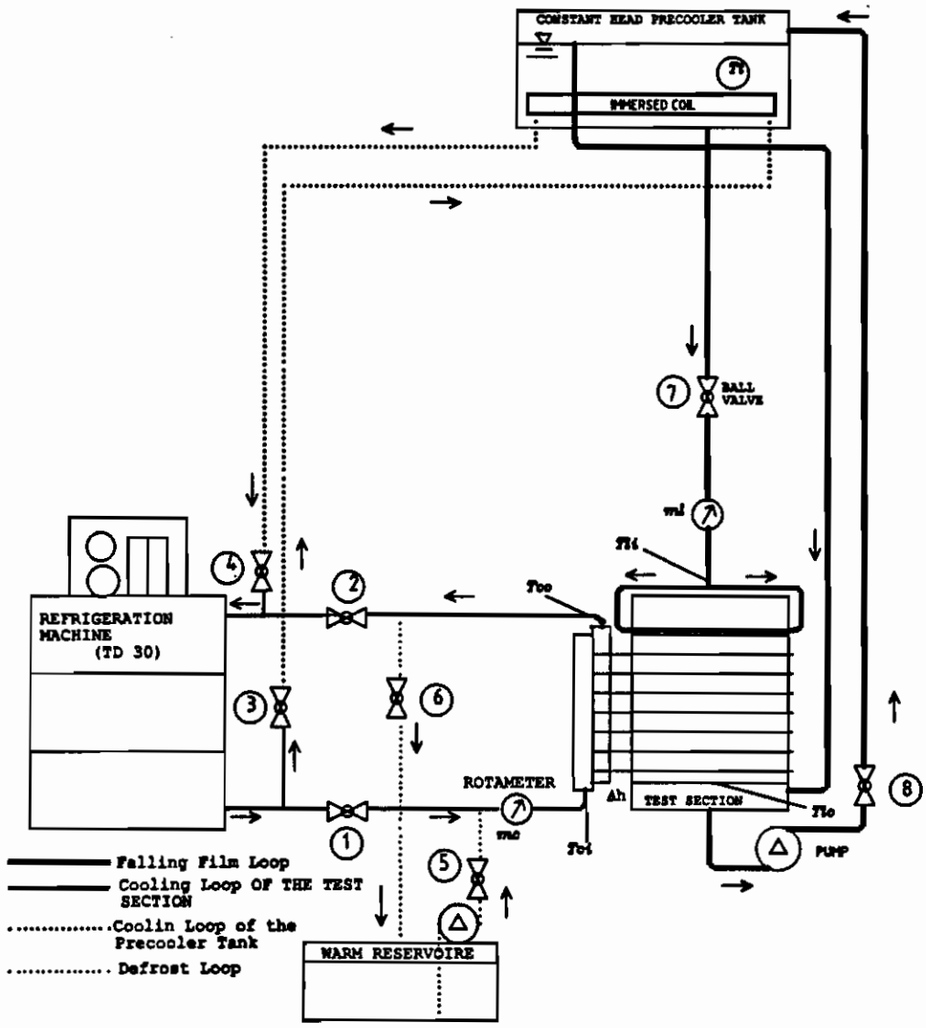

Figure 3.1:A schematic of the experimental apparatus showing the measuring points.

Then, the average rate of heat transfer from the test tubes to the coolant at a specific time, $\dot{Q}_{c,ave}$, is calculated by the following equation:

$$\dot{Q}_{c,ave} = \frac{\int_{t=0}^{t=n} \dot{Q}_c \, dt}{time} \qquad (3.2)$$

where:

t : is the interval times in minutes

n : is the indicated time

$\int_{t=0}^{t=n} \dot{Q}_c \, dt$ = Area under the curve of $\dot{Q}_c$ vs.time

This integration can be obtained by the trapezoidal rule of integration:

$$\int_a^b f(x)\, dx = \frac{b-a}{2n} [\, f(x_0) + 2f(x_1) + 2f(x_2) + \ldots + 2f(x_{n-1}) + f(x_n)\,] \qquad (3.3)$$

The rate of heat transfer from the test tubes to the coolant, $\dot{Q}_c$, is compared with the calculated rate of heat transfer to the coolant, $\dot{Q}_{c,cal}$. Considering figure 3.2 and section 1.4.1:

$$\dot{Q}_{c,cal} = U\, A\, (T_i - T_c) \qquad (3.4)$$

Where:

$$\frac{1}{UA} = \frac{1}{h_i\, \pi\, D_{i,o}\, l} + \frac{\ln(D_{o,o} / D_{i,o})}{2\, \pi\, k_c\, l} + \frac{\ln(D_{ice} / D_{o,o})}{2\, \pi\, k_{ice}\, l} + \frac{1}{h_o\, \pi\, D_{ice}\, l} \qquad (3.5)$$

Or,

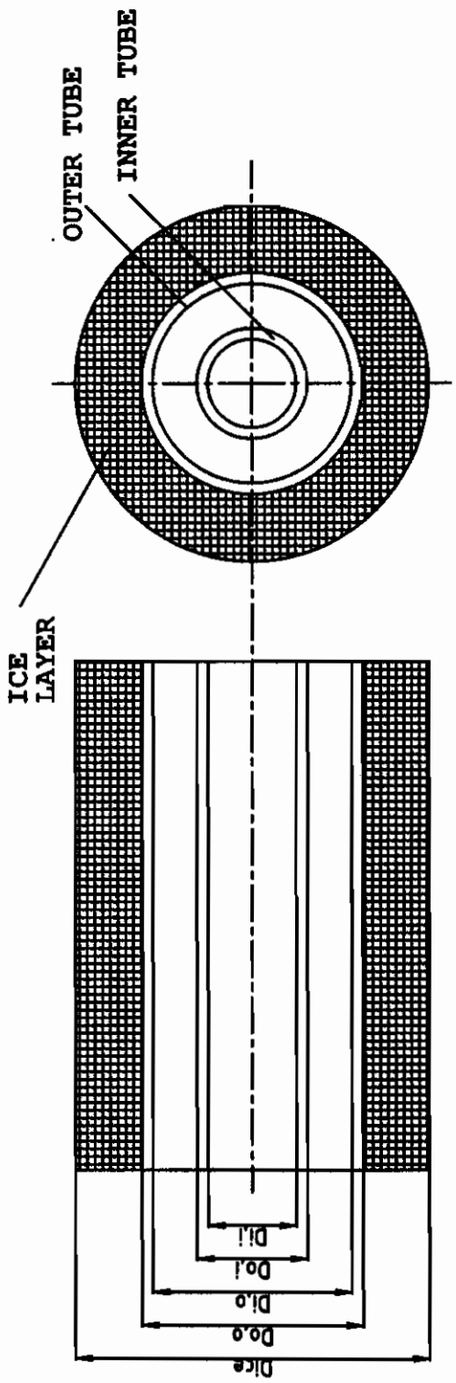

Figure 3.2: A schematic of the annulus of the test tube

$$UA = \frac{1}{R_1 + R_2 + R_3 + R_4}$$

Where:

$R_1 = 1/(h_i \pi D_{i,o} l)$

$R_2 = \ln(D_{o,o} / D_{i,c}) / (2 \pi k_c l)$

$R_3 = \ln(D_{ice} / D_{o,o}) / (2 \pi k_{ice} l)$

$R_4 = 1/(h_o \pi D_{ice} l)$

In the falling film loop, liquid falls from the constant head precooler tank (refer to figure 3.1) which is kept at a temperature of about 0.2°C. The falling film freezes outside the tubes in which the coolant is passed at a temperature of about -10°C and the falling film loses heat to the coolant. This heat includes: sensible cooling rate of the falling film, rate of latent heat transfer, which contributes to freezing, and sensible average cooling rate of ice.

Sensible cooling rate of the falling film, $\dot{Q}_{s,l}$, is evaluated by measuring the flow rate of the falling film m_l and the falling film inlet and outlet temperatures T_{li} & T_{lo}. Then $\dot{Q}_{s,l}$ is evaluated as follows:

$$\dot{Q}_{s,l} = \dot{m}_l C_{pl} (T_{li} - T_{lo}) \qquad (3.6)$$

The rate of heat transfer, which contributes to freezing, $\dot{Q}_{fr}$, is evaluated by measuring the quantity of the frozen ice at a certain time. The discharge cycle is activated to remove ice from the test tubes. Part of ice melts and the rest falls below. Water pool height due to ice defrosting is measured by a fixed ruler on the edge of the supporting box and $\dot{Q}_{fr}$ is calculated as:

$$\dot{Q}_{fr} = \frac{M_{ice}L}{Time} \qquad (3.7)$$

On the other hand, the formed ice loses sensible heat to the coolant, from the freezing point of ice "0°C for water" to half of the average coolant temperature. The average cooling rate of ice, $\dot{Q}_{s,s}$, is calculated as:

$$\dot{Q}_{s,s} = \frac{M_{ice}\, C_{pice}\, (T_f - T_o/2)}{Time} \qquad (3.8)$$

Loss from the test tubes is mainly due to convection from the outside layer (falling film) to the air inside the supporting box:

$$\dot{Q}_{ls,o} = h_l A_l (T_\infty - T_l) \qquad (3.9)$$

Then , the absorbed heat from the falling film, $\dot{Q}_{a,f}$, is :

$$\dot{Q}_{a,f} = \dot{Q}_{s,l} + \dot{Q}_{fr} + \dot{Q}_{s,s} \qquad (3.10)$$

The ratio (ε) between the absorbed heat from the falling film, $\dot{Q}_{a,f}$, and the average rate of heat transfer from the

test tubes to the coolant at a specific time, $\dot{Q}_{c,ave}$, is defined as:

$$\varepsilon = \frac{\dot{Q}_{a,f}}{\dot{Q}_{c,ave}} \qquad (3.11)$$

The experimental overall heat transfer coefficient, h_{ov}, is:

$$h_{ov} = \frac{\dot{Q}_{a,f}}{[A_{ice}(T_f - T_c)]} \qquad (3.12)$$

Losses from the test section $\dot{Q}_{ls}$ are calculated by measuring T_{ci}&T_{co} without introducing the falling film of liquid. Then, $\dot{Q}_{ls}$ is calculated as:

$$\dot{Q}_{ls} = \dot{m}_c C_{pc}(T_{co} - T_{ci}) \qquad (3.13)$$

3.2 Experimental Procedure

In these experiments commercial ethylene glycol solution (40% by weight) is used as a coolant. The concentration is obtained by measuring its specific gravity experimentally, then using its value to get the concentration from the specific gravity graph of the ethylene glycol from Perry [7]. The following values were obtained, for the coolant at -10°C:

$\mu = 0.008$ N.s/m^2

$\rho = 1060$ kg/m^3

$k = 0.4671$ W/m.K

$C_p = 3.3488$ kJ/kg.K

Physical properties of water at 0.25°C were as follows [9]:

$\mu = 1750 \times 10^{-6}$ N.s/m^2

$\rho = 1000$ kg/m^3

$k = 569.6 \times 10^{-3}$ W/m.K

$C_p = 4200$ J/kg.K

$\nu = 1.79 \times 10^{-6}$ m^2/s

Also, the physical properties of ice at 0°C [9] were as follows:

$\rho = 920$ kg/m^3

$k = 1.88$ W/m.K

$C_p = 2040$ J/kg.K

The experiment is started by running the TD30 to reduce liquid coolant temperature to about -10°C. The pressure regulator valve is adjusted carefully until the desired temperature remains approximately constant. The coolant is first admitted to the constant head precooler tank by opening valves 3 and 4,refer to Figure (3.1), and the stirrer is activated to accelerate the heat transfer. It takes about two hours(depending on the initial temperature) to bring the water temperature to about 0.2°C. During this time, some ice is accumulated around the coil, which helps

to keep the temperature of the precooler tank at the prescribed temperature (0.2°C). On-Off cooling of the precooler tank may be used if necessary to keep its temperature approximately constant. The coolant flows to the test section by opening valves 1 and 2, which are used to control the required coolant flow rate. When the temperature of the coolant in the test tubes reaches -10°C valves 7 and 8 are opened to start the falling film.

The falling film can be droplet, jet or sheet mode. The mode is selected by adjusting valve 7 to obtain the desired mode and the flow rate is recorded. Part of the liquid falling film freezes and accumulates around the test tubes. The ice formation is observed and photographed and the rest falls down to the bottom of the test section. Then it is pumped back to the constant head precooler tank.

The flow rate of the coolant and the liquid falling film is recorded every run. The inlet and outlet temperatures of the coolant, inlet and outlet temperatures of the liquid falling film and surface temperature are recorded using selector switch and read out temperature. The temperature of the constant head precooler tank is checked periodically to insure that it remains nearly constant.

In order to measure the quantity of the formed ice, the defrost loop is activated. The defrost loop is activated by opening valves 5 and 6 and closing valves 1,2,3,4,7 and 8. The warm liquid is of the same type and concentration as the coolant, since the remaining liquid inside the test tubes will pumped to TD30 during the coolant loop. Defrost loop is activated for some times depending on the quantity of the formed ice. It is activated about ten times during each run, to measure the formed ice at different periods. The ice falls down to the bottom of the test section and floats on the remaining water. Difference in height of water pool before and after the defrost loop activates is recorded.

3.3 Observations

More than ninety experimental runs are made to observe and measure the quantity of ice formation around the test tubes. The following are the main observations from these experiments:

1-When the liquid falling film falls on the horizontal test tubes, the flow is observed to be one of the main three modes: discrete droplets, jets or a continuos sheet, depending on the flow rate. When the valve is fully opened sheet mode is observed with high velocity hitting the first

test tube. The flow velocity decreases as the flow reaches the last test tube. The sheet mode is observed clearly on the top tubes and sheet-jet mode or jet takes place on the bottom ones. In this mode a small quantity (it may reach up to 10% of the liquid falling film) is observed to fall outside of the test tubes. This is due to hard hitting of the liquid with the tube.

As the falling film flow rate is reduced gradually, sheet-jet or jet mode takes place. The flow rate can be adjusted to get a steady jet mode as shown in figure (3.3). The flow covers the whole test tubes and the surface is wetted. A negligible quantity of the liquid splashes out of the test tubes. As the falling film flow rate decreases further, a jet-droplet or droplet is observed. Droplet mode is steady in flow and all the tubes are wetted.

The jet mode prevailed most of the experiments, and some experiments are carried out for droplets and sheet modes.

2-Ice formation starts to form at the bottom side of the tube. This is due to the fact that the falling film losses heat through the test tubes as it falls down until it reaches its freezing point. The ice formation reduces heat transfer at the bottom tubes rather than at the top

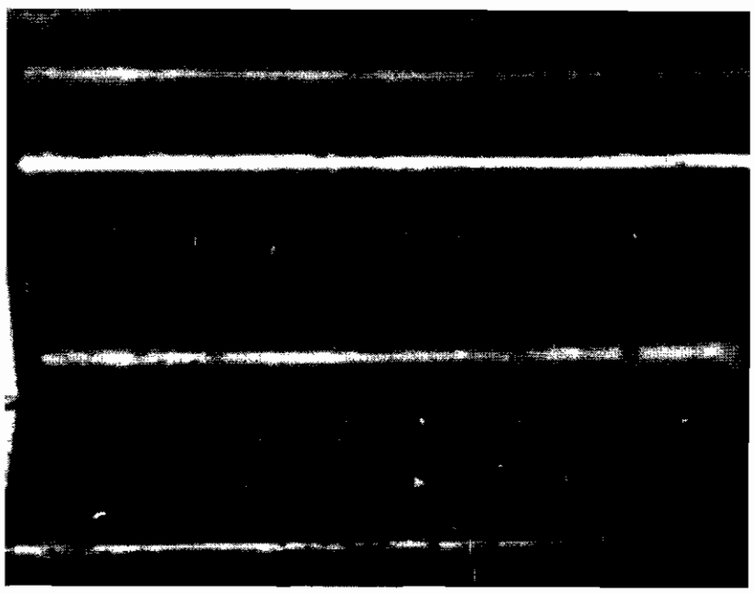

Figure 3.3: A steady jet mode is shown clearly at falling film flow, $\dot{m}_f$=0.025 kg/s.

especially in series arrangement. This increases the temperature difference between the falling film and the coolant at the upper tubes.

3- It has been noticed that the ice formation is more accumulated at the entrance of the coolant to the tube than the outlet (figure3.4) and gradually decreases as it gets further away from the entrance. This is due to the reduction of the coolant temperature a long the tube because of the heat transfer.

In addition, the formation of ice is more accumulated on the bottom tubes than in the upper tubes (figure3.5). This is because the falling film temperature is reduced as it flows down to the bottom test tubes. Moreover, in series arrangements the temperature at the bottom test tubes is much lower than in the upper tubes.

4-More ice accumulation is noticed at the bottom of the tube than its top, due to drag force of the water falling stream.

5-Ice formation on the first test tube is not regular in jet mode because it acts as an impact on the ice in the first test tube. Regularity is notified in the rest of the tubes, due to drag force. However, regularity is notified

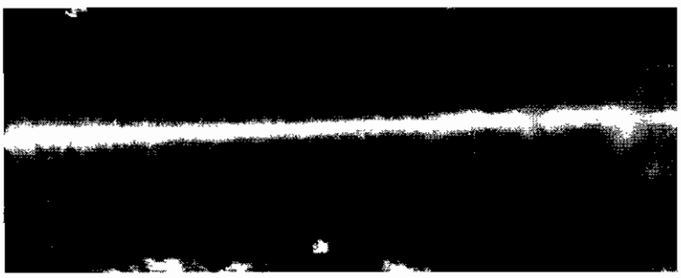

Figure 3.4: Distribution of ice accumulation on the test tube surface.

Figure 3.5: Ice accumulation for different tubes.

on the first test tube in sheet mode because the sheet covers the whole tube. Less regularity is notified in the droplet mode due to an increase in drag force.

6-Ice accumulates circumferentially on the test tubes surface until the tube spacing is filled by ice. The ice then increases by sides as shown in figure (3.5).

7-It is obvious that the formation of ice increases with time (see figures 3.6-3.9). However, the rate of formation is decreased with time due to an increase in the insulation of ice (increased thickness of ice causes an increase in thermal resistance and consequently reduction of heat transfer through ice layer).

8-It has been observed that as the ice accumulates on the test tubes, it takes longer time to remove it from the test tubes by the discharge cycle and relatively large quantity of ice is melted.

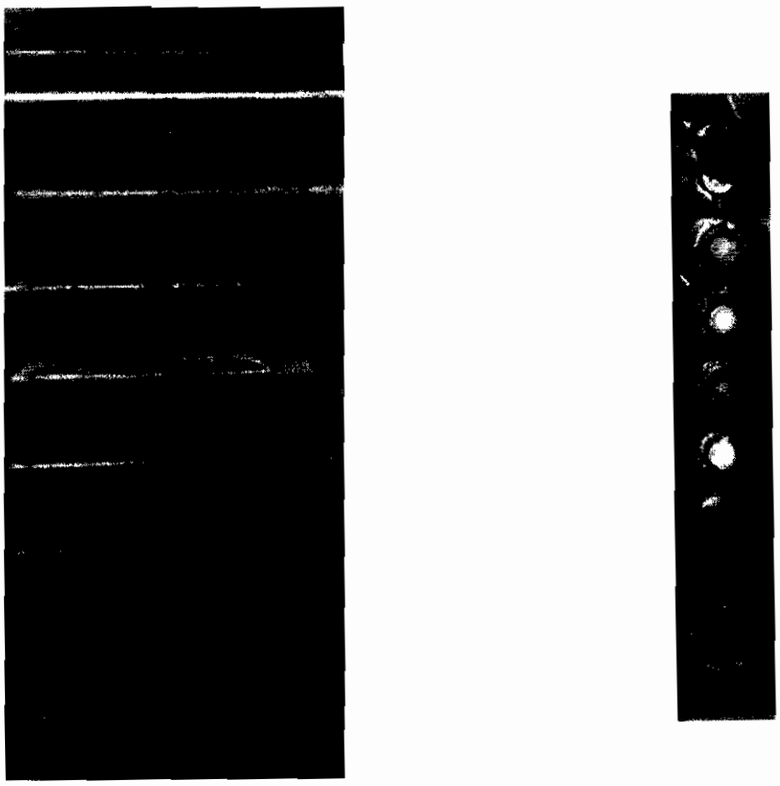

(a) front view (b) side view

Figure 3.6,Ice formation on the test tubes after 15 minutes, run 6(S) for $\dot{m}_c$=0.162 kg/s & $\dot{m}_i$=0.025 kg/s "Series arrangement, jet mode"

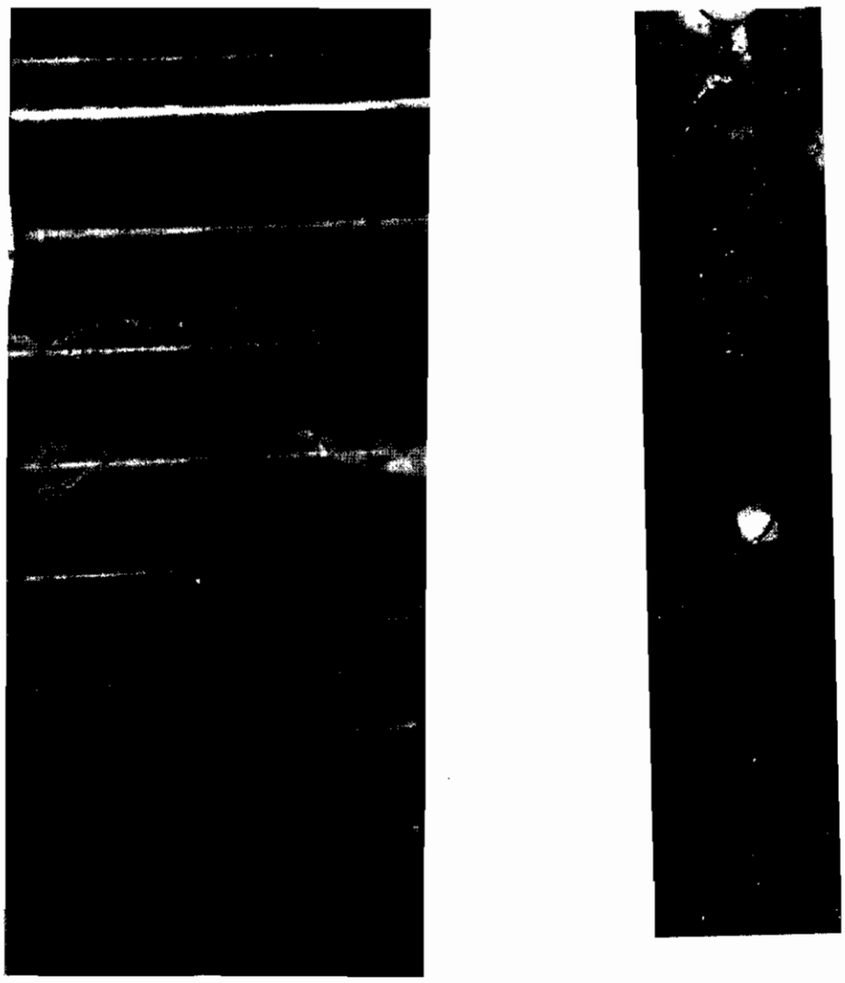

(a) front view (b) side view

Figure 3.7,Ice formation on the test tubes after 30 minutes, run 6(S) for $\dot{m}_c$=0.162 kg/s & $\dot{m}_1$=0.025 kg/s "Series arrangement, jet mode"

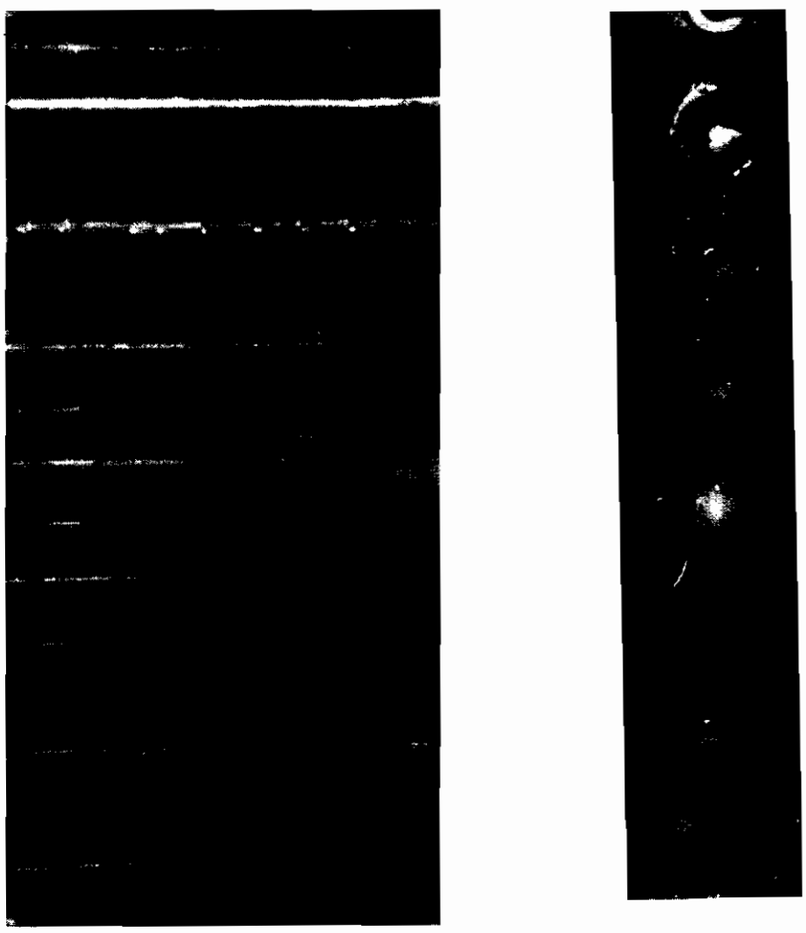

(a) front view (b) side view

Figure 3.8,Ice formation on the test tubes after 45 minutes, run 6(S) for $\dot{m}_c$=0.162 kg/s & $\dot{m}_l$=0.025 kg/s "Series arrangement, jet mode"

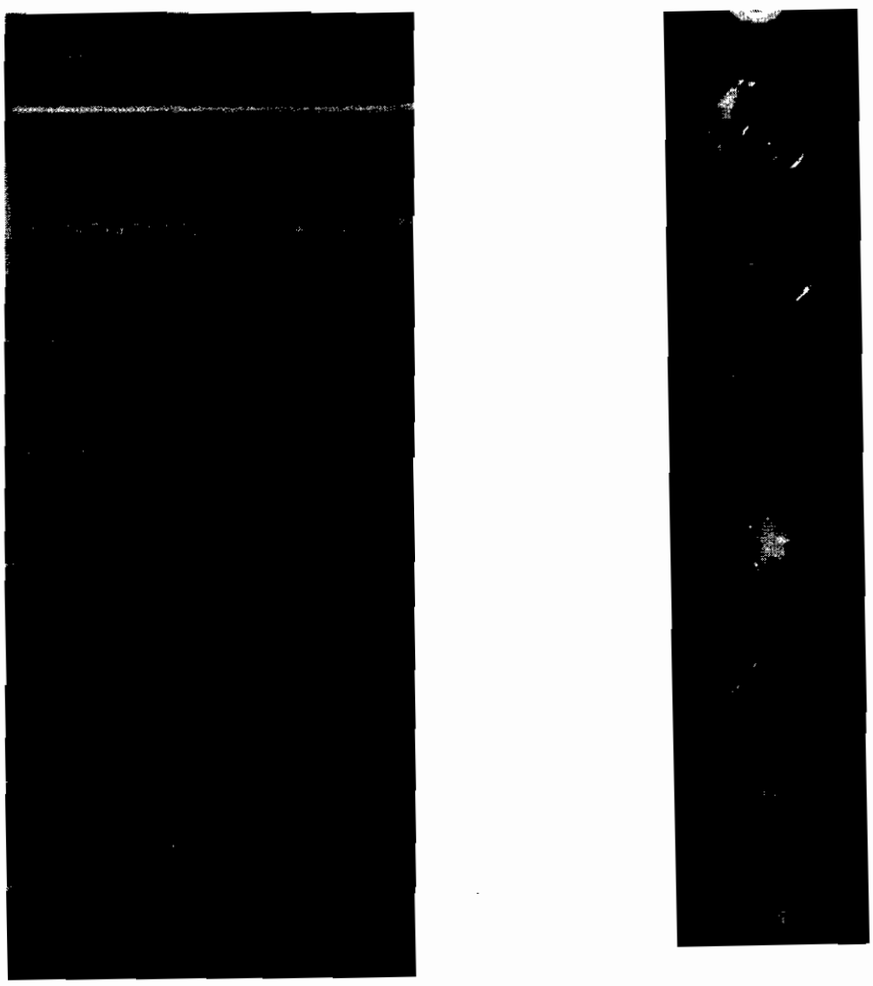

(a) front view (b) side view

Figure 3.9,Ice formation on the test tubes after 60 minutes, run 6(S) for $\dot{m}_c$=0.162 kg/s & $\dot{m}_l$=0.025 kg/s "Series arrangement, jet mode"

3.4 RESULTS

This section includes a sample calculation for a case study of 1(P). Also the rest of all results are given with discussion.

3.4-1 Experimental run 1(P):

This experimental run is carried out under the following conditions:

1-Parallel arrangement,jet mode

2-Falling film liquid: water

3-Room temperature: 23°C

4-Mass flow rate of coolant: 0.38 kg/s

5-Mass flow rate of the falling liquid: 0.025 kg/s

The results and calculations for this run are shown in Table (3.1). Such calculations are carried out using the equations outlined in section (3.1) and employing MS Excel Software. The following is an example for how the values in Table (3.1) were calculated.

For the 15 minutes run under the condition of Experimental run 1(P), the height of water level before and after the discharge cycle activated is recorded to get ice weight.

$\Delta h = 18$ mm

The volume of this quantity,

$V = \Delta h \, W \, l$, where

W : inside width of the supporting box

l : inside length of the supporting box

$V = 18 \times 235 \times 273 = 1154.8 \times 10^{-6}$ m^3

The mass of the formed ice:

$$M = V \times \rho$$

Where ρ is the density of the collected water [9],

$\rho = 1000$ kg/m^3

$M = (1154.8 \times 10^{-6}) \times 1000 = 1.155$ kg

Average ice thickness,c is:

$$c = \frac{V}{A_o}$$

A_o = total outside area of the test tubes:

$= 7(\pi D_{o,o} \, l)$

$= 7(\pi \, 0.0285 \times 0.235)$

$= 0.147$ m^2

$$c = \frac{1154.8 \times 10^{-6}}{0.147} = 7.86 \times 10^{-3} \text{ m} = 7.86 \text{ mm}$$

3.4-1.1 Energy balance:

The average rate of heat transfer from the test tubes to the coolant, $\dot{Q}_{c,ave}$, with losses is compared with the absorbed heat from the falling film, $\dot{Q}_{a,f}$, as follows:

From equation 3.1,

$$\dot{Q}_c = m_c C_{pc}(T_{co} - T_{ci})$$

$$= 0.38x3348.8x(-7.8-(-8.1))$$

$$= 381.76 \text{ W}$$

where, T_{co} and T_{ci} are taken from the recorded data from table B.1(Appendix B).

From equation (3.2),

$$\dot{Q}_{c,ave} = \left(\int_{t=0}^{t=n} \dot{Q}_c \, x \, dt \right) / time$$

where n is 15 minutes for this run and the values of $\dot{Q}_{c,n}$ are taken from table B.1.Then, applying trapezoidal rule:

$\dot{Q}_{c,ave} = 547.19$ W

The sensible cooling rate of the falling film, $\dot{Q}_{s,l}$, is evaluated from equation 3.5:

$$\dot{Q}_{s,l} = \dot{m}_l C_{pl}(T_{li} - T_{lo})$$

$$= 0.025x4200x(0.3-0)$$

$$= 31.5 \text{ W}$$

From equation 3.6 the rate of heat transfer which contributes to freezing, $\dot{Q}_{fr}$, is:

$$\dot{Q}_{fr} = \frac{M_{ice}L}{Time}$$

Where L = 335 kJ/kg

$$\dot{Q}_{fr} = \frac{1.155x335x10^3}{(15x60)} = 429.91 \text{ W}$$

The average subcooling rate of ice, $\dot{Q}_{s,s}$,is calculated as follows:

$$\dot{Q}_{s,s} = \frac{M_{ice}\, C_{pice}\, (T_f - T_c/2)}{Time}$$

$$= \frac{1.155x\ 2040x(0-(-7.9)/2)}{15x60}$$

$$= 10.34 \text{ W}$$

Loss from the falling film due to convection, $\dot{Q}_{ls}$, is:

$$\dot{Q}_{ls,c} = h_c\, A_l\, (T_\infty - T_l)$$

h_c :the heat transfer coefficient due free convection is approximated to be = 10 $W/m^2.K$ [12]

A_l : area which is covered by the falling film is:

$$A_l = l \; h$$

h = height of the falling film which covers the test tubes and the spaces between them:

= 0.3705 m

A_l = 0.235x0.3705x2 =0.174 m^2

$\dot{Q}_{ls,c}$ = 10x0.175x(15-0.15)

$= 26.12$ W

Then , the absorbed heat from the falling film, $\dot{Q}_{a,f}$, is :

$$\dot{Q}_{a,f} = \dot{Q}_{s,l} + \dot{Q}_{fr} + \dot{Q}_{s,s}$$

$$= 31.5 + 429.91 + 10.34$$

$$= 471.75 \text{ W}$$

The prcentage ratio, ε, of the absorbed heat from the falling film, $\dot{Q}_{a,f}$ to the average rate of heat transfer from the test tubes to the coolant , $\dot{Q}_{c,ave}$, and, is given by equation 3.9:

$$\varepsilon = \frac{\dot{Q}_{a,f}}{\dot{Q}_{c,ave}}$$

$$\varepsilon = \frac{471.75}{547.19}$$

$$= 0.86$$

<u>The experimental overall heat transfer coefficient:</u>

The experimental overall heat transfer coefficient, h_{ov}, is obtained from equation 3.10 as:

$$h_{ov} = \frac{\dot{Q}_{a,f}}{A_{ice}(T_l - T_c)}$$

A_{ice} = total surface area of the ice is:

$$A_{ice} = 7\pi(D_{o,o} + 2\ c)\ l$$

$$= 7\pi(0.0285 + 2 \times 7.86 \times 10^{-3}) \times 0.235$$

$$= 0.228 \text{ m}^2$$

$T_o = (T_{ci} + T_{co})/2 = (-8.1+(-7.7))/2 = -7.9\ °C$

$T_l = (0.3+0)/2 = 0.15\ °C$

$T_l - T_c = 8.05$

$$h_{ov} = \frac{471.75}{0.228\ (8.05)}$$

$$= 257.03\ W/m^2.K$$

<u>The calculated heat transfer rat from the test tubes to the coolant:</u>

To verify the experimental work, the rate of heat transfer from the test tubes to the coolant at a specific ice thickness, $\dot{Q}_c$, is compared with the calculated one, $\dot{Q}_{c,cal}$, at that thickness.

From equation, 3.4

$$\dot{Q}_{c,cal} = U\ A\ (T_l - T_c)$$

Where:

$$\frac{1}{UA} = \frac{1}{h_i\ \pi\ D_{i,o}\ /} + \frac{\ln(D_{o,o}/D_{i,o})}{2\ \pi k_c\ /} + \frac{\ln(D_{ice}/D_{o,o})}{2\ \pi k_{ice}\ /} + \frac{1}{h_o\ \pi\ D_{ice}\ /}$$

<u>Heat transfer coefficient inside the tube:</u>

Using equation 1.15 the inside heat transfer coefficient is:

$$h_i = \frac{Nu\ k}{D_h}$$

Where:

D_h = Equivalent Diameter = $4\ A_i\ /\ \pi(D_{i,o} + D_{o,i})$

A_i = Inside cross sectional area, figure 3.2, is

$$A_i = \frac{\pi\,(D_{i,o}^2 - D_{o,i}^2)}{4}$$

$$= \frac{\pi(0.0265^2 - 0.0158^2)}{4}$$

$$= 3.55\text{x}10^{-4}\ m^2$$

$D_h = 4\text{x}3.55\text{x}10^{-4}/\ \pi\,(0.0265+0.0158) = 0.0107$ m

In order to get Nu, Re must be calculated to select the suitable equation,

$$Re = \frac{\rho\, u_m\, D_h}{\mu}$$

Velocity of the coolant at the test tube, u_m is:

$$u_m = \dot{m}_c\ /\rho A_i$$

$\dot{m}_c$ = mass flow rate of the coolant which enters to the test section = 0.38 kg/s

The average mass flow rate in each test tube = 0.38/7

= 0.0543 kg/s

Then,

$u_m = 0.0543/(1060\text{x}0.000355) = 0.144$ m/s

From equation 1.14

$$Re_c = \frac{1060\,(0.144)\,(0.0107)}{0.008} = 204.52$$

From equation 1.9, it is indicated that the flow is laminar and its Nusselt number is determined from equation 1.12:

$$Nu = 1.86 \left(\frac{Re\ Pr}{//D_h} \right)^{1/3} \left(\frac{\mu}{\mu_s} \right)^{0.14}$$

Where μ=0.008 N.s/m at a coolant temperature -8°C and μ_s=0.0065 N.s/m at surface temperature -5.5°C

$(\mu / \mu_s)^{0.14} = 1.03$

$Pr = C_p\mu/k = 3348.8x0.008/0.4671 = 57.35$

$$Nu = 1.86\left(\frac{204.52x57.35}{0.235/0.0107} \right)^{(1/3)} \left(\frac{0.008}{0.0065} \right)^{0.14}$$

$= 15.53$

from equation 1.15

$$h_i = \frac{15.53x0.4671}{0.0107} = 678.39\ W/m^2.K$$

<u>Heat transfer Coefficient outside the tube</u>

The outside heat transfer coefficient is calculated using equation (1.18)

$$h_o = \frac{Nu\ k}{(\nu^2/g)^{1/3}}$$

Since the falling film shows a jet mode on most test tubes equation (1.16) is used to calculate Nusselt number:

$$Nu = 1.378 Re_f^{0.42} Pr^{0.26} Ar^{(-0.23)} (s/d)^{0.08}$$

Where s/d = 1 in the existed setup

Re_f, Pr and Ar values are computed using equations 1.19,1.120 and 1.21 respectively.

$Re_f = 2\Gamma/\mu$

$\dot{m}_l$ = The flow rate of the falling film = 0.025 kg/s

$\Gamma = 0.025/0.235 = 0.1064$ kg/s.m

$Re_f = 2x0.106/(1750x10^{-6}) = 121.58$

$Pr = C_p\mu/k = 4216x1750x10^{-6}/0.569 = 12.96$

$Ar = d_{ice}^3 g/\nu^2 = (0.04416^3)(9.81)/(1.79x10^{-6})^2 = 26.36x10^7$

Then,

$Nu = 1.378(121.6)^{0.42}(12.96)^{0.26}(26.36x10^7)^{-0.23}$

$= 0.233$

$$h_o = \frac{Nu\ k}{(\nu^2/g)^{1/3}} = \frac{0.215x0.569}{(1.79x10^{-6})^2/9.81)^{1/3}} = 1922.2\ W/m^2.K$$

The overall heat transfer coefficient can be obtained from equation 3.3,

$$UA = \frac{1}{R_1 + R_2 + R_3 + R_3}$$

$R_1 = 1/(h_i\ \pi\ D_{i,o}\ell) = 1/(678.39x3.14x0.0265x0.235) = 0.075$ K/W

The thermal resistance of the copper tube(k_c=405 W/m.K,[9]) is calculated using equation (1.2)

$$R_2 = \frac{\ln(D_{o,o}/D_{i,o})}{2\pi k_c /} = \frac{\ln[28.5/26.5]}{2x3.14x405x0.235} = 1.21x10^{-4}\ K/W$$

The thermal resistance of the iced layer is calculated using equation (1.2)

$$R_3 = \frac{\ln(D_{ice}/D_{o,o})}{2\pi k_{ice} /} = \frac{\ln[2(14.25+7.83)/28.5]}{2x3.14x1.88x0.235} = 0.158\ K/W$$

$R_4 = 1/(h_o \pi D_{ice} /) = 1/(1922.2x3.14x.0.04416x0.235)$

$= 0.016$ K/W

It is clear that R_2 is smaller than all the other resistances and can be neglected. In this current study R_2 has been taken to be zero.

$$UA = \frac{1}{0.075 + 0.158 + 0.016} = \frac{1}{0.249}$$

$= 4.016$ W/K

Then, the calculated rate of heat transfer to the coolant for the seven test tubes, $\dot{Q}_{c,cal}$:

$\dot{Q}_{c,cal} = 7x4.016x8.05 = 226.3$ W

From equation 3.13, losses in test section are calculated to overcome the error that may exist in measuring temperature especially for small ΔT_c.

$\dot{Q}_{ls} = m_c C_{pc}(T_{co} - T_{ci})$

$= 0.38x3348.8x(-8-(-8.1)) = 127.25$ W

where T_{co} and T_{ci} for no falling film are -8 and-8.1°C respectively.

$\dot{Q}_{c,act} = \dot{Q}_c - \dot{Q}_{ls} = 381.76-127.25 = 254.51$ W

The percentage difference is then calculated as follows:

$$\text{Percentage difference, P.D} = \left(\frac{\dot{Q}_{c,act} - \dot{Q}_{c,cal}}{\dot{Q}_{c,act}} \right) x100$$

$$= \left(\frac{254.51 - 226.3}{254.51} \right) X100 = 11.08\%$$

3.4-1.2 Error analysis:

Relative error in the overall heat transfer coefficient, h_{ov} is:

$$\frac{\Delta h_{ov}}{h_{ov}} = \frac{\Delta \dot{Q}_{a,f}}{\dot{Q}_{a,f}} + \frac{\Delta A_{ice}}{A_{ice}} + \left(\frac{(\Delta T_l + \Delta T_c)_r}{(T_l - T_c)} + \frac{(\Delta T_l + \Delta T_c)_{fl}}{(T_l - T_c)} \right)$$

Where subscript $_r$ and $_{fl}$ refer to error in reading and fluctuation respectively

For the 15 minutes run in experimental run 1P:

The error in the absorbed heat from the falling film, $\dot{Q}_{a,f}$ is:

$$\Delta \dot{Q}_{a,f} = \Delta \dot{Q}_{s,l} + \Delta \dot{Q}_{fr} + \Delta \dot{Q}_{s,s}$$

The relative error in $\dot{Q}_{s,l}$ is:

$$\frac{\Delta \dot{Q}_{s,l}}{\dot{Q}_{s,l}} = \frac{\Delta m_l}{m_l} + \frac{\Delta C_p}{C_p} + \left(\frac{(\Delta T_{ll} + \Delta T_{lo})_r}{T_{li} - T_{lo}} + \frac{(\Delta T_{ll} + \Delta T_{lo})_{fl}}{T_{li} - T_{lo}} \right)$$

$$= \frac{0.006}{0.025} + 0 + \frac{0.1+0.1}{0.5-0} + \frac{0.1 + 0.1}{0.5-0}$$

$$= 1.04$$

$$\Delta\dot{Q}_{s,l} = 1.04(31.5)$$

$$= 32.76 \text{ W}$$

The relative error in $\dot{Q}_{fr}$ is:

$$\frac{\Delta \dot{Q}_{fr}}{\dot{Q}_{fr}} = \frac{\Delta M_{ice}}{M_{ice}} + \frac{\Delta t}{t} + \frac{\Delta L}{L}$$

$$\frac{\Delta M_{ice}}{M_{ice}} = \frac{\Delta(\Delta h)}{\Delta h} + \frac{\Delta w}{w} + \frac{\Delta l}{l}$$

$$= \frac{1+1}{18} + \frac{1}{273} + \frac{1}{235}$$

$$= 0.1188$$

$$\frac{\Delta t}{t} = \frac{1}{15x60} = 0.0011$$

$$\Delta \dot{Q}_{fr} = 429.8(0.1188+0.0011+0) = 51.53 \text{ W}$$

The relative error in $\dot{Q}_{s,s}$ is:

$$\frac{\Delta \dot{Q}_{s,s}}{\dot{Q}_{s,s}} = \frac{\Delta M_{ice}}{M_{ice}} + \frac{\Delta t}{t} + \frac{(\Delta T_f + \Delta T_c/2)_r}{T_f - T_c/2}$$

$$\Delta T_c = \frac{(\Delta T_{ci} + \Delta T_{co})_r}{2} + \frac{(\Delta T_{ci} + \Delta T_{co})_{fl}}{2} = \frac{0.1+0.1}{2} + \frac{0.1+0.1}{2} = 0.2$$

$$\frac{\Delta \dot{Q}_{s,s}}{\dot{Q}_{s,s}} = 0.1188 + \frac{0 + 0.2/2}{0 - (-7.9)/2}$$

$$\Delta \dot{Q}_{s,s} = 10.34(0.1188+0.0253) = 1.489 \text{ W}$$

So, the error in the absorbed heat from the falling film is:

$$\Delta \dot{Q}_{a,f} = 32.76 + 51.53 + 1.489 = 85.78 \text{ W}$$

and the relative error is:

$$\frac{\Delta \dot{Q}_{a,f}}{\dot{Q}_{a,f}} = \frac{85.78}{471.68} = 0.18$$

The relative error in total surface area of ice, A_{ice} is:

$$\frac{\Delta A_{ice}}{A_{ice}} = \frac{(\Delta D_{o,o} + 2\Delta c)}{D_{o,o} + 2c} + \frac{\Delta l}{l}$$

$$\frac{\Delta c}{c} = \frac{\Delta(\Delta h)}{\Delta h} + \frac{\Delta w}{w} + \frac{\Delta D_{o,o}}{D_{o,o}}$$

$$= \frac{1+1}{18} + \frac{1}{273} + \frac{0.1}{28.5}$$

$$\Delta c = 7.84\ (0.1182) = 0.93 \text{ mm}$$

$$\frac{\Delta A_{ice}}{A_{ice}} = \frac{0.1 + 2(0.93)}{28.5 + 2(7.84)} + \frac{1}{235}$$

$$= 0.0486$$

Error in temperature difference between falling film and the coolant:

$$\left(\frac{(\Delta T_l + \Delta T_c)_r}{T_l - T_c} + \frac{(\Delta T_l + \Delta T_c)_{fl}}{T_l - T_o} \right) =$$

$$\Delta T_l = \frac{(\Delta T_{li} + \Delta T_{lo})_r}{2} + \frac{(\Delta T_{li} + \Delta T_{lo})_{fl}}{2} = \frac{0.1+0.1}{2} + \frac{0.1 + 0.1}{2} = 0.2$$

$$\Delta T_c = \frac{(\Delta T_{ci} + \Delta T_{co})_r}{2} + \frac{(\Delta T_{ci} + \Delta T_{co})_{fl}}{2} = \frac{0.1+0.1}{2} + \frac{0.1 + 0.1}{2} = 0.2$$

$$\left(\frac{\Delta T_l + \Delta T_c}{T_l - T_c} \right)_{r+fl} = \frac{0.2 + 0.2}{0.25 - (-7.9)} = 0.049$$

So, the relative error in the experimental overall heat transfer coefficient is:

$$\frac{\Delta h_{ov}}{h_{ov}} = 0.18 + 0.0486 + 0.049 = 0.278 = 27.8\%$$

Table (3.1): Energy balance analysis, at m_c=0.38 kg/s & m_f=0.025 kg/s "Parallel arrangement, jet mode"

	Run# 1	Run#2	Run#3	Run#4	Run#5	Run#6	Run#7	Run#8	Run#9	Run#10
t(min)	0.25	5	10	15	20	25	30	45	60	80
Δh(cm)		0.7	1.3	1.8	2.4	3	3.5	4.8	5.9	6.4
$Vx10^{-6}(m^3)$	27	449	834	1155	1540	1925	2245	3079	3785	4106
M(Kg)	0.03	0.45	0.83	1.155	1.54	1.92	2.25	3.08	3.79	4.11
c (mm)	0.18	3.05	5.67	7.86	10.46	13.07	15.25	20.92	25.71	27.89
$\Delta T_c(^oC)$	0.60	0.40	0.40	0.30	0.30	0.30	0.30	0.20	0.20	0.20
Q_c(W)	763.53	509.02	509.02	381.76	381.76	381.76	381.76	254.51	254.51	254.51
$Q_{c,ave}$(W)	763.53	636.27	598.09	547.19	531.29	514.00	494.17	463.77	422.06	391.31
$Q_{s,l}$ (W)	31.50	31.50	31.50	31.50	31.50	31.50	31.50	31.50	31.50	31.50
Q_{fr}(W)	603.00	501.48	465.66	429.91	429.84	429.84	417.90	382.08	352.23	286.56
$Q_{s,s}$ (W)	14.50	12.06	11.20	10.34	10.34	10.34	10.05	9.19	8.47	6.89
$Q_{ls,c}$ (W)	26.12	26.12	26.12	26.12	26.12	26.12	26.12	26.12	26.12	26.12
$Q_{s,f}$ (W)	649.00	545.04	508.36	471.75	471.68	471.68	459.45	422.77	392.20	324.95
$\varepsilon = Q_{s,f}/Q_{c,ave}$	0.85	0.86	0.85	0.86	0.89	0.92	0.93	0.91	0.93	0.83
$T_i - T_c$ (^oC)	8.15	8.15	8.15	8.05	8.15	8.18	8.30	8.15	8.15	8.15
h_{ov}(W/m^2.K)	534.07	374.18	303.18	257.03	226.73	204.28	181.62	142.78	116.57	91.59
Re_c	204.53	204.53	204.53	204.53	204.53	204.53	204.53	204.53	204.53	204.53
$(\mu/\mu_s)^{0.14}$	1.070	1.038	1.032	1.030	1.025	1.022	1.020	1.017	1.016	1.010
h_i(W/m^2.K)	704.89	683.81	679.86	678.39	675.25	673.27	671.95	669.98	669.32	665.37
Re_f	121.58	121.58	121.58	121.58	121.58	121.58	121.58	121.58	121.58	121.58
h_o(W/m^2.K)	2578.6	2275.6	2065.0	1922.2	1779.4	1660.1	1574.5	1394.8	1277.1	1231.1
R_1(K/W)	0.073	0.075	0.075	0.075	0.076	0.076	0.076	0.076	0.076	0.077
R_3(ice) (K/W)	0.005	0.070	0.121	0.158	0.198	0.235	0.262	0.326	0.372	0.391
R_4(K/W)	0.018	0.017	0.016	0.016	0.015	0.015	0.015	0.014	0.013	0.013
UA(W/K)	10.49	6.18	4.71	4.016	3.45	3.07	2.83	2.41	2.17	2.08
$Q_{c,cal}$ (W)	598.23	352.35	268.67	226.3	197.04	175.25	161.62	137.22	123.66	118.68
$Q_{c,act}$ (W)	636.27	381.76	381.76	254.51	254.51	254.51	254.51	127.25	127.25	127.25
P.D= $\frac{(Q_{c,act}-Q_{c,cal})}{Q_{c,act}}$x100	5.979	7.706	29.625	11.08	22.579	31.142	36.497	-7.833	2.825	6.741

The results of such experimental run are also shown in figures (3.10 to 3.15). Figure (3.10) shows that the coolant temperature difference $\Delta T_c=(T_{co}-T_{ci})$ is small as expected, due to the high flow rate and the low coolant velocity in the test tubes. The temperature difference decreases with time as ice accumulates on the test tubes. It decreases rapidly from 0.6 to 0.4°C and gradually from 0.4 to 0.2°C. Further accumulation of ice on the test tubes increases its thermal resistance, and causes the rate of heat transfer from the test tubes to the coolant $\dot{Q}_c$ to decrease as shown in figure (3.11). The ice formation increases gradually up to 2.2 kg in 30 minutes, and slightly in the following period up to 4.1 kg in 80 minutes as shown in figure (3.12). The rate of ice formation also decreases with time. The experimental overall heat transfer coefficient, h_{ov}, decreases as ice thickness increases as shown in figure(3.13). Figure (3.14) shows the energy balance of this case of study. It indicates that the average rate of heat transfer from the test tubes to the coolant, $\dot{Q}_{c,ave}$ is approximately close to the absorbed heat from the falling film, $\dot{Q}_{a,f}$. The ratio ε, of $\dot{Q}_{a,f}$ to $\dot{Q}_{c,ave}$ is about 0.86 which is considered reasonable.The remaining is due to losses,which is limited by careful insulation of the test section. Figure (3.15) indicates that the actual heat

transfer from the test tubes to the coolant, $\dot{Q}_{c,act}$ shows the same trend as the calculated one, $\dot{Q}_{c,cal}$. The average percentage difference between $\dot{Q}_{c,act}$ and $\dot{Q}_{c,cal}$ is about 16%. This is may be due to an accuracy in the measurement of T_{ci} & T_{co}, the assumptions used in the theoretical equations (inside and outside heat transfer coefficient, hi and h_o) and the assumption of the ice formation increases circularly.

This case of study, yields a reasonable amount of ice (3.8kg/hr), however, ΔT_c is between 0.6 and 0.2°C due to high flow rate (0.38 kg/s) and low velocity inside the test tubes (0.144 m/s). As a result, an error in reading thermocouples may cause a relatively high error in the results as it has been appeared in this case of study. So, the flow rate is reduced in the following run to increase the temperature difference ΔT_c.

3.4-2 Experimental run 2(P):

This experimental run is carried out under the following conditions:

1-Parallel arrangement, jet mode

2-Falling film liquid: water

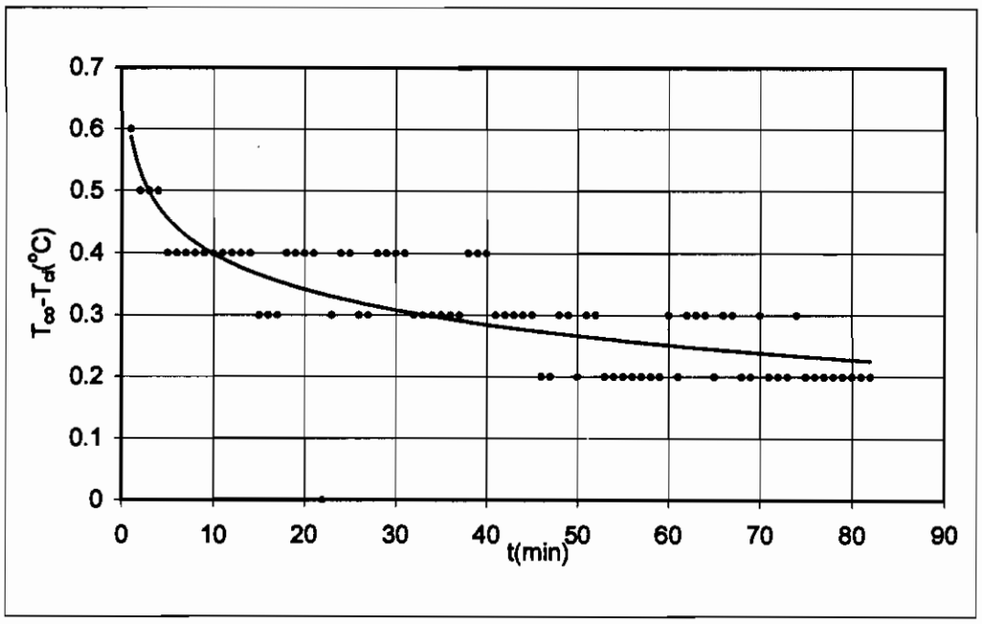

Figure 3.10: Change of ΔT_c with time for $\dot{m}_c$ = 0.38 kg/s & $\dot{m}_j$=0.025 kg/s "parallel arrangement, jet mode"

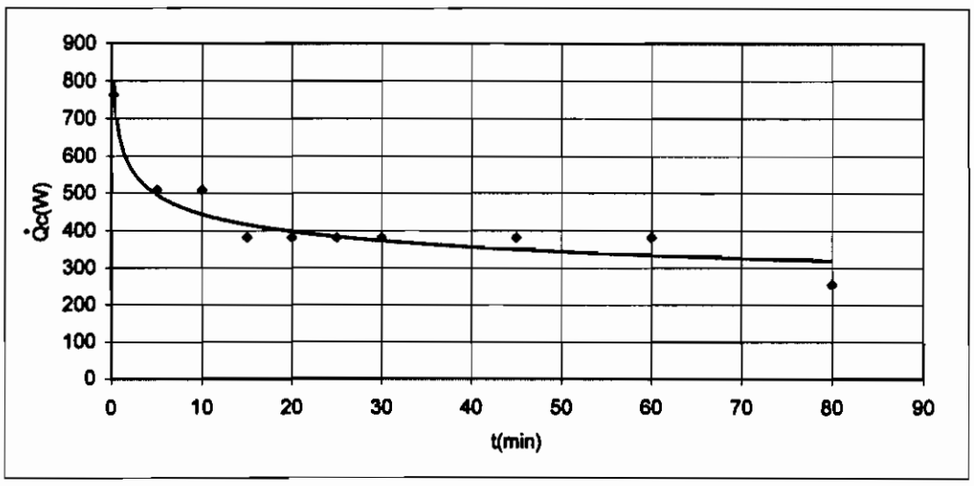

Figure 3.11: Variation of the rate of heat transfer from the test tubes to the coolant with time for $\dot{m}_c$ =0.38kg/s & $\dot{m}_j$=0.025 kg/s "parallel arrangement, jet mode"

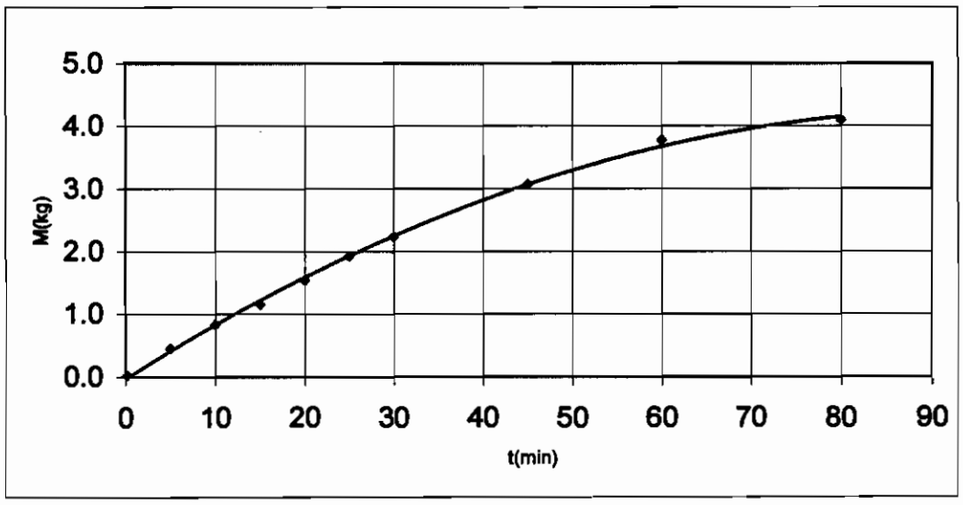

Figure 3.12:Variation of the formed ice on the test tubes with time for $\dot{m}_c$=0.38 kg/s & $\dot{m}_l$=0.025 kg/s "parallel arrangement, jet mode"

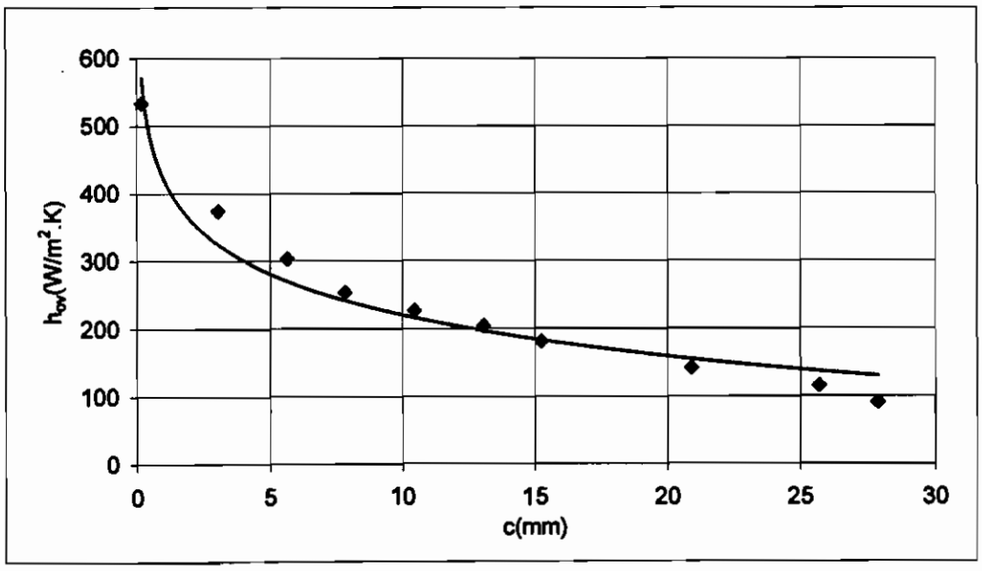

Figure 3.13: Variation of the experimental overall heat transfer coefficient with ice thickness for $\dot{m}_c$ =0.38 kg/s & $\dot{m}_l$=0.025 kg/s "parallel arrangement,jet mode"

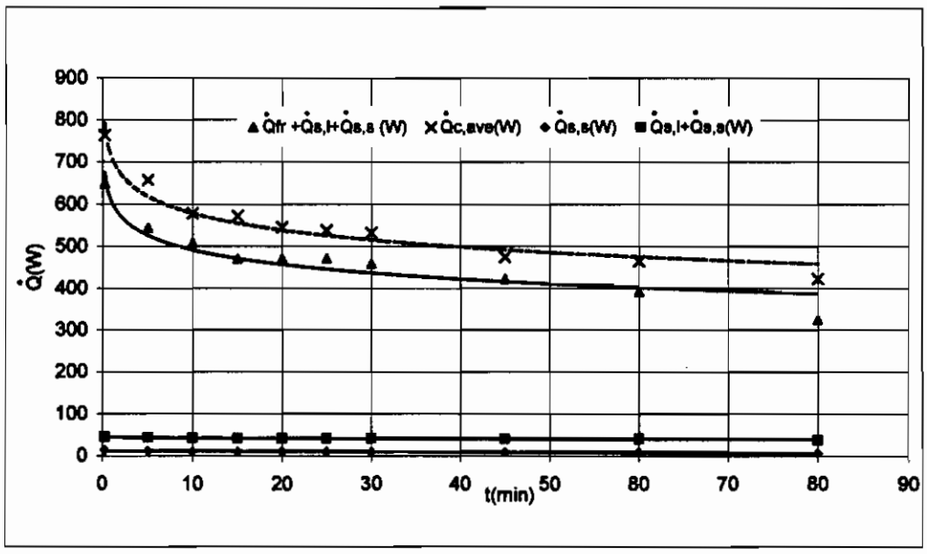

Figure 3.14:Energy balance for $\dot{m}_c$=0.38 kg/s & $\dot{m}_l$=0.025 kg/s "parallel arrangement, jet mode"

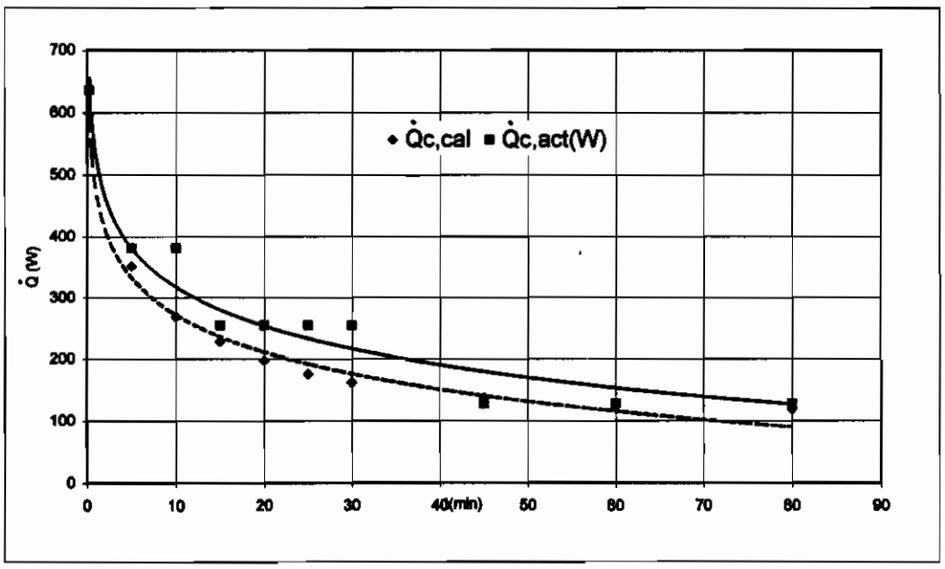

Figure 3.15:Comparison between actual and calculated rate of heat transfer from the test tubes to the coolant for $\dot{m}_c$=0.38 kg/s& $\dot{m}_l$=0.025 kg/s "parallel arrangement, jet mode"

3-Room temperature: 23°C

4-Mass flow rate of coolant :0.162 kg/s

5-Mass flow rate of the falling liquid:0.025 kg/s

Calculations and energy balance for this run are shown in table (3.2). The results of such experimental run are also shown in figures (3.16 to 3.20). In this experimental run, the change of ΔT_c starts from 1.1°C down to 0.4°C.In comparison with run 1(P), in which the temperature difference varies in the range (0.6°C to 0.2°C), errors in temperature measurements may be less effective on the results (Figure 3.16). However, the quantity of the ice formed is reduced due to reduction of the inside heat transfer coefficient (figure 3.17). The experimental overall heat transfer coefficient is less than that of run 1(P) as shown in figure (3.18). A reasonable energy balance is shown in figure (3.19). Comparison between actual $\dot{Q}_{c,act}$ and calculated $\dot{Q}_{c,cal}$ rate of heat transfer from the test tubes to the coolant is shown in figure (3.20). Although, curve of $\dot{Q}_{c,cal}$ is above curve of $\dot{Q}_{o,act}$ the two curves show the same trend with small percentage error.

Table (3.2): Energy balance analysis, at $\dot{m}_c$=0.162kg/s & $\dot{m}_j$=0.025kg/s "Parallel arrangement, jet mode"

	Run#1	Run#2	Run#3	Run#4	Run#5	Run#6	Run#7	Run#8	Run#9	Run#10
t(min)	0.25	5	10	15	20	25	30	45	60	80
Δh(cm)	0.28	0.6	0.9	1.4	1.6	2	2.2	3.1588	3.7906	4.5
$Vx10^{-6}(m^3)$	22	383	575	894	1022	1278	1405	2000	2400	2875
M(Kg)	0.02	0.38	0.57	0.89	1.02	1.28	1.41	2.00	2.40	2.87
c (mm)	0.15	2.64	3.96	6.16	7.04	8.80	9.68	13.78	16.54	19.81
$\Delta T_c(^oC)$	1.1	0.8	0.7	0.6	0.6	0.6	0.6	0.5	0.5	0.4
$\dot{Q}_c$(W)	596.76	434.00	379.75	325.50	325.50	325.50	325.50	271.25	271.25	217.00
$\dot{Q}_{c,ave}$(W)	596.76	494	420	401	369	346	340	333	320	302
$\dot{Q}_{s,i}$ (W)	31.50	31.50	31.50	31.50	31.50	31.50	31.50	31.50	31.50	31.50
$\dot{Q}_{fr}$(W)	488.40	427.27	320.45	332.32	284.85	284.85	261.11	246.67	222.00	200.28
$\dot{Q}_{s,s}$ (W)	14.96	13.09	9.82	10.18	8.73	8.73	8.00	7.56	6.80	6.13
$\dot{Q}_{ls,c}$(W)	26.12	26.12	26.12	26.12	26.12	26.12	26.12	26.12	26.12	26.12
$\dot{Q}_{a,f}$ (W)	534.86	471.86	361.77	374.00	325.07	325.07	300.61	285.72	260.30	237.92
$\varepsilon = \dot{Q}_{a,f}/\dot{Q}_{c,ave}$	0.90	0.96	0.86	0.93	0.88	0.94	0.88	0.86	0.81	0.79
$T_i - T_c$ (^oC)	10.00	10.00	10.00	10.00	10.00	10.00	10.00	10.00	10.00	10.00
h_{ov}(W/m^2.K)	359.50	269.35	191.55	176.67	147.22	135.98	121.12	98.67	81.85	67.38
Re_c	87.6	87.6	87.6	87.6	87.6	87.6	87.6	87.6	87.6	87.6
$(\mu/\mu_s)^{0.14}$	1.070	1.040	1.035	1.030	1.028	1.026	1.025	1.022	1.018	1.010
h_i(W/m^2.K)	531.38	516.48	513.99	511.51	510.52	509.53	509.03	507.54	505.55	501.58
Re_f	121.60	121.60	121.60	121.60	121.60	121.60	121.60	121.60	121.60	121.60
h_o(W/m^2.K)	2582.7	2312.6	2195.2	2028.5	1970.1	1864.7	1817.0	1625.5	1520.2	1423.7
R_1(K/W)	0.096	0.099	0.099	0.100	0.100	0.100	0.100	0.101	0.101	0.102
R_3(ice) (K/W)	0.004	0.062	0.089	0.130	0.145	0.174	0.187	0.246	0.281	0.315
R_4(K/W)	0.018	0.017	0.017	0.016	0.016	0.016	0.016	0.015	0.014	0.014
UA(W/K)	8.46	5.62	4.87	4.06	3.82	3.45	3.29	2.77	2.52	2.32
$\dot{Q}_{c,cal}$ (W)	592	394	341	284	268	241	231	194	177	162
$\dot{Q}_{c,act}$ (W)	488.26	325.50	271.25	217.00	217.00	217.00	217.00	162.75	162.75	108.50
$P.D = \frac{(\dot{Q}_{c,cal} - \dot{Q}_{c,act})}{\dot{Q}_{c,cal}} \times 100$	17.505	17.291	20.497	23.644	18.919	10.080	5.91	16.01	7.89	33.224

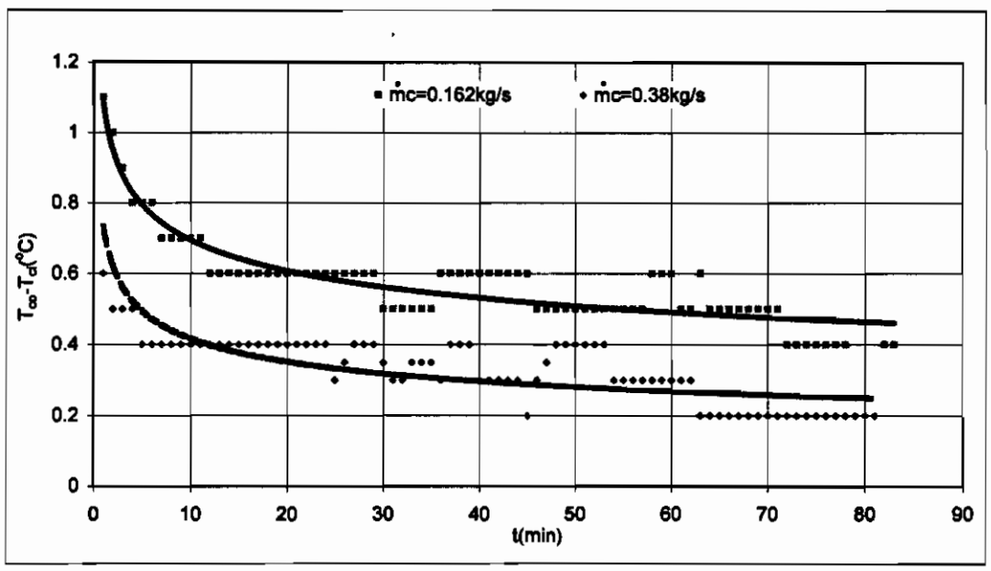

Figure 3.16: Comparison of ΔT_c changing with time between $\dot{m}_c$=0.162 kg/s & $\dot{m}_c$ =0.38 kg/s for $\dot{m}_j$=0.025 kg/s "parallel arrangement, jet mode"

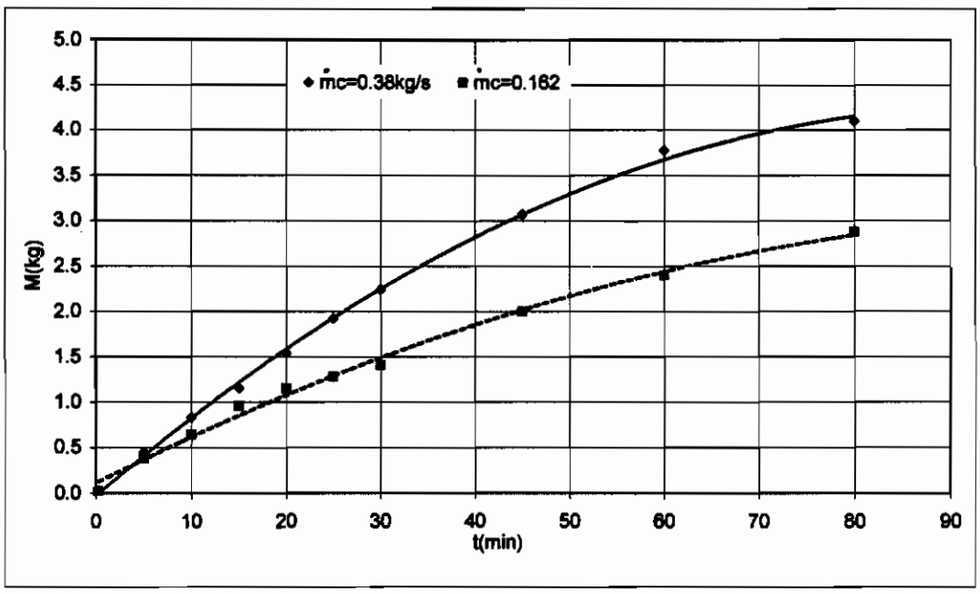

Figure 3.17: Comparison of the formed ice between $\dot{m}_c$ = 0.162 kg/s & $\dot{m}_c$ =0.38 kg/s for $\dot{m}_l$=0.025 kg/s "Parallel arrangement, jet mode"

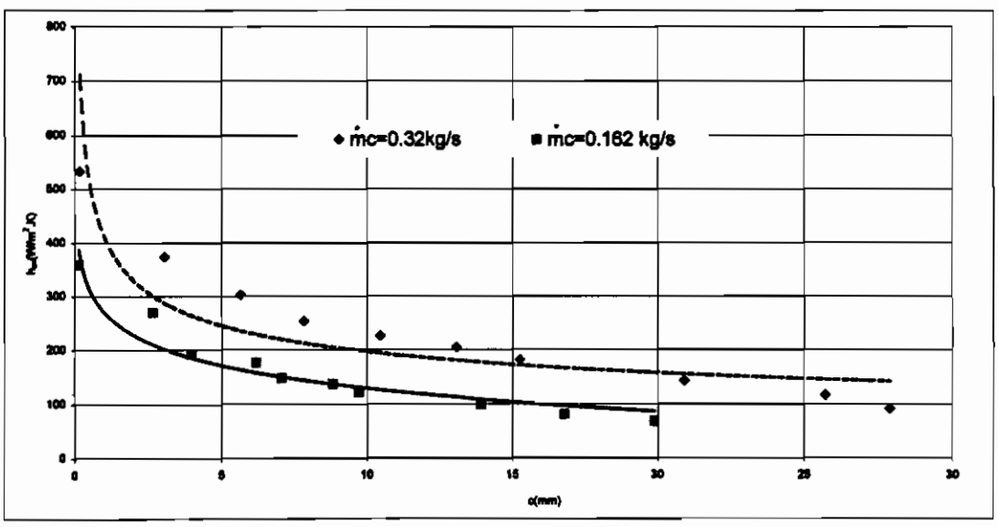

Figure 3.18:Comparison of the experimental overall heat transfer coefficient between $\dot{m}_c$ =0.162 kg/s & $\dot{m}_c$ = 0.38 kg/s for $\dot{m}_l$=0.025 kg/s "parallel arrangement, jet mode"

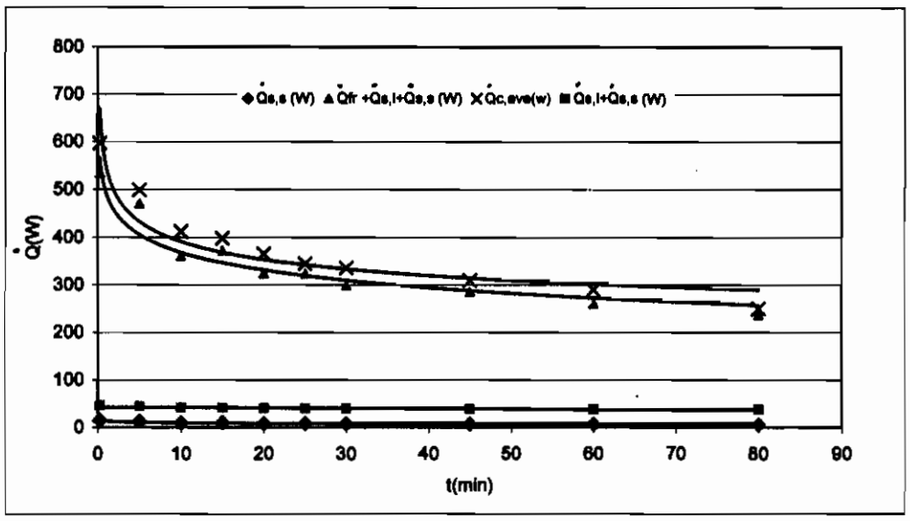

Figure 3.19:Energy balance for $\dot{m}_c$ =0.162 kg/s & $\dot{m}_l$=0.025 kg/s "parallel arrangement, jet mode"

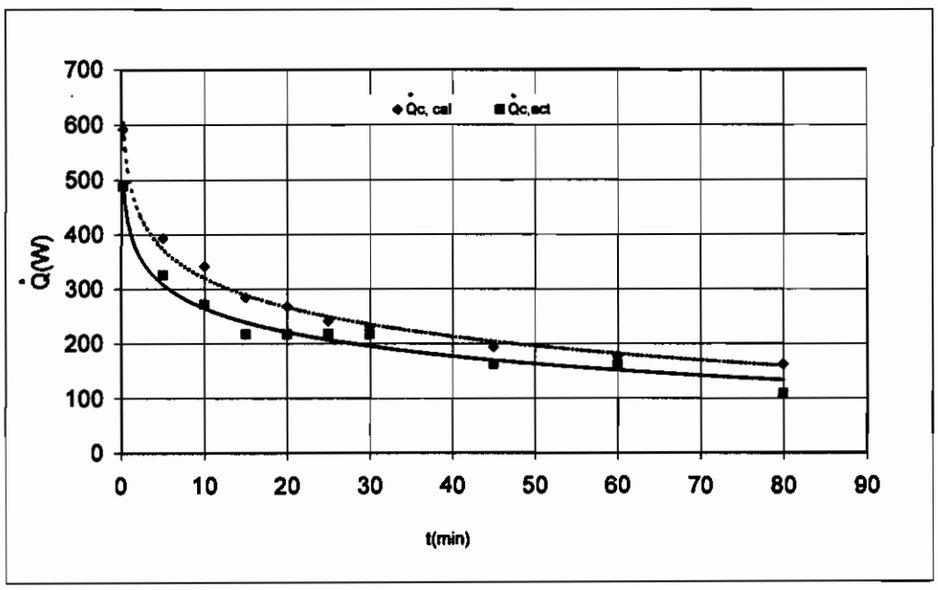

Figure 3.20:Comparison between actual and calculated rate of heat transfer from the test tubes to the coolant for $\dot{m}_c$ =0.162 kg/s & $\dot{m}_l$ =0.025 kg/s "parallel arrangement, jet mode"

From the previous run, it has been seen that, the ice formation rate and the heat transfer coefficient are reduced and ΔT_c is still low. To improve these items, series arrangement is utilized (refer to figure 2.5). In the series arrangement, the coolant velocity inside the tube increases and the flow rate is reduced to increase ΔT_c. Four different flow rates are tested as follows.

3.4-3 Experimental run 3(S):

This experimental run is carried out under the following conditions:

1-Series arrangement, jet mode

2-Falling film liquid: water

3-Room temperature: 23°C

4-Mass flow rate of coolant: 0.023 kg/s

5-Mass flow rate of the falling liquid:0.025kg/s

Calculations and energy balance for this run are shown in table (3.3). The results of such experimental run are also shown in figures (3.21 to 3.26). Figure (3.21) shows that the coolant temperature difference ΔT_c for series arrangement decreases rapidly from 6.1 to 4°C and then smoothly to about 2.1°C with time as ice accumulates on the test tubes. The change of ΔT_c starts from 6.1°C down to

2.1°C,which is higher than run 2(P) in which ΔT_c ranges from 1.1°C to 0.4°C,in which the errors in temperatures measurements are less effective on the experimental results. The rate of heat transfer from the test tubes to the coolant, the rate of the formed ice and the experimental overall heat transfer coefficient figure (3.22,23,24), show the same trend as those in parallel arrangement figure (3.11,12,13). Comparison between $Q_{c,act}$ and $Q_{c,cal}$,and the energy balance are shown in figures (3.25) and (3.26)respectively, which give a reasonable balance. The equations used to calculate the outside heat transfer coefficient,h_o ,and the thermal resistance of the ice,R_{ice} ,are valid until the tube spacing is filled with ice, since the ice increases in radial direction. After that the problem is no longer falling film on horizontal tubes and the flow forms like a falling film on a vertical corrugated plate in which the ice accumulates by sides. The flow rate of the coolant is increased to study the effect of increasing the heat transfer coefficient inside the tubes, in the two following runs.

Table (3.3): Energy balance analysis at $\dot{m}_c$=0.023 kg/s & $\dot{m}_j$=0.025kg/s "series arrangement, jet mode"

	Run#1	Run#2	Run#3	Run#4	Run#5	Run#6	Run#7	Run#8	Run#9	Run#10
t(min)	3	5	10	15	20	25	30	60	90	120
Δh(cm)	0.25	0.5	0.95	1.3	1.7	1.9	2.2	3.7	4.6	5.5
$Vx10^{-6}(m^3)$	160	320.1	608.2	832.2	1088	1216	1408	2400	3000	3521
M(Kg)	0.154	0.32	0.608	0.832	1.088	1.216	1.408	2.4	3	3.521
c (mm)	1.103	2.205	4.19	5.734	7.498	8.38	9.703	16.54	20.67	24.26
$\Delta T_c(^oC)$	6.3	5.7	5	4.4	4	3.9	3.5	3.4	2.6	2.4
$\dot{Q}_c(W)$	485.2	439	385.1	338.9	308.1	300.4	269.6	261.9	200.3	184.9
$\dot{Q}_{c,ave}(W)$	374.9	422	409	389.8	417.9	356.6	347.9	340.4	290.6	264.2
$\dot{Q}_{s,l}(W)$	31.5	31.5	31.5	31.5	31.5	31.5	31.5	31.5	31.5	31.5
$\dot{Q}_{fr}(W)$	284.2	355.3	337.5	309.8	302	270	260.6	222	185	162.8
$\dot{Q}_{s,s}(W)$	8.707	10.88	10.34	9.432	9.251	8.271	7.981	6.8	5.667	4.988
$\dot{Q}_{ls,c}(W)$	26.12	26.12	26.12	26.12	26.12	26.12	26.12	26.12	26.12	26.12
$\dot{Q}_{a,f}(W)$	324.4	397.7	379.4	350.7	342.8	309.8	300	260.3	222.2	199.3
$\varepsilon=\dot{Q}_{a,f}/\dot{Q}_{c,ave}$	0.865	0.942	0.928	0.9	0.82	0.869	0.862	0.765	0.765	0.754
T_i-T_c (^oC)	8	9.5	9.95	9.85	9.8	9.82	10	10.65	11.35	12.55
h_{ov}(W/m^2.K)	255.7	246.3	200.2	172.5	155.7	134.9	121.2	76.85	54.26	39.93
Re_c	86.65	86.65	86.65	86.65	86.65	86.65	86.65	86.65	86.65	86.65
$(\mu/\mu_s)^{0.14}$	1.068	1.046	1.038	1.036	1.034	1.032	1.029	1.023	1.018	1
$h_i(W/m^2.K)$	528.4	517.5	513.6	512.6	511.6	510.6	509.1	506.2	503.7	494.8
Re_f	121.6	121.6	121.6	121.6	121.6	121.6	121.6	121.6	121.6	121.6
$h_o(W/m^2.K)$	2471.2	2355.7	2177.7	2060.2	1943.4	1890.8	1818.1	1529.1	1401.7	1310.2
R_1(K/W)	0.097	0.099	0.1	0.1	0.1	0.1	0.1	0.101	0.102	0.103
R_3(ice) (K/W)	0.027	0.052	0.093	0.122	0.152	0.167	0.187	0.278	0.323	0.358
R_4(K/W)	0.018	0.017	0.017	0.016	0.016	0.016	0.016	0.014	0.014	0.013
UA(W/K)	7.067	5.947	4.777	4.2	3.726	3.537	3.298	2.544	2.281	2.105
$\dot{Q}_{c,cal}(W)$	395.8	395.5	332.7	289.6	255.6	243.2	230.9	189.7	181.2	184.9
$\dot{Q}_{c,act}(W)$	418.3	372.1	318.1	271.9	241.1	240.1	209.3	208.3	146.7	131.3
$P.D=\frac{(\dot{Q}_{c,cal}-\dot{Q}_{c,act})}{\dot{Q}_{c,cal}}\times 100$	-5.7	5.9	4.4	6.1	5.7	1.3	9.3	-9.8	19.1	29.0

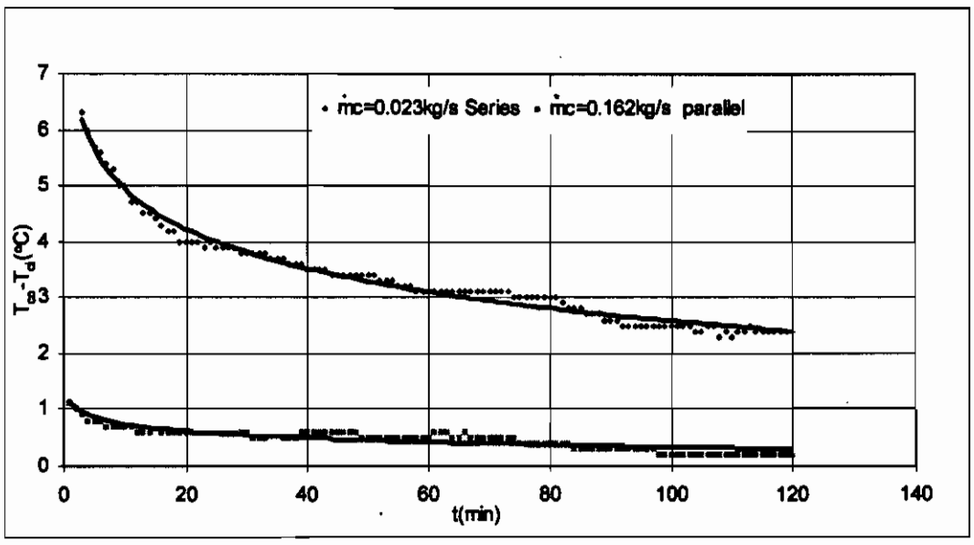

Figure 3-21: Comparison of ΔT_c changing with time between $\dot{m}_c$=0.023 kg/s "series arrangement, jet mode" & $\dot{m}_c$=0.162 kg/s "parallel arrangement, jet mode" for $\dot{m}_l$=0.025 Kg/s

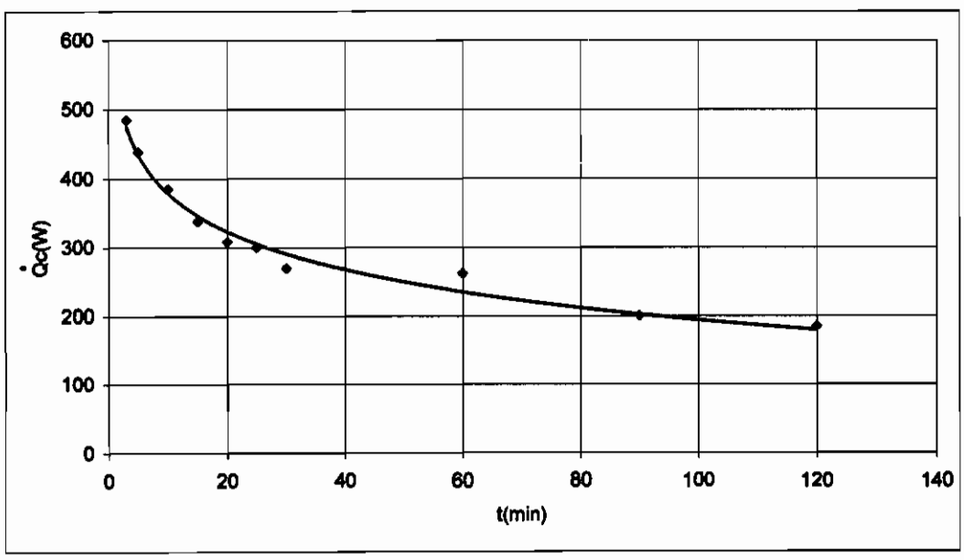

Figure 3.22: Variation of the rate of heat transfer from the test tubes to the coolant for $\dot{m}_c$=0.023kg/s & $\dot{m}_l$=0.025 Kg/s "series arrangement, jet mode"

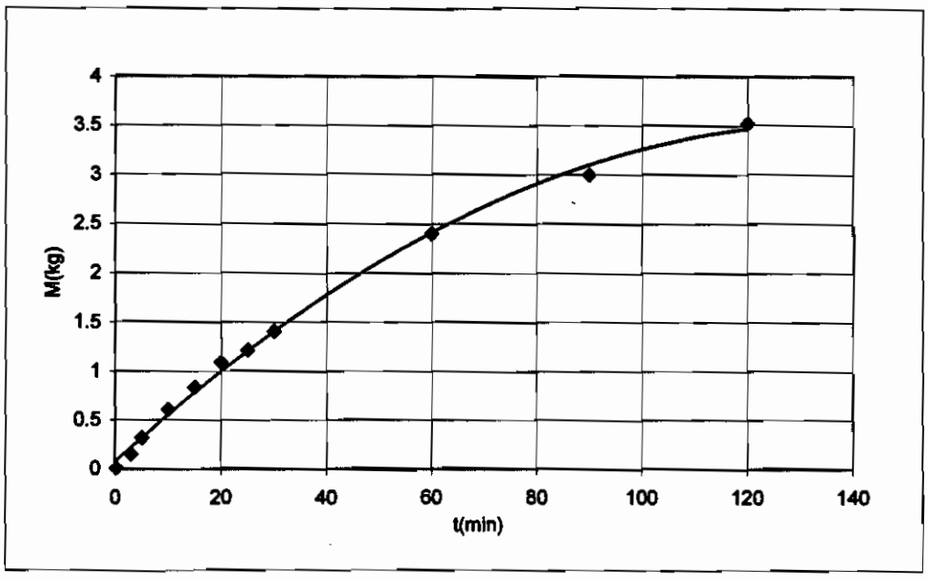

Figure 3.23: Variation of the formed ice on the test tubes with time for m_c =0.023 kg/s & m_f=0.025 Kg/s, "series arrangement, jet mode"

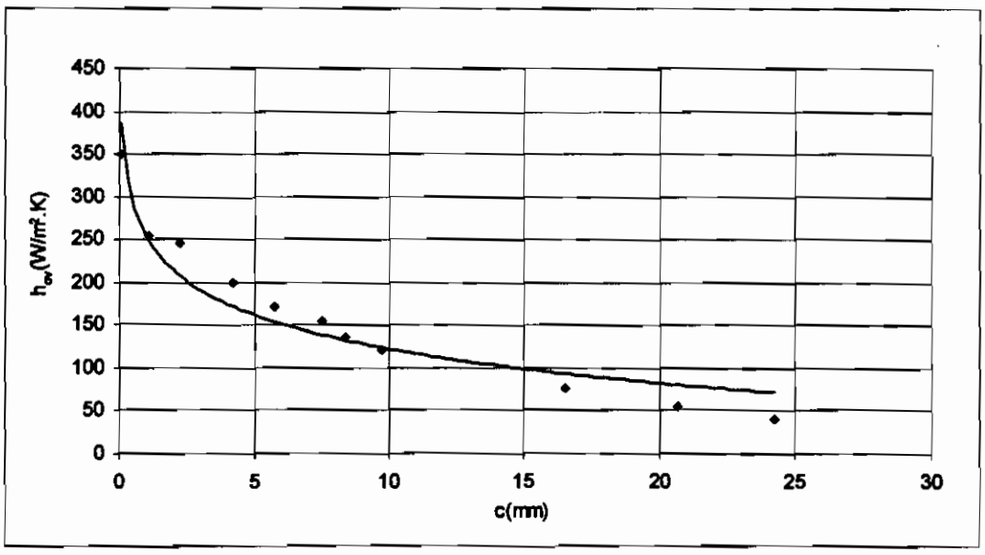

Figure 3.24: Variation of the experimental overall heat transfer coefficient with thickness for m_c=0.023 kg/s & m_f=0.025 Kg/s, "series arrangement, jet mode"

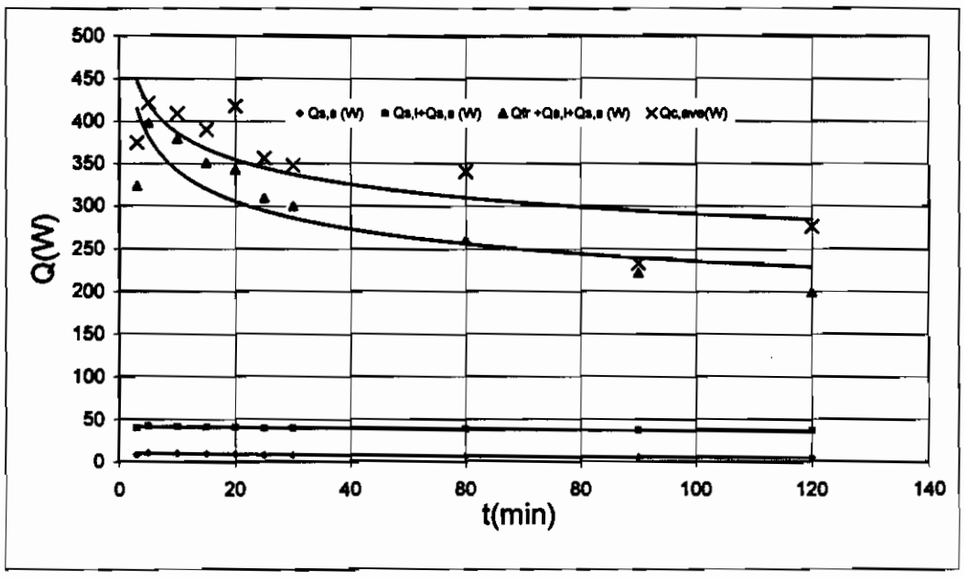

Figure 3-25: Energy Balance for m_c =0.023 kg/s & m_l=0.025 Kg/s "series arrangement, jet mode"

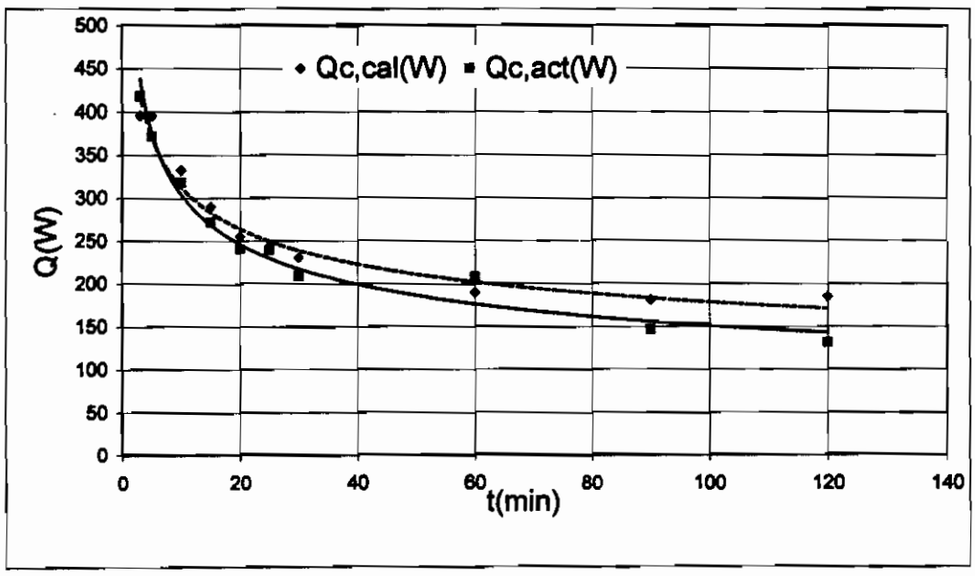

Figure 3-26: Comparison between actual and calculated rate of heat transfer from the test tubes to the coolant for m_c=0.023 kg/s & m_l=0.025 Kg/s "series arrangement, jet mode"

3.4-4 Experimental run 4(S):

This experimental run is carried out under the following conditions:

1-Series arrangement, jet mode

2-Falling film liquid: water

3-Room temperature: 23°C

4-Mass flow rate of coolant: 0.06 kg/s

5-Mass flow rate of the falling liquid: 0.025 kg/s

Calculations and energy balance for this run are shown in table (3.4). Energy balance and comparison between $\dot{Q}_{c,act}$ and $\dot{Q}_{c,cal}$, the are shown in figures (3.27) and (3.28) respectively, which give a reasonable balance. In this experimental run, the change of ΔT_c reduces to (3.3°C to 1.2°C) as shown in figure (3.29). It is clear that ΔT_c decreases as m_c increase due to higher velocity. The quantity of ice increases as planned due to the increase in the inside heat transfer coefficient (figure 3.30 and figure 3.31).

Table (3.4): Energy balance analysis at $\dot{m}_c$=0.06 kg/s & $\dot{m}_l$=0.025kg/s "series arrangement, jet mode"

	Run#1	Run#2	Run#3	Run#4	Run#5	Run#6	Run#7	Run#8	Run#9	Run#10
t(min)	0.217	5	10	15	20	25	30	45	60	70
Δh(cm)	____	0.7	1.1	1.6	2	2.3	2.7	3.8	4.7	5.4
$Vx10^{-6}(m^3)$	20	448.1	704.2	1024	1280	1472	1728	2433	3009	3307
M(Kg)	0.02	0.448	0.704	1.024	1.28	1.472	1.728	2.433	3.009	3.307
c (mm)	0.137	3.077	4.835	7.032	8.79	10.11	11.87	16.7	20.66	22.7
$\Delta T_c(^oC)$	3.7	2.7	2.1	1.8	1.6	1.4	1.4	1.4	1.2	1.2
$\dot{Q}_c$(W)	743.3	542.5	421.9	361.7	321.5	281.3	281.3	281.3	241.1	241.1
$\dot{Q}_{c,ave}$(W)	639	626.9	541.5	502.3	446.1	410.2	391	358.2	333.5	314.7
$\dot{Q}_{s,l}$(W)	31.5	31.5	31.5	31.5	31.5	31.5	31.5	31.5	31.5	31.5
$\dot{Q}_{fr}$(W)	512.3	497.4	390.8	379	355.3	326.9	319.8	300	278.3	262.2
$\dot{Q}_{s,s}$ (W)	28.33	13.94	10.88	11.33	10.97	10.4	9.973	6.649	4.987	4.778
$\dot{Q}_{ls,c}$ (W)	26.1	26.1	26.1	26.1	26.1	26.1	26.1	26.1	26.1	26.1
$\dot{Q}_{a,f}$ (W)	572.1	542.9	433.2	421.8	397.8	368.8	361.2	338.2	314.8	298.5
$\varepsilon = \dot{Q}_{a,f} / \dot{Q}_{c,ave}$	0.90	0.87	0.80	0.84	0.89	0.90	0.92	0.94	0.94	0.95
$T_l - T_c$ (^oC)	12.05	11.5	11.3	11.45	11.45	11.55	11.65	11.75	12	12.85
h_{ov}(W/m^2.K)	319.5	263.7	194.5	167.6	146	126.9	114.9	90.01	72.75	60.85
Re_c	199.7	199.7	199.7	199.7	199.7	199.7	199.7	199.7	199.7	199.7
$(\mu/\mu_s)^{0.14}$	1.07	1.04	1.035	1.03	1.028	1.025	1.023	1.021	1.018	1.01
h_i(W/m^2.K)	699.3	679.7	676.4	673.1	671.8	669.9	668.6	667.3	665.3	660.1
Re_f	121.6	121.6	121.6	121.6	121.6	121.6	121.6	121.6	121.6	121.6
H_o(W/m^2.K)	2584	2273	2127	1973	1868	1797	1713	1523	1414	1371
R_1(K/W)	0.073	0.075	0.076	0.076	0.076	0.076	0.076	0.077	0.077	0.077
R_3(ice) (K/W)	0.003	0.071	0.106	0.146	0.175	0.195	0.22	0.282	0.321	0.337
R_4(K/W)	0.018	0.017	0.017	0.016	0.016	0.015	0.015	0.014	0.014	0.014
UA(W/K)	10.54	6.113	5.036	4.203	3.752	3.489	3.208	2.684	2.431	2.335
$\dot{Q}_{c,cal}$ (W)	889.3	492.1	398.4	336.8	300.7	282.1	261.6	220.7	204.2	210
$\dot{Q}_{c,act}$ (W)	663.1	482.2	361.7	301.4	261.2	221	221	221	180.8	180.8
P.D= $\frac{(\dot{Q}_{c,cal} - \dot{Q}_{c,act})}{\dot{Q}_{c,cal}} \times 100$	25.44	2.009	9.214	10.52	13.15	21.64	15.51	0.135	11.44	13.9

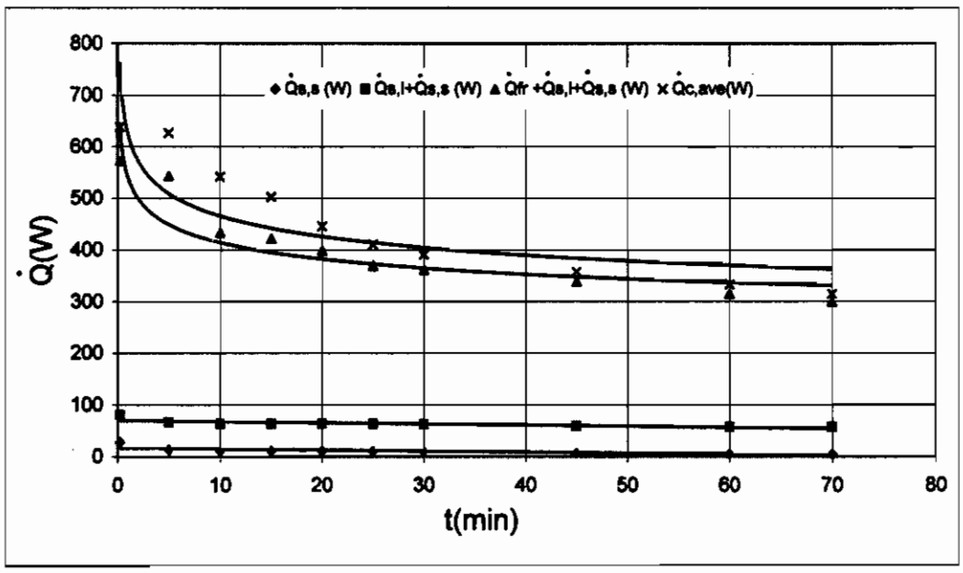

Figure 3-27: Energy Balance for $\dot{m}_c$ =0.06 kg/s & $\dot{m}_l$=0.025 kg/s "series arrangement, jet mode"

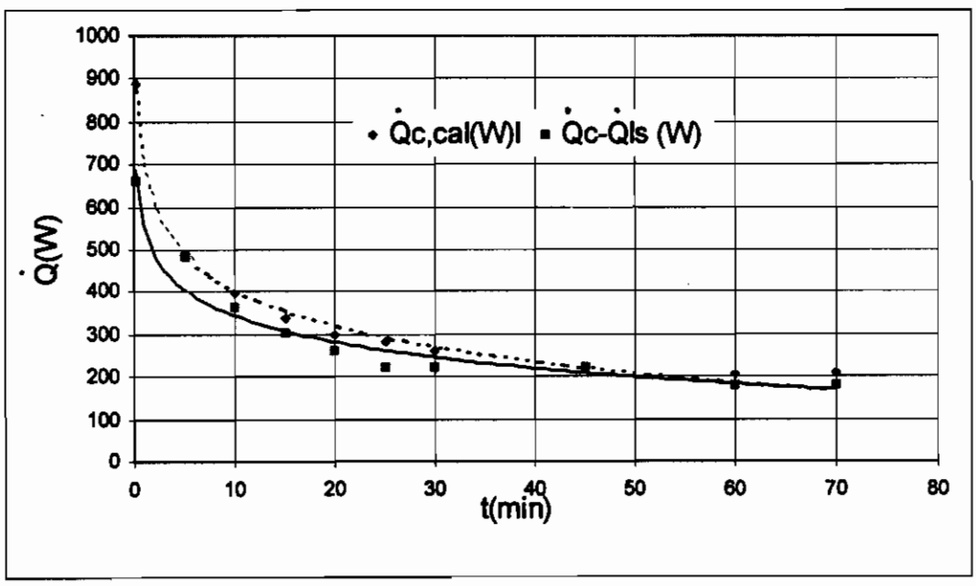

Figure 3-28: Comparison between actual and calculated rate of heat transfer from the test tubes to the coolant for $\dot{m}_c$=0.06 kg/s & $\dot{m}_l$=0.025 kg/s "series arrangement, jet mode"

3.4-5 Experimental run 5(S):

The coolant flow rate is further increased in the present series mode to improve the heat transfer coefficient inside the annulus.

This experimental run is carried out under the following conditions:

1-Series arrangement, jet mode

2-Falling film liquid: water

3-Room temperature: 23°C

4-Mass flow rate of coolant: 0.128 kg/s

5-Mass flow rate of the falling liquid: 0.025 kg/s

Calculations and energy balance for this run are shown in table (3.5) and in figures (3.29 to 3.33). ΔT_c is further decreased as shown in figure (3.29). Figures (3.30) and (3.31) show that the ice formation and h_{ov} increases as the flow rate of the coolant is increased. Comparison between $\dot{Q}_{c,act}$ and $\dot{Q}_{c,cal}$, and the energy balance are shown in figures (3.32) and (3.33) respectively, which give a reasonable balance.

Table (3.5): Energy balance analysis at $\dot{m}_c$=0.128 kg/s & $\dot{m}_i$=0.025kg/s "series arrangement, jet mode"

	Run#1	Run#2	Run#3	Run#4	Run#5	Run#6	Run#7	Run#8	Run#9	Run#10
t(min)	0.2	5	10	15	20	25	30	40	50	60
Δh(cm)	____	0.8	1.2	1.75	2.2	2.7	3.1	3.7	4.3	4.9
$Vx10^{-6}(m^3)$	25	512.1	768.2	1120	1408	1728	1985	2369	2753	3137
M(Kg)	0.025	0.512	0.768	1.12	1.408	1.728	1.985	2.369	2.753	3.137
c (mm)	0.172	3.516	5.274	7.691	9.669	11.87	13.62	16.26	18.9	21.54
ΔT_c(°C)	2	1.4	1	1	0.9	0.9	0.8	0.7	0.6	0.6
$\dot{Q}_c$(W)	857.3	600.1	428.6	428.6	385.8	385.8	342.9	300.1	257.2	257.2
$\dot{Q}_{c,ave}$(W)	857.3	685.8	623.5	623	498	478.1	495.8	446.4	416.9	393.5
$\dot{Q}_{s,i}$(W)	31.5	31.5	31.5	31.5	31.5	31.5	31.5	31.5	31.5	31.5
$\dot{Q}_{fr}$(W)	693.8	568.5	426.4	414.5	390.8	383.7	367.1	328.7	305.6	290.2
$\dot{Q}_{s,s}$ (W)	21.25	17.41	13.06	12.70	11.97	11.75	11.25	10.07	9.36	8.89
$\dot{Q}_{ls,c}$ (W)	26.10	26.10	26.10	26.10	26.10	26.10	26.10	26.10	26.10	26.10
$\dot{Q}_{a,f}$ (W)	746.5	617.4	470.9	458.7	434.3	427	409.9	370.2	346.4	330.6
$\varepsilon = \dot{Q}_{a,f} / \dot{Q}_{c,ave}$	0.87	0.90	0.76	0.74	0.87	0.89	0.83	0.83	0.83	0.84
$T_i - T_c$ (°C)	10	10.05	9.85	10.55	10.4	11.8	12.05	12.4	12.6	12.9
h_{ov}(W/m^2.K)	475.8	314.9	219.3	177.1	155.4	123.2	108.1	85.91	72.36	62.17
Re_c	485	485	485	485	485	485	485	485	485	485
$(\mu/\mu_s)^{0.14}$	1.07	1.038	1.035	1.03	1.026	1.025	1.023	1.022	1.02	1.01
h_i(W/m^2.K)	940.0	911.9	909.2	904.8	901.3	900.4	898.7	897.8	896.0	887.3
Re_f	121.6	121.6	121.6	121.6	121.6	121.6	121.6	121.6	121.6	121.6
h_o(W/m^2.K)	2580	2234	2094	1932	1820	1713	1638	1539	1453	1378
R_1(K/W)	0.054	0.056	0.056	0.057	0.057	0.057	0.057	0.057	0.057	0.058
R_3(ice) (K/W)	0.004	0.08	0.115	0.157	0.188	0.22	0.244	0.276	0.306	0.334
R_4(K/W)	0.018	0.017	0.017	0.016	0.016	0.015	0.015	0.015	0.014	0.014
UA(W/K)	12.96	6.513	5.334	4.357	3.837	3.423	3.169	2.874	2.648	2.465
$\dot{Q}_{c,cal}$ (W)	1089	547.1	448.1	366	322.3	287.6	266.2	241.4	222.4	207.1
$\dot{Q}_{c,act}$ (W)	793	535.8	364.3	364.3	321.5	278.6	235.8	192.9	192.9	192.9
$P.D = \frac{(\dot{Q}_{c,cal} - \dot{Q}_{c,act})}{\dot{Q}_{c,cal}} \times 100$	27.15	2.06	18.68	0.44	0.26	3.11	11.44	20.11	13.27	6.86

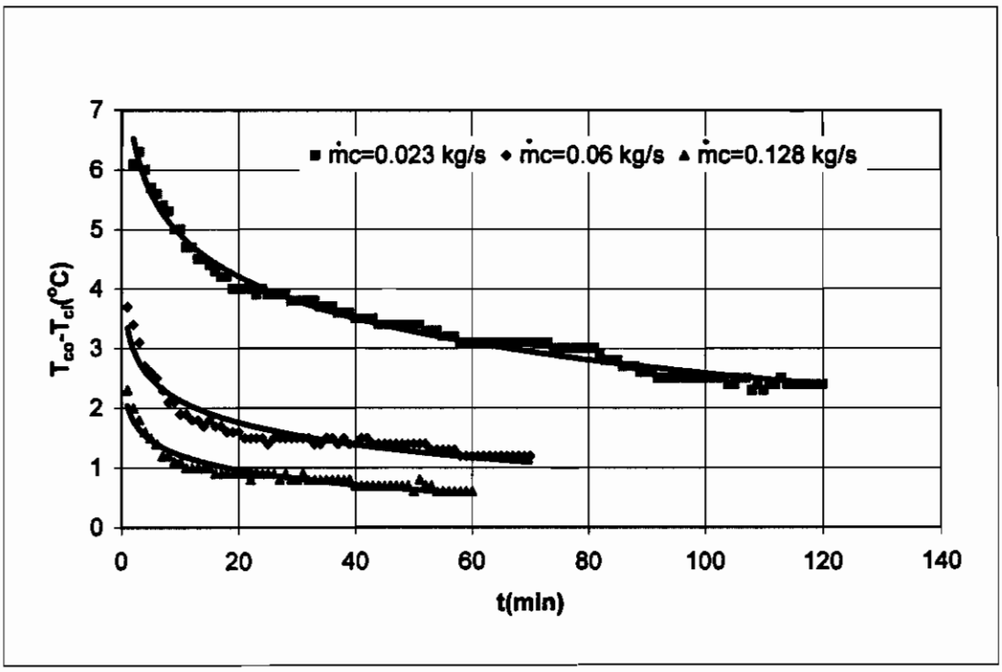

Figure 3.29: Comparison of ΔT_c changing with time for different coolant flow rate, at same falling film flow rate of $\dot{m}_f$=0.025 kg/s "series arrangement, jet mode"

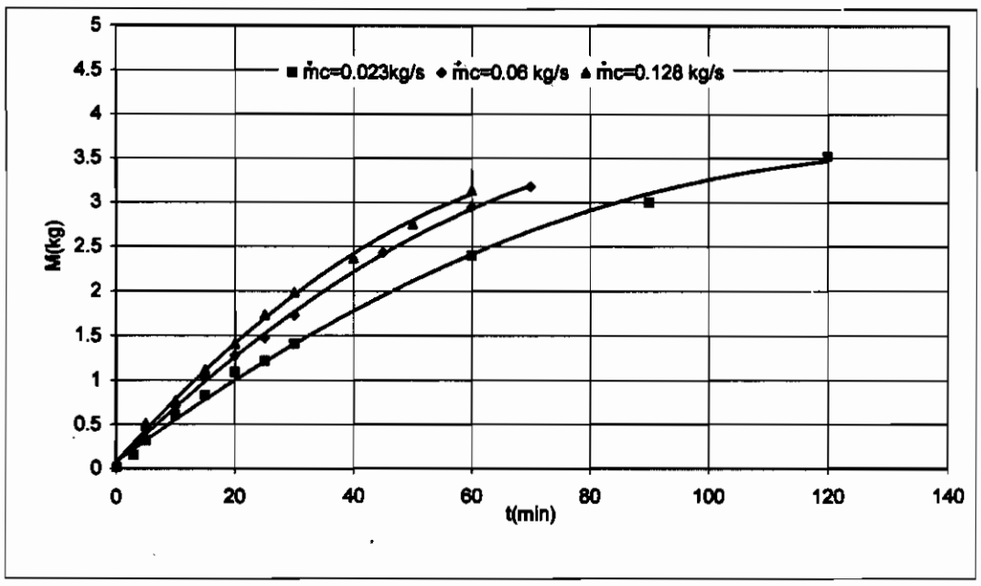

Figure 3.30: Comparison of the formed ice on the test tubes for different coolant flow rate, with same falling film flow rate of $\dot{m}_f$=0.025 kg/s "series arrangement, jet mode"

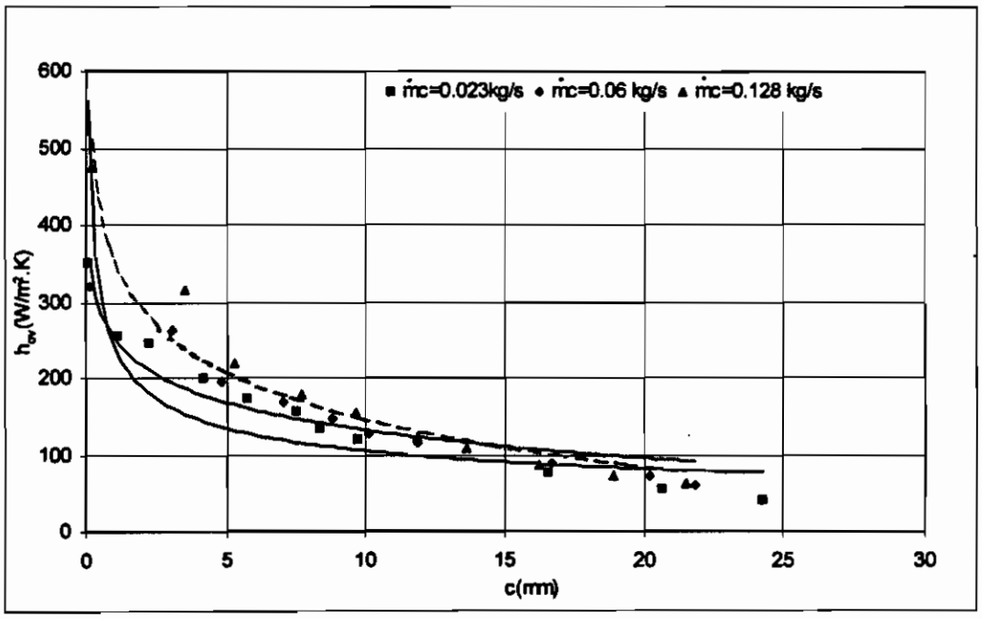

Figure 3.31: Comparison of the experimental overall heat transfer coefficient changing with thickness for different coolant flow rate, with same falling film flow rate of $\dot{m}_f$=0.025 kg/s "series arrangement, jet mode"

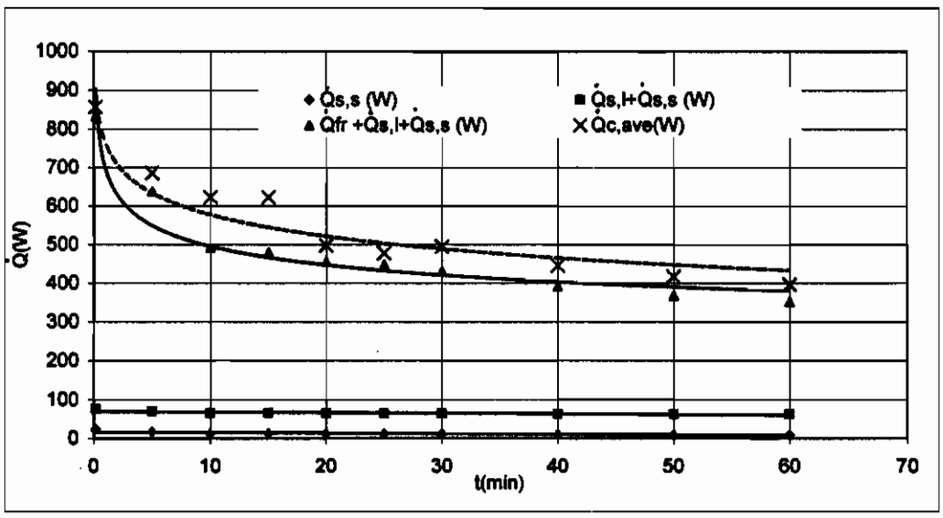

Figure 3.32: Energy Balance for $\dot{m}_c$ =0.128 kg/s & $\dot{m}_l$=0.025 kg/s "series arrangement, jet mode"

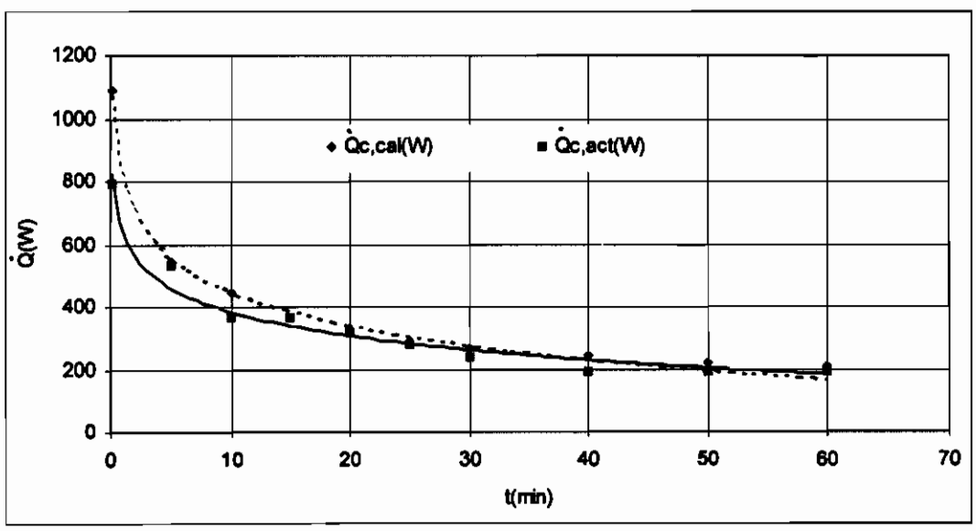

Figure 3.33: Comparison between actual and calculated rate of heat transfer from the test tubes to the coolant for $\dot{m}_c$=0.128 kg/s & $\dot{m}_l$=0.025 kg/s "series arrangement, jet mode"

3.4-6 Experimental run 6(S):

The coolant flow rate is further increased to $\dot{m}_c$=0.162 kg/s in the present run, to compare the performance of the series arrangement with the parallel one.

This experimental run is carried out under the following conditions:

1-Series arrangement, jet mode

2-Falling film liquid: water

3-Room temperature: 23°C

4-Mass flow rate of coolant: 0.162 kg/s

5-Mass flow rate of the falling liquid: 0.025 kg/s

Calculations and energy balance for this run are shown in table (3.5) and in figures (3.34 to 3.37). Figure (3.34) shows that the series arrangement gives more ice than in parallel one. This is due to an increase of both inside heat transfer coefficient h_i and the difference in coolant temperature ΔT_c. In addition, the experimental overall heat transfer coefficient of the series arrangement is higher than that of parallel one as shown in figure (3.35).

Table (3.6): Energy balance analysis at $\dot{m}_c$=0.162 kg/s & $\dot{m}_l$=0.025kg/s "series arrangement, jet mode"

	Run#1	Run#2	Run#3	Run#4	Run#5	Run#6	Run#7	Run#8	Run#9	Run#10
t(min)	0.22	5	10	15	20	25	30	40	50	60
Δh(cm)	____	0.80	1.30	1.80	2.30	2.80	3.10	3.70	4.35	5.00
$Vx10^{-6}(m^3)$	28.0	512.1	832.2	1152.3	1472.4	1792.5	1984.6	2368.7	2784.8	3200.9
M(Kg)	0.04	0.51	0.83	1.15	1.47	1.79	1.98	2.37	2.78	3.20
c (mm)	0.19	3.52	5.71	7.91	10.11	12.31	13.62	16.26	19.12	21.98
ΔT_c(°C)	2.1	1.2	1	0.8	0.7	0.7	0.6	0.6	0.5	0.5
$\dot{Q}_c$(W)	1139.3	651.01	542.51	434.00	379.75	379.75	325.50	325.50	271.25	271.25
$\dot{Q}_{c,ave}$(W)	1139.3	797.50	680.80	604.00	550.00	500.00	434.00	393.30	385.20	366.20
$\dot{Q}_{s,l}$ (W)	31.50	31.50	31.50	31.50	31.50	31.50	31.50	31.50	31.50	31.50
$\dot{Q}_{fr}$(W)	901.92	571.90	464.67	428.92	411.05	400.33	369.35	330.63	310.97	297.86
$\dot{Q}_{s,s}$ (W)	27.46	17.41	14.15	13.06	12.52	12.19	11.25	10.07	9.47	9.07
$\dot{Q}_{s,f}$ (W)	960.88	620.81	510.32	473.48	455.07	444.02	412.10	372.20	351.94	338.43
$\varepsilon = \dot{Q}_{s,f} / \dot{Q}_{c,ave}$	0.84	0.78	0.75	0.78	0.83	0.89	0.95	0.95	0.91	0.92
$T_l - T_c$ (°C)	9.8	9.85	10.15	10.2	10.3	10.3	10.4	10.4	10.4	10.4
h_{ov}(W/m^2.K)	657.18	343.41	243.79	202.76	175.57	157.14	137.6	113.54	98.169	86.957
Re_c	613.81	613.81	613.81	613.81	613.81	613.81	613.81	613.81	613.81	613.81
$(\mu/\mu_s)^{0.14}$	1.07	1.038	1.037	1.03	1.028	1.025	1.022	1.02	1.09	1.01
h_i(W/m^2.K)	1016.8	986.3	985.4	978.7	976.8	974.0	971.1	969.2	1035.8	959.7
Re_f	121.6	121.6	121.6	121.6	121.6	121.6	121.6	121.6	121.6	121.6
h_o(W/m^2.K)	2578	2234	2062	1918	1797	1693	1638	1539	1446	1367
R_1(K/W)	0.050	0.052	0.052	0.052	0.052	0.053	0.053	0.053	0.049	0.053
R_3(ice) (K/W)	0.005	0.080	0.123	0.161	0.195	0.226	0.244	0.276	0.309	0.339
R_4(K/W)	0.018	0.017	0.017	0.016	0.016	0.015	0.015	0.015	0.014	0.014
UA(W/K)	13.59	6.70	5.23	4.37	3.81	3.40	3.21	2.91	2.69	2.47
$\dot{Q}_{c,cal}$ (W)	1027.6	506.35	395.61	330.39	287.73	257.32	242.87	219.95	203.04	186.38
$\dot{Q}_{c,act}$ (W)	1057.9	569.63	461.13	352.63	298.38	298.38	244.13	244.13	189.88	189.88
P.D= $\frac{(\dot{Q}_{c,cal} - \dot{Q}_{c,act})}{\dot{Q}_{c,cal}} \times 100$	-2.95	12.50	-16.56	6.73	3.70	15.96	0.52	10.99	-6.48	1.88

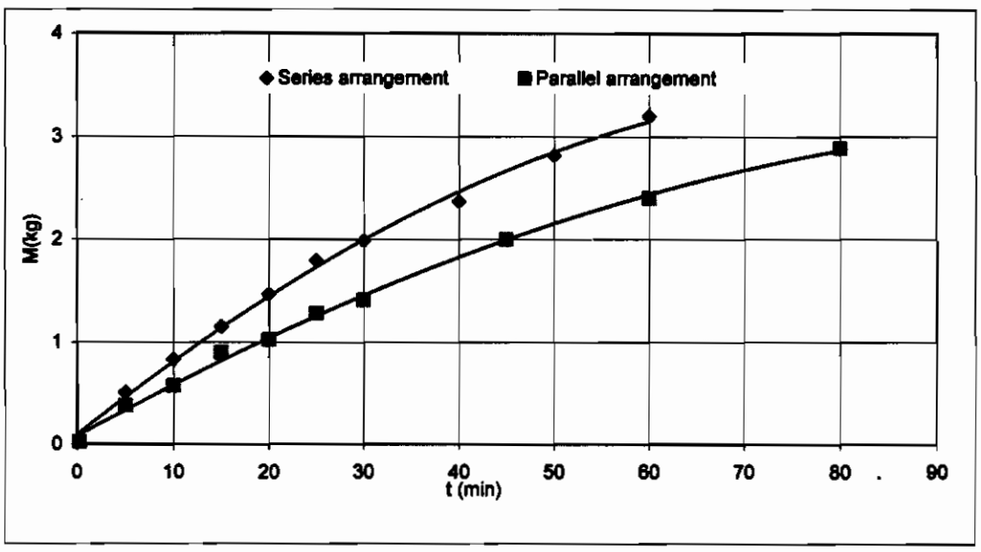

Figure 3.34: Comparison of the ice formed between series and parallel arrangements for $\dot{m}_c$=0.162 kg/s & $\dot{m}_l$=0.025 kg/s "jet mode".

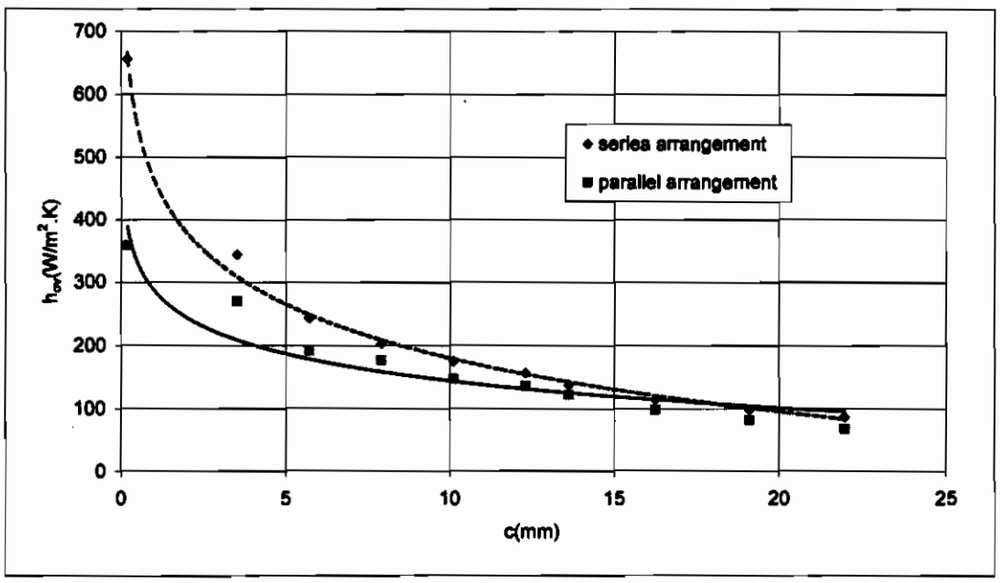

Figure 3.35: Comparison of the experimental overall heat transfer coefficient between series and parallel arrangements for $\dot{m}_c$=0.162 kg/s & $\dot{m}_l$=0.025 kg/s "jet mode".

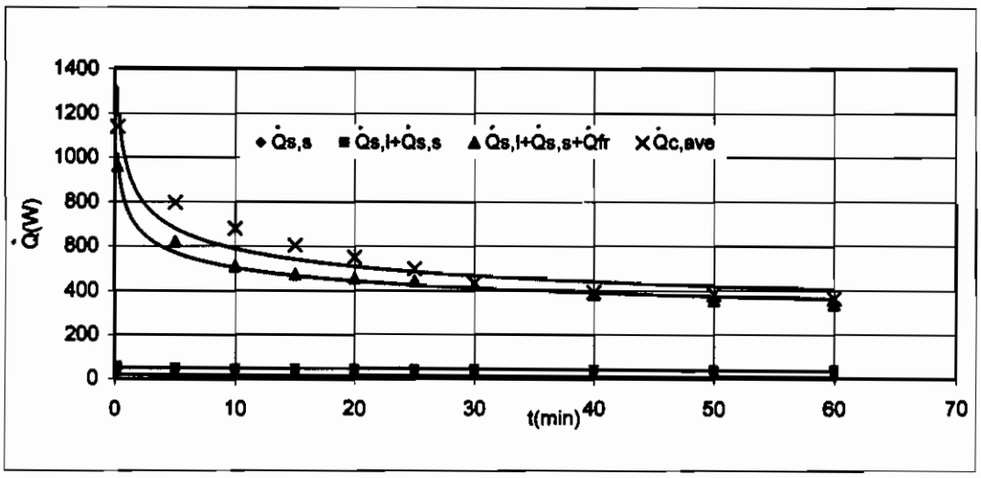

Figure 3.36: Energy balance for $\dot{m}_c$=0.162 & $\dot{m}_l$=0.025 kg/s "series arrangement, jet mode"

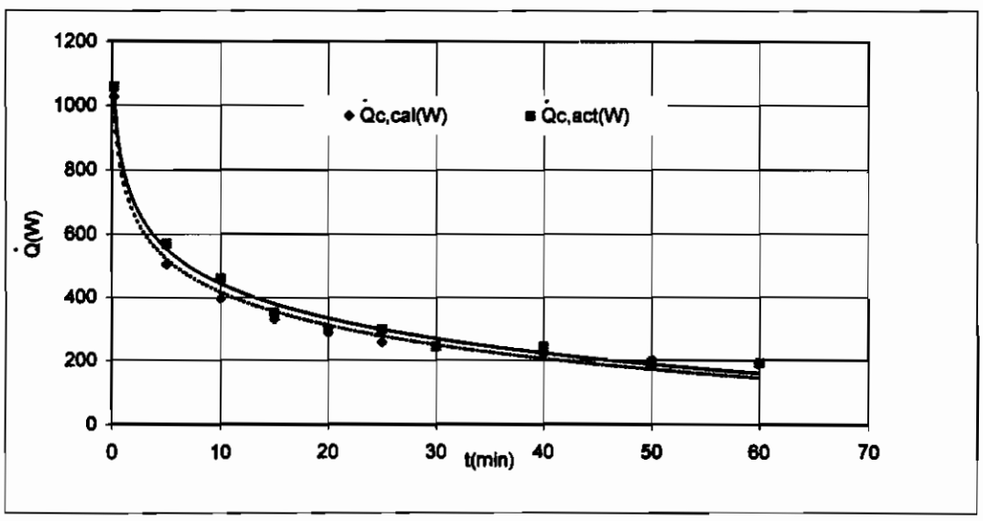

Figure 3.37: Comparison between calculated rate of heat transfer from the test tubes to the coolant and actual one, for $\dot{m}_c$=0.162 kg/s & $\dot{m}_l$=0.025 kg/s "series arrangement, jet mode"

To study the effect of the falling film various modes on the ice formation, two runs were made. In the first run the falling film flow rate increased to get sheet mode. In the second run the flow rate is decreased to get droplet mode.

3.4-7 Experimental run 7(S):

The falling film flow rate is increased to $\dot{m}_f$=0.075 kg/s in the present run, to get sheet mode.This experimental run is carried out under the following conditions:

1-Series arrangement, sheet mode

2-Falling film liquid: water

3-Room temperature: 23°C

4-Mass flow rate of coolant: 0.162 kg/s

5-Mass flow rate of the falling liquid: 0.075 kg/s

Calculations and energy balance for this run are shown in table (3.7) and in figures (3.38 to 3.41).

Sheet mode increases the amount of the formed ice and the experimental overall heat transfer coefficient h_{ov} for the system. Tubes surfaces are highly wetted by the falling film, but some water falls outside them, due to an increase in drag force. Sheet mode is observed clearly in the two upper test tubes. The rest of the test tubes are

covered by sheet-jet mode, which leads us to use equation (1.15) of Hu [8] to approximate h_o since there is no equation for such mixing mode.

Table (3.7): Energy balance analysis at $\dot{m}_c$=0.162 kg/s & $\dot{m}_f$=0.075kg/s "series arrangement, sheet mode"

	Run#1	Run#2	Run#3	Run#4	Run#5	Run#6	Run#7	Run#8	Run#9	Run#10
t(min)	0.2	5	10	15	20	25	30	40	50	60
Δh(cm)	____	0.85	1.45	2.1	2.5	2.9	3.2	3.85	4.4	5.2
$Vx10^{-6}(m^3)$	30	544.16	928.27	1344.4	1600	1856.5	2049	2464.7	2816.8	3329
M(Kg)	0.035	0.5442	0.9283	1.3444	1.6	1.8565	2.049	2.4647	2.8168	3.329
c (mm)	0.2059	3.7358	6.3728	9.2295	10.99	12.746	14.06	16.921	19.338	22.854
ΔT_c(°C)	2.2	1.2	0.9	0.8	0.7	0.7	0.6	0.6	0.5	0.5
$\dot{Q}_c$(W)	1193.5	651.01	488.26	434	379.8	379.75	325.5	325.5	271.25	271.25
$\dot{Q}_{c,ave}$(W)	1139.2	754.08	640.16	625.7	562	534.4	490.1	450.13	423.41	414.56
$\dot{Q}_{a,l}$ (W)	75.6	75.6	75.6	75.6	75.6	75.6	75.6	75.6	75.6	75.6
$\dot{Q}_{fr}$(W)	971.25	604.01	515.19	497.42	444.1	412.15	379	341.98	312.67	307.93
$\dot{Q}_{a,s}$ (W)	29.75	18.50	15.78	15.24	13.60	12.62	11.61	10.48	9.58	9.43
$\dot{Q}_{a,f}$ (W)	1076.6	698.12	606.57	588.26	533.3	500.38	466.2	428.05	397.84	392.96
$\varepsilon = \dot{Q}_{a,f}/\dot{Q}_{c,ave}$	0.94	0.93	0.95	0.94	0.95	0.94	0.95	0.95	0.94	0.95
$T_1 - T_c$ (°C)	8.90	9.35	9.95	10.2	9.55	9.95	10.15	9.85	9.9	9.9
h_{ov}(W/m^2.K)	810.01	401.85	286.14	237.77	214.2	180.32	157	134.95	115.82	103.55
Re_c	613.81	613.81	613.81	613.81	613.8	613.81	613.8	613.81	613.81	613.81
$(\mu/\mu_s)^{0.14}$	1.07	1.037	1.03	1.028	1.025	1.022	1.021	1.02	1.08	1.01
h_i(W/m^2.K)	1016.8	985.4	978.7	976.8	974.0	971.1	970.2	969.2	1026.3	959.7
Re_f	364.7	364.7	364.7	364.7	364.7	364.7	364.7	364.7	364.7	364.7
h_o(W/m^2.K)	3609	3165	2916	2698	2583	2481	2411	2276	2176	2050
R_1(K/W)	0.0503	0.0519	0.0522	0.0524	0.053	0.0527	0.053	0.0528	0.0498	0.0533
R_3(ice) (K/W)	0.00523	0.0847	0.1344	0.1815	0.208	0.2321	0.249	0.2842	0.3112	0.3473
R_4(K/W)	0.0131	0.012	0.0114	0.0108	0.01	0.0102	0.01	0.0096	0.0093	0.0089
UA(W/K)	14.567	6.729	5.0502	4.0882	3.695	3.3908	3.205	2.8856	2.6999	2.442
$\dot{Q}_{c,cal}$ (W)	1040.0	480.45	360.59	291.89	263.8	242.1	228.8	206.03	192.78	174.36
$\dot{Q}_{c,act}$ (W)	1112.1	569.63	406.88	352.63	298.4	298.38	244.1	244.13	189.88	189.88
$P.D=\frac{(\dot{Q}_{c,cal}-\dot{Q}_{c,act})}{\dot{Q}_{c,cal}}x100$	-6.93	-18.56	-12.84	-20.81	-13.10	-23.25	-6.70	-18.49	1.50	-8.90

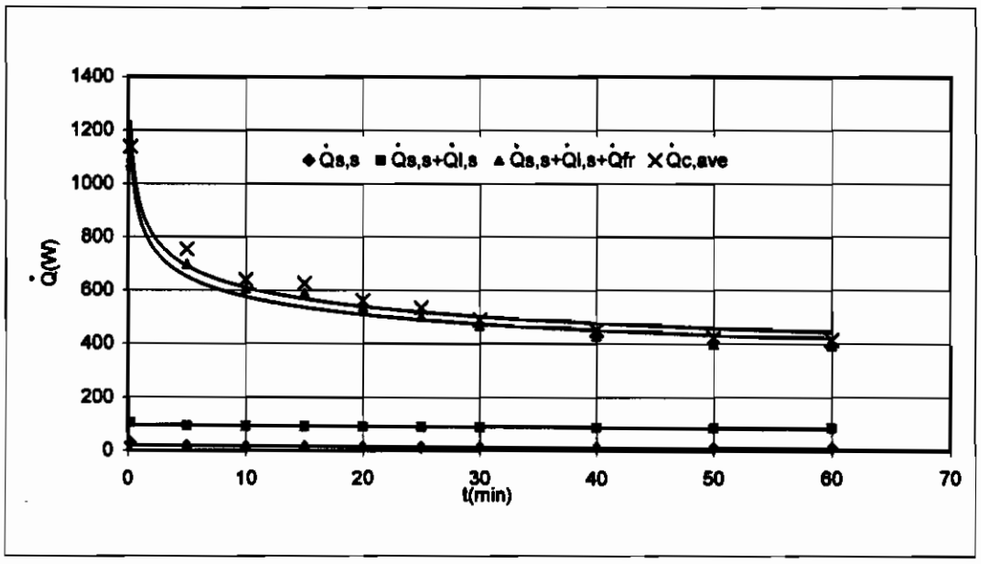

Figure 3.38: Energy balance for $\dot{m}_c$=0.162 kg/s and $\dot{m}_l$ =0.075 kg/s "series arrangement, sheet mode"

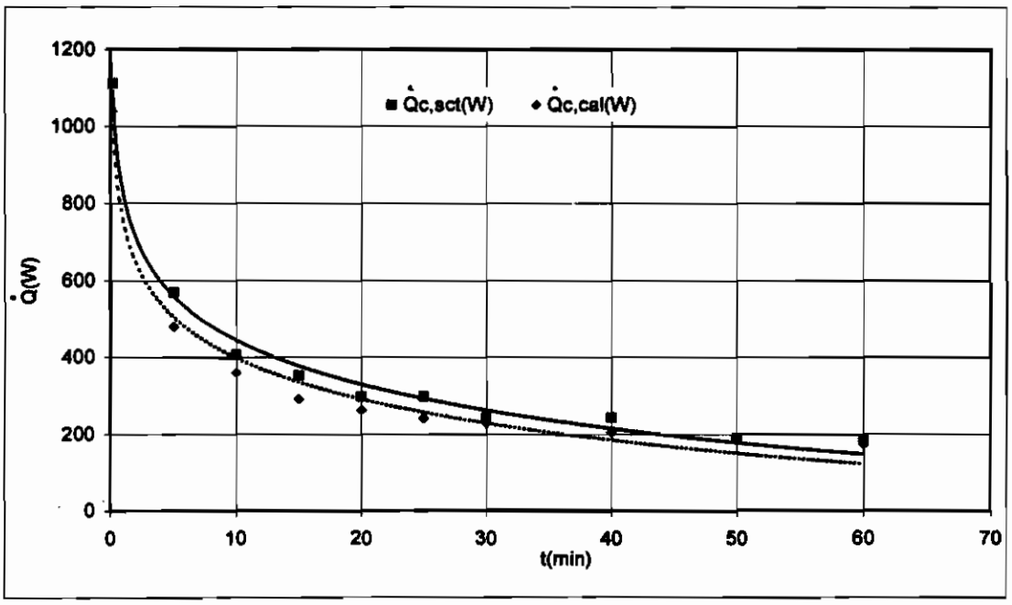

Figure 3.39: Comparison between actual and calculated rate of heat transfer from the test tubes to the coolant, for $\dot{m}_c$=0.162 kg/s & $\dot{m}_l$=0.075 kg/s "series arrangement, sheet mode"

3.4-8 Experimental run 8(S):

The falling film flow rate is decreased to m_f=0.0125 kg/s in the present series, to get droplet mode, to study the effect of such mode on the performance of the heat exchanger.

This experimental run is carried out under the following conditions:

1-Series arrangement, droplet mode

2-Falling film liquid: water

3-Room temperature: 23°C

4-Mass flow rate of coolant: 0.162 kg/s

5-Mass flow rate of the falling liquid: 0.0125 kg/s

Calculations and energy balance for this run are shown in table (3.7) and in figures (3.40 to 3.43).

Droplet mode shows a steady flow in which the droplets cover the whole test tubes and no flow falls outside the test tubes. Equation (1.17) are used to calculate h_o for this mode. However, less ice accumulates on the test tubes, (figure 3.40) due to less h_o. The experimental overall heat transfer coefficient increases as the falling film flow rate increases as shown in figure (3.41).

Table (3.8): Energy balance analysis at $\dot{m}_c$=0.162 kg/s & $\dot{m}_l$=0.0125kg/s "series arrangement, droplet mode"

	Run#1	Run#2	Run#3	Run#4	Run#5	Run#6	Run#7	Run#8	Run#9	Run#10
t(min)	0.25	5	10	15	20	25	30	40	50	60
Δh(cm)	———	0.8	1.2	1.6	2	2.4	2.7	3.2	3.8	4.2
$Vx10^{-6}(m^3)$	30	512.15	768.22	1024.3	1280.4	1536.4	1728.5	2048.6	2432.7	2688.8
M(Kg)	0.035	0.5121	0.7682	1.0243	1.2804	1.5364	1.7285	2.0486	2.4327	2.6888
c (mm)	0.206	3.516	5.274	7.032	8.79	10.548	11.867	14.064	16.701	18.459
$\Delta T_c(^oC)$	1.8	1.1	0.9	0.8	0.7	0.7	0.6	0.6	0.5	0.5
$\dot{Q}_c$(W)	976.51	596.76	488.26	434	379.75	379.75	325.5	325.5	271.25	271.25
$\dot{Q}_{c,ave}$(W)	976.51	678.13	596.7	587.7	535.12	495.22	461.13	434.15	405.32	366.64
$\dot{Q}_{s,l}$ (W)	26.25	26.25	26.25	26.25	26.25	26.25	26.25	26.25	26.25	26.25
$\dot{Q}_{fr}$(W)	777	568.48	426.36	378.99	355.3	341.09	319.77	284.24	270.03	248.71
$\dot{Q}_{s,s}$ (W)	23.80	17.41	13.06	11.61	10.88	10.45	9.79	8.71	8.27	7.62
$\dot{Q}_{a,f}$ (W)	827.05	612.15	465.67	416.85	392.44	377.79	355.82	319.2	304.55	282.58
$\varepsilon = \dot{Q}_{a,f} / \dot{Q}_{c,ave}$	0.85	0.90	0.78	0.71	0.73	0.76	0.77	0.74	0.75	0.77
$T_l - T_c$ (^oC)	9.05	9.30	9.95	10.20	9.55	9.95	10.15	9.85	9.90	9.90
$h_{ov}(W/m^2.K)$	611.94	358.64	232.04	185.88	172.65	148.21	129.93	110.79	96.211	84.472
Re_c	613.81	613.81	613.81	613.81	613.81	613.81	613.81	613.81	613.81	613.81
$(\mu/\mu_s)^{0.14}$	1.071	1.038	1.035	1.03	1.028	1.026	1.025	1.022	1.021	1.02
$h_i(W/m^2.K)$	1017.7	986.3	983.5	978.7	976.8	974.9	974.0	971.1	970.2	969.2
Re_f	60.8	60.8	60.8	60.8	60.8	60.8	60.8	60.8	60.8	60.8
$h_o(W/m^2.K)$	2023	1712	1586	1479	1387	1307	1253	1174	1092	1044
R_1(K/W)	0.0502	0.0518	0.052	0.0522	0.0524	0.0525	0.0525	0.0527	0.0527	0.0528
R_3(ice) (K/W)	0.0052	0.0802	0.1145	0.1458	0.1746	0.2013	0.2201	0.2494	0.2816	0.3016
R_4(K/W)	0.0232	0.0223	0.0219	0.0215	0.0212	0.0209	0.0207	0.0204	0.02	0.0198
UA(W/K)	12.716	6.4782	5.3077	4.5536	4.0292	3.6408	3.4095	3.1016	2.8218	2.6721
$\dot{Q}_{c,cal}$ (W)	907.92	462.54	378.97	325.13	287.68	259.95	243.44	221.45	201.48	190.79
$\dot{Q}_{c,act}$ (W)	895.13	515.38	406.88	352.63	298.38	298.38	244.13	244.13	189.88	189.88
$P.D = \frac{(\dot{Q}_{c,cal} - \dot{Q}_{c,act})}{\dot{Q}_{c,cal}} \times 100$	1.41	-11.42	-7.36	-8.46	-3.72	-14.78	-0.28	-10.24	5.76	0.48

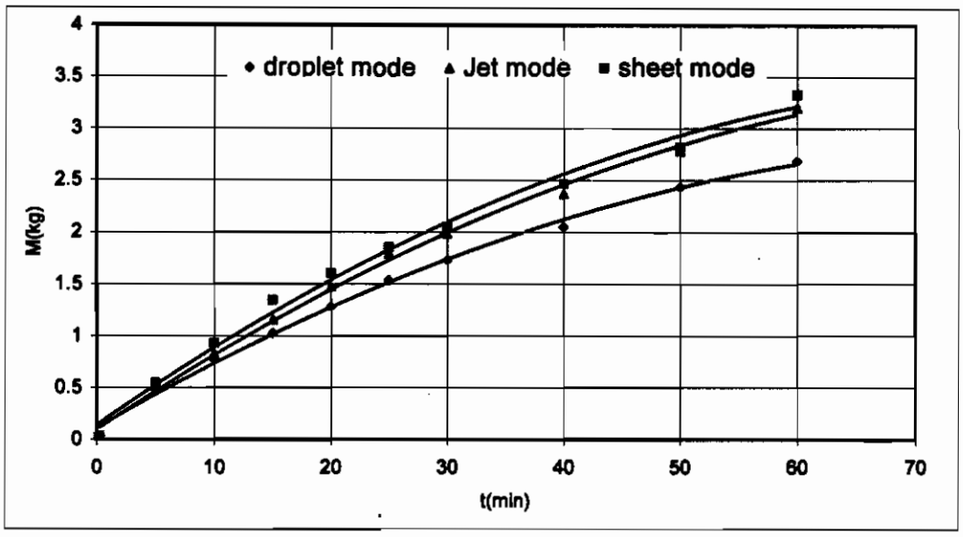

Figure 3.40: Comparison of the formed ice between droplet, jet and sheet mode for $\dot{m}_c$=0.162 kg/s "series arrangement".

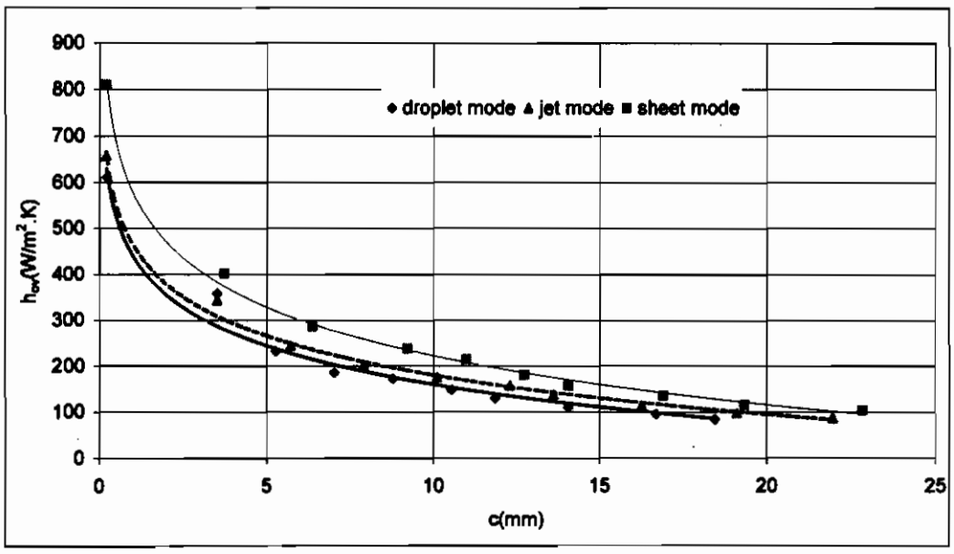

Figure 3.41: Comparison of the experimental overall heat transfer coefficient between droplet, jet and sheet modes for $\dot{m}_c$=0.162 kg/s "series arrangement".

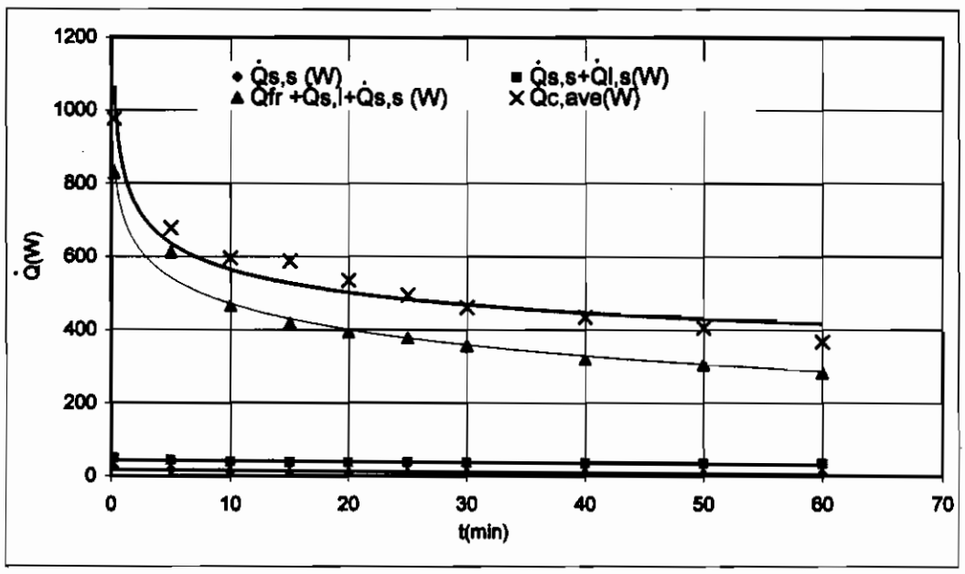

Figure 3.42: Energy balance for $\dot{m}_c$=0.162 &$\dot{m}_l$=0.0125 kg/s "series arrangement, droplet mode"

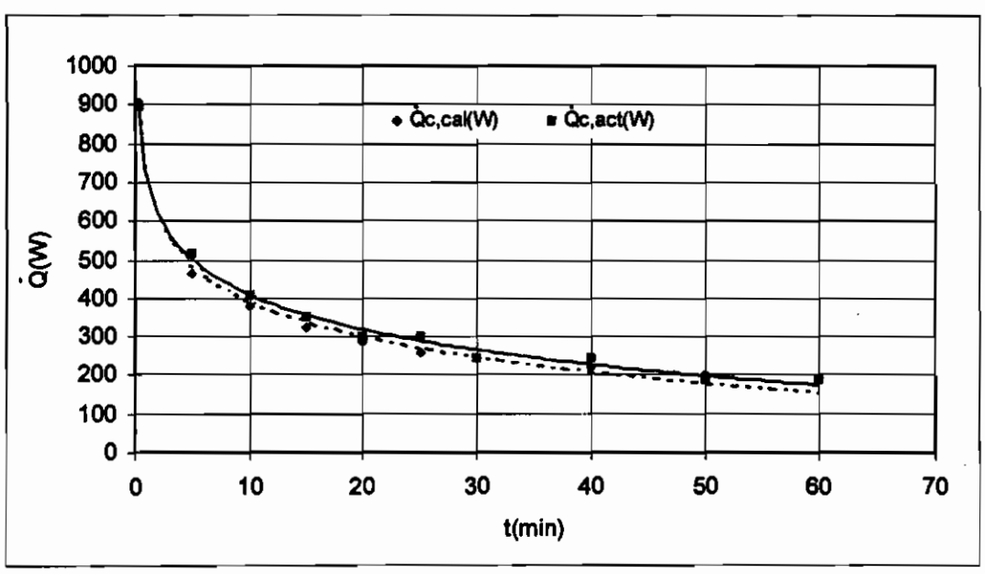

Figure 3.43: Comparison between actual and calculated rate of heat transfer from the test tubes to the coolant, for $\dot{m}_c$=0.162 kg/s & $\dot{m}_l$=0.0125 kg/s "series arrangement, droplet mode"

From the previous runs, one may note that: the ice formation rate, the heat transfer rate and the heat transfer coefficient decreases as ice accumulates on the tubes. One solution to meet this problem is to yield soft ice, which is then carried out with water as slurry. Consequently less ice will accumulate on the test tubes. This leads to better heat transfer process. This can be achieved by adding an additive like (acetone) to the water. [13]

Results are shown in the following run.

3.4-9 Experimental run 9(S, 2%acetone in water):

This experimental run is carried out under the following conditions:

1-Series arrangement, jet mode

2-Falling film liquid: 2% acetone in water

3-Room temperature: 23°C

4-Mass flow rate of coolant: 0.023 kg/s

5-Mass flow rate of the falling liquid: 0.025 kg/s

Calculations and energy balance for this run are shown in table (3.6) and figures (3.44 to 3.49). Figure (3.44) shows that the change of ΔT_c stops at 3.3°C which is higher than run 3(S), in which the change of ΔT_c stops at 2.3 °C for the same period.

Although, the experimental overall heat transfer coefficient h_{ov} increases, the accumulated ice on the test tubes is slightly reduced than that in run 3(S)(figure 3.45). This is due the reduction of the freezing point of the solution (water, with 2% acetone) to -5.6 °C [13]. The solution leaves the last test tube at a temperature, $T_{l,o}$ of -4 °C.For such case, the temperature potential for freezing reduces to (-10-(-5.6)=-4.4 °C). The test tubes surface temperature of the 2% acetone is a little higher than that of a pure water, due to less accumulation of ice on the tubes surfaces figure (3.49). Energy balance and comparison between $\dot{Q}_{c,act}$ and $\dot{Q}_{c,cal}$,are shown in figures (3.47) and (3.48) respectively ,which give a reasonable balance.

Table (3.9): Energy balance analysis for 2% acetone in water at $\dot{m}_c$=0.023 kg/s & $\dot{m}_f$=0.025kg/s "series arrangement, jet mode"

	Run#1	Run#2	Run#3	Run#4	Run#5	Run#6	Run#7	Run#8	Run#9	Run#10
t(min)	3	5	10	15	20	25	30	60	90	120
Δh(cm)		0.35	0.75	1.1	1.35	1.6	1.8	3.2	4.2	5
$Vx10^{-6}(m^3)$	140	224.1	480.1	704.2	864.2	1024	1152	2049	2689	3201
M(Kg)	0.14	0.224	0.48	0.704	0.864	1.024	1.152	2.049	2.689	3.201
c (mm)	0.965	1.522	3.308	4.852	5.954	7.057	7.939	14.11	18.52	22.05
$\Delta T_c(^oC)$	6	4.9	4.6	4.4	4.2	4.3	4.1	3.5	3.2	3.2
$\dot{Q}_c$(W)	462.1	377.4	354.3	338.9	323.5	331.2	315.8	269.6	246.5	246.5
$\dot{Q}_{c,ave}$(W)	360.7	349.7	359.3	373.1	344.1	331.2	333.4	315.3	295.3	286.1
$\dot{Q}_{s,l}$(W)	52.5	52.5	52.5	52.5	52.5	52.5	52.5	52.5	52.5	52.5
$\dot{Q}_{fr}$(W)	259	248.7	266.5	260.6	239.8	227.4	213.2	189.5	165.8	148
$\dot{Q}_{s,s}$(W)	7.933	7.618	8.162	7.981	7.346	6.965	6.53	5.804	5.079	4.535
$\dot{Q}_{ls,c}$(W)	26.12	26.12	26.12	26.12	26.12	26.12	26.12	26.12	26.12	26.12
$\dot{Q}_{a,f}$(W)	319.4	308.8	327.1	321	299.7	286.9	272.2	247.8	223.4	205.1
$\varepsilon = \dot{Q}_{a,f} / \dot{Q}_{c,ave}$	0.886	0.883	0.91	0.86	0.871	0.866	0.817	0.786	0.756	0.718
$T_i - T_c$ (^oC)	9.55	9.3	9.75	10.2	10.1	10.2	10.2	11.35	11.5	11.7
h_{ov}(W/m^2.K)	227.2	225.6	227.9	213.8	201.6	191	181.3	148.3	132	119.1
Re_c	86.65	86.65	86.65	86.65	86.65	86.65	86.65	86.65	86.65	86.65
$(\mu/\mu_s)^{0.14}$	1.068	1.046	1.038	1.036	1.034	1.032	1.029	1.023	1.018	1
h_i(W/m^2.K)	528.4	517.5	513.6	512.6	511.6	510.6	509.1	506.2	503.7	494.8
Re_f	121.6	121.6	121.6	121.6	121.6	121.6	121.6	121.6	121.6	121.6
h_o(W/m^2.K)	2487	2426	2253	2125	2045	1971	1917	1618	1464	1365
R_1(K/W)	0.098	0.1	0.101	0.101	0.101	0.102	0.102	0.103	0.103	0.105
R_3(ice) (K/W)	0.024	0.037	0.076	0.107	0.127	0.146	0.161	0.25	0.302	0.339
R_4(K/W)	0.018	0.018	0.017	0.017	0.017	0.016	0.016	0.015	0.014	0.014
UA(W/K)	7.133	6.445	5.146	4.45	4.082	3.785	3.584	2.722	2.383	2.183
$\dot{Q}_{c,cal}$ (W)	476.8	419.6	351.2	317.8	288.6	270.3	255.9	216.2	191.8	178.8
$\dot{Q}_{c,act}$ (W)	400.5	315.8	292.7	277.3	261.9	254.2	238.8	208	184.9	169.4
P.D= $\frac{(\dot{Q}_{c,cal} - \dot{Q}_{c,act})}{\dot{Q}_{c,cal}}$x100	16	24.74	16.66	12.74	9.257	5.95	6.697	3.825	3.64	5.231

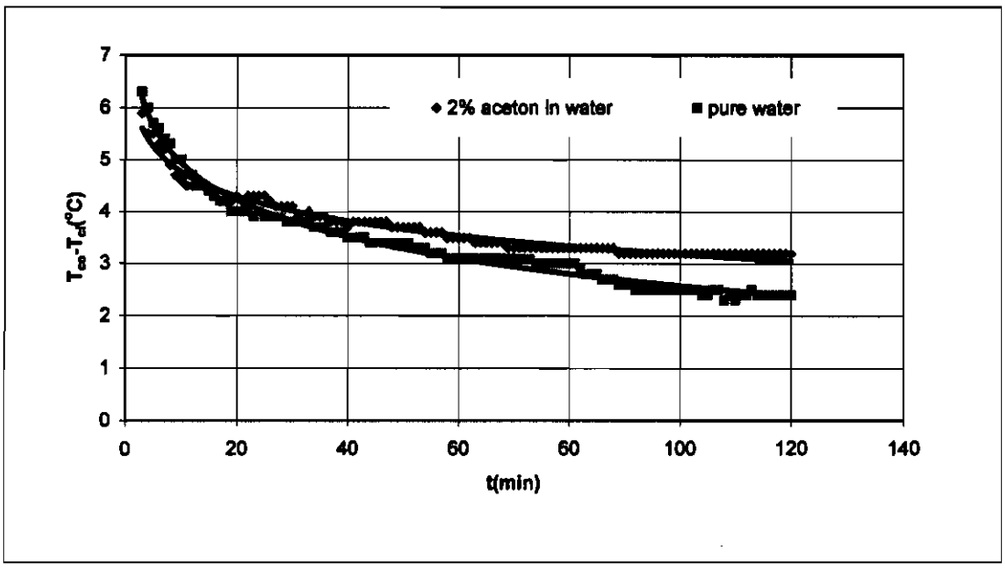

Figure 3.44:Comparison of ΔT_c changing with time between 2% aceton in water and pure water for $\dot{m}_c$=0.023 kg/s & $\dot{m}_l$=0.025 kg/s "series arrangement, jet mode"

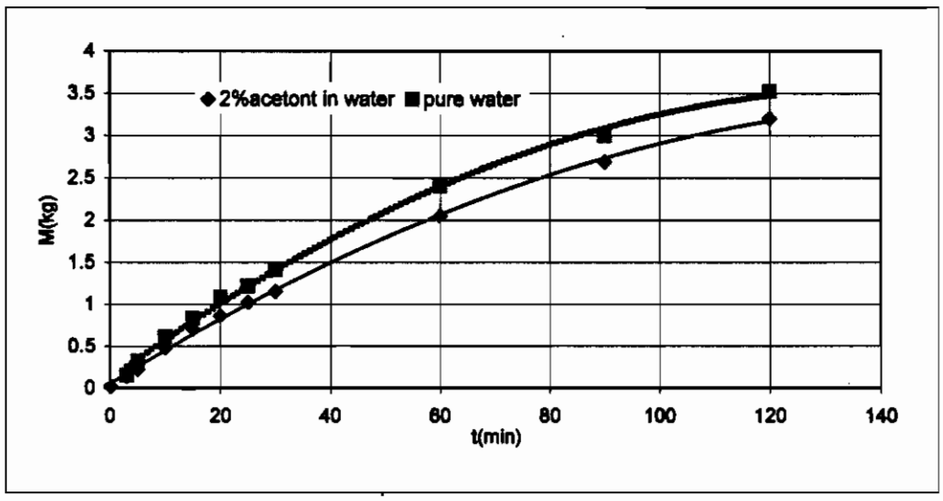

Figure 3.45,Comparison of the formed ice on the test tubes between 2%aceton in water & pure water, for $\dot{m}_c$=0.023 kg/s & $\dot{m}_l$=0.025 kg/s "series arrangement, jet mode"

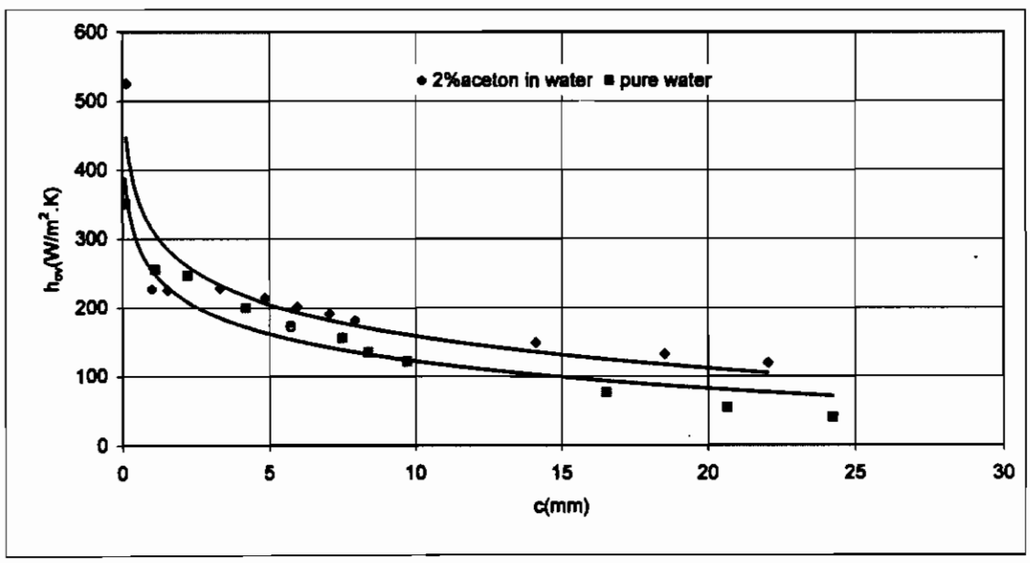

Figure 3.46: comparison of the experimental overall heat transfer coefficient between 2%aceton in water & pure water, for $\dot{m}_c$=0.023 kg/s & $\dot{m}_l$=0.025 kg/s "series arrangement, jet mode"

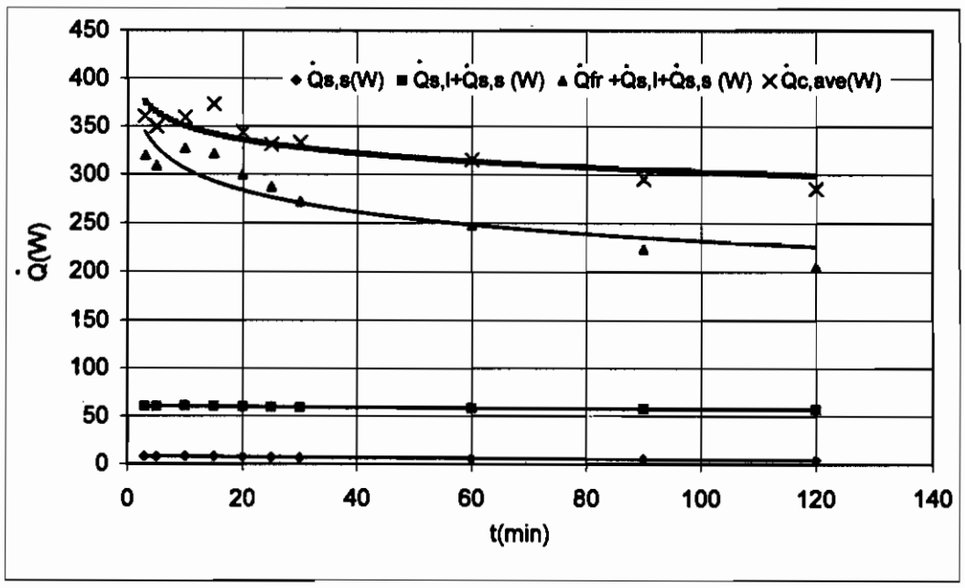

Figure 3.47: Energy balance for 2% aceton in water $\dot{m}_c$=0.023 kg/s & $\dot{m}_l$=0.025 kg/s "series arrangement, jet mode"

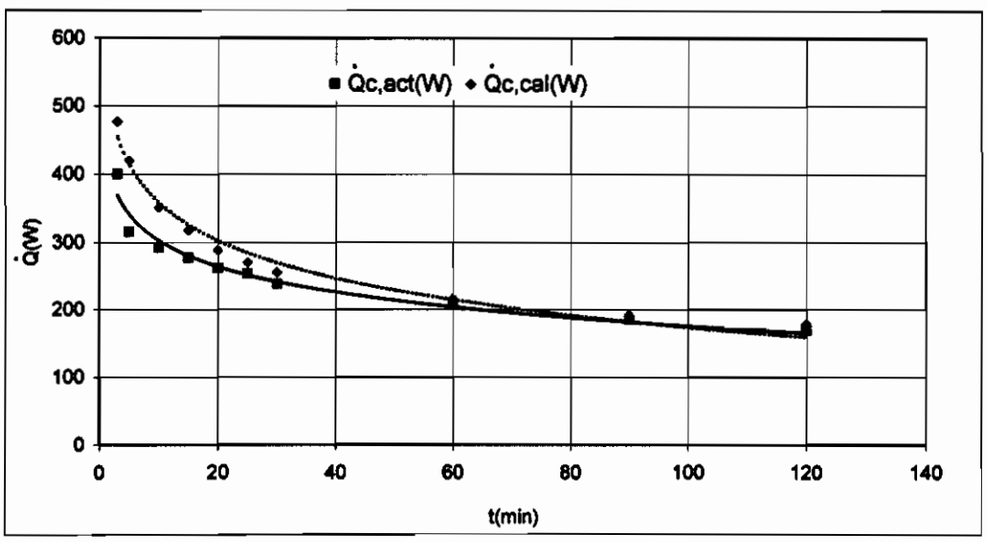

Figure 3.48: Comparison between actual and calculated rate of heat transfer from the test tubes to the coolant, for 2% aceton in water, $\dot{m}_c$=0.023 kg/s & $\dot{m}_l$=0.025 kg/s "series arrangement, jet mode"

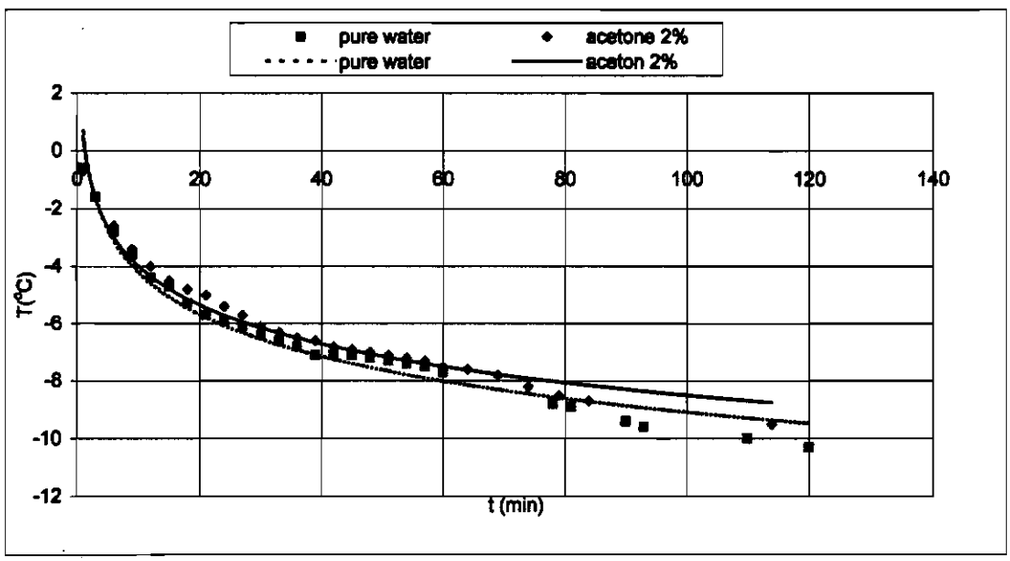

Figure 3-49: Comparison of test tubes surface temperature between pure water and 2% aceton in water with at $\dot{m}_c$=0.023 kg/s & $\dot{m}_l$=0.025 kg/s "series arrangement, jet mode"

3.5 Summary of results and discussion

The previous results can be summarized as follows:

1-The quantity of ice is highly affected by the flow rate of both the coolant and the falling film. Increasing either of them or both will increase the amount of ice formed. This is due to an increase in either or both of the inside or the outside heat transfer coefficient.

2-Within the experimental range tested, the series arrangement produces a larger quantity of ice (for coolant flow rate $\dot{m}_c$=0.162 kg/s, per tube) than the parallel one (for $\dot{m}_c$=0.162/7 kg/s per tube), due to an increase of the inside heat transfer coefficient and the coolant temperature difference.

3-The equations used to calculate the outside heat transfer coefficient, h_o, and the thermal resistance of the ice, R_{ice}, are valid until the tube spacing is filled with ice, since the ice increases in radial direction. After that the problem is no longer a falling film on horizontal tubes and the flow forms like a falling film on a vertical corrugated plate in which the ice accumulates normal to the central plane.

4-The experimental overall heat transfer coefficient, h_{ov}, is highly affected by the coolant and falling film flow rate, the resistance of the ice layer and the used arrangement.

5-Different modes of the falling film were investigated. When the valve of the feeding tubes is fully opened, the flow shows a sheet mode. This mode is shown clearly in the upper two test tubes, the rest shows sheet-jet mode. Jet mode is achieved by reducing the flow rate and it is observed clearly on the upper five tubes and the rest is a jet-droplet mode. With further decrease in the flow rate, a steady droplet mode on all over the test tubes was noticed.

6-Adding 2% acetone to water causes less accumulation of ice on the test tubes. However, no slurry of ice has been notified. Further studies are needed to study this phenomenon.

CHAPTER IV

CONCLUSIONS AND RECOMENDATIONS

4.1 Conclusions:

This experimental research will help in the analyzing and the constructing of cold thermal storage systems which are necessary for areas having hot climate such as Saudi Arabia. Electric utilities companies are recommended to encourage the use of such technique in order to reduce the peak demand on their generation and distribution systems. Manufacturers of air conditioning and refrigeration machines can also utilize such technique as an additional unite to save energy by their A/C chillers. Large projects that construct a central air conditioning system are also recommended to consider utilizing a similar technique.
The following are the conclusions derived from this experimental research:

1-Droplet, jet and sheet modes were shown clearly in the experimental runs. As the falling film flow increases, the mode changes from droplet to jet and finally to sheet mode. The droplet mode is the only steady falling flow on

the all test tubes. The jet mode is nearly steady for the upper five tubes, while the remained two tubes flow is a jet-droplet transition mode. The sheet mode shows a steady flow on the upper two test tubes only, while the rest of the tubes show sheet-jet transition mode.

2-The overall heat transfer coefficient is highly affected by the thermal resistance of the ice layer (x/k_{ice}). The heat transfer coefficient decreases with time as ice accumulates on the tube surfaces. As the thickness of ice increases, it acts as an insulating material. The heat transfer coefficient is also affected by the coolant flow rate, which affect the inside heat transfer coefficients the coolant flow rate is increased, the overall heat transfer coefficient increased. The same is true for the falling film flow rate. The overall heat transfer coefficient is also affected by the type of arrangement of the tubes used (parallel or series).

3-the rate of the ice formation is also dependable on: the coolant flow rate, the falling film flow rate and the arrangement of the tubes, due to the previous reasons.

4-It has been noticed that as the flow rate of the coolant or the falling film flow rate increases the ice

accumulation increases. Although, at high flow rate the temperature difference between the inlet and the outlet coolant temperatures ΔT_c is low and more accuracy in temperature measurements is required.

5-Series arrangement shows better performance in producing ice than parallel one for the same coolant flow rate to the test section, in the range of experimental runs tested. The series arrangement increases temperature difference and improves the inside heat transfer coefficient but reduces the inlet temperature to the test tube.

6-Adding 2% acetone to water was carried out in order to produce some ice as a slurry form in the water to reduce its accumulation over the tubes. It was found that less accumulation of ice on the test tubes is appeared. However, no slurry of ice has been notified.

4.2 Recommendation for future studies:

1-Further study is needed to obtain the optimum quantity of ice and the best method for discharging to minimize the melted ice and to compare between the falling film freezing on horizontal tubes and the immersed one.

2-Elaborate study of additives such as acetone is recommended to explore the possibility of producing ice in a slurry form. Refrigerant such as R-134a or similar is recommended to be used as a coolant in the experiments to allow study of ice formation as a slurry, since refrigerant could be allowed to evaporate at say (-2 °C to -3 °C).

3-Emulsion with freezing point of higher than 0 °C (say 6 °C to 13 °C) is highly recommended to be studied, these freezing points are about the same as chiller operating temperature. In this case the same traditional chiller can be used for thermal storage sources.

REFERENCES

1. ALDIGHAITHER,M.M. "A study of Alternatives of Conventional Roof Thermal Installation". A thesis submitted in partial fulfillment of the requirements for the degree of Science in Mechanical Engineering,1997.

2. ASHRAE.Design Guide for Cool Thermal Storage, 1993.

3. Intemann,P.A and M.Kazmierczak. "Heat Transfer and Ice Formation Deposited upon Cold Tube Bundles Immersed in Flowing Water-1. Convective Analysis". Int Journal of Heat Fluid Flow Vol.40.No.3,pp.557-572,1997.

4. Intemann,P.A and M.Kazmierczak."Convective heat transfer for cold tube bundles with ice formations in a stream of water at steady state ". Int Journal of Heat Fluid Flow 15,491-500,1994.

5. Inaba H.and S.Morita. "Flow and Cold Heat-Storage

Characteristics of Phase-Change Emulsion in a Coiled Double-Tube Heat Exchanger". Journal of Heat Transfer ,Vol.117,pp440-446, 1995.

6. Inaba,H.and K.Sato."Fundemental Study on Latent Cold Heat Storage by Means of Direct-Contact-Freezing between Oil Droplets and Cold Water Solution". Journal of Heat Transfer,Vol.118,pp 799-802,August 1996.

7. Perry,R.H, Chemical engineering handbook,6th Ed,1984.

8. Hu,X and A.M.Jacobi. "The Intertube Falling Film: Part 1-Flow characteristics, Mode Transitions and Hysteresis". Journal of Heat Transfer.Vol.118,pp 616-625 ,August 1996.

9. Incropera,F.P. and D.P.DeWitt.Introduction To Heat Transfer.Second Edition,1990.

10. Hu,X and A.M.Jacobi."The Intertube Falling Film:Part-2 Mode Effects on Sensible Heat Transfer to a Falling Liquid Film".Journal of Heat Transfer.Vol.118,pp 626-633 ,1996.

11. Tequipment Limited,The Refrigeration Test Bench TD30,1973.

12. ASHRAE,Fundamentals Handbook, "Natural Convection Heat Transfer Coefficients"1985.

13 Breck,W.,Brown,R. and Mc Cowan,J."Chemistry for Science and Engineering" McGrow.Hill 1st.Ed., Chemistry Series,2nd.Ed.1989.

APPENDEX-A

CONTROLLED TEMPERATURE COOLING MACHINE TD30

A.1 PURPOSE

A.2 DESCRIPTION OF CHIEF CYCLES

A.1 PURPOSE

The purpose of the controlled temperature cooling machine TD30 is that of a liquid-chilling unit, employing R.12 refrigerant to cool a solution of ethylene glycol. The unite is provided with instrumentation for the measurement of temperatures, pressures, flow-rates, and energy inputs so that a wide range of heat balance studies can be made while a group of additional experiments can be "plugged-in" to the bench, using either R.12 or glycol solution as a source of cooling.

A.2 DESCRIPTION OF CHIEF CYCLES

Controlled temperature cooling machine TD30, consists of three cycles namely: R12 cycle, glycol cycle and condensing water cycle.

A.2.1 R12 Cycle

R12 cycle is shown in figure (A.1). The open type-reciprocating compressor sucks R12 vapor and delivers it to the water-cooled condenser. The refrigerant is condensed and goes to the heat exchanger to be subcooled. Then it goes through the rotameter to the filter drier. The thermostatic expansion valve throttles R12 to the

chiller pressure and temperature. The refrigerant absorbs glycol thermal load and evaporates. R12 vapor goes back through pressure regulator and heat exchanger to compressor suction. Pressure regulator is adjusted to get nearly constant suction pressure (i,e constant temperature).

A.2.2 Ethylene glycol solution cycle

Glycol cycle is shown in figure (A.2).The pump delivers glycol through the chiller to loose its thermal heat there. Glycol goes through rotameter and bypass valve to glycol storage tank, back to the pump suction. After precooling glycol in the storage tank, the by pass valve is opened to use the glycol in the experiment .The glycol returns back to the storage tank. An electric heater is immersed to heat the glycol if required.

A.2.3 Water coolant cycle

Water comes down from cooling tower to water pump and then through flowmeter valve to the condenser as shown in figure A.3, to absorb its thermal load. Then, water is returned back to the cooling tower through rotameter. Water flow rate is adjusted by flowmeter valve to get the

required condensing water, to keep nearly constant condenser pressure.

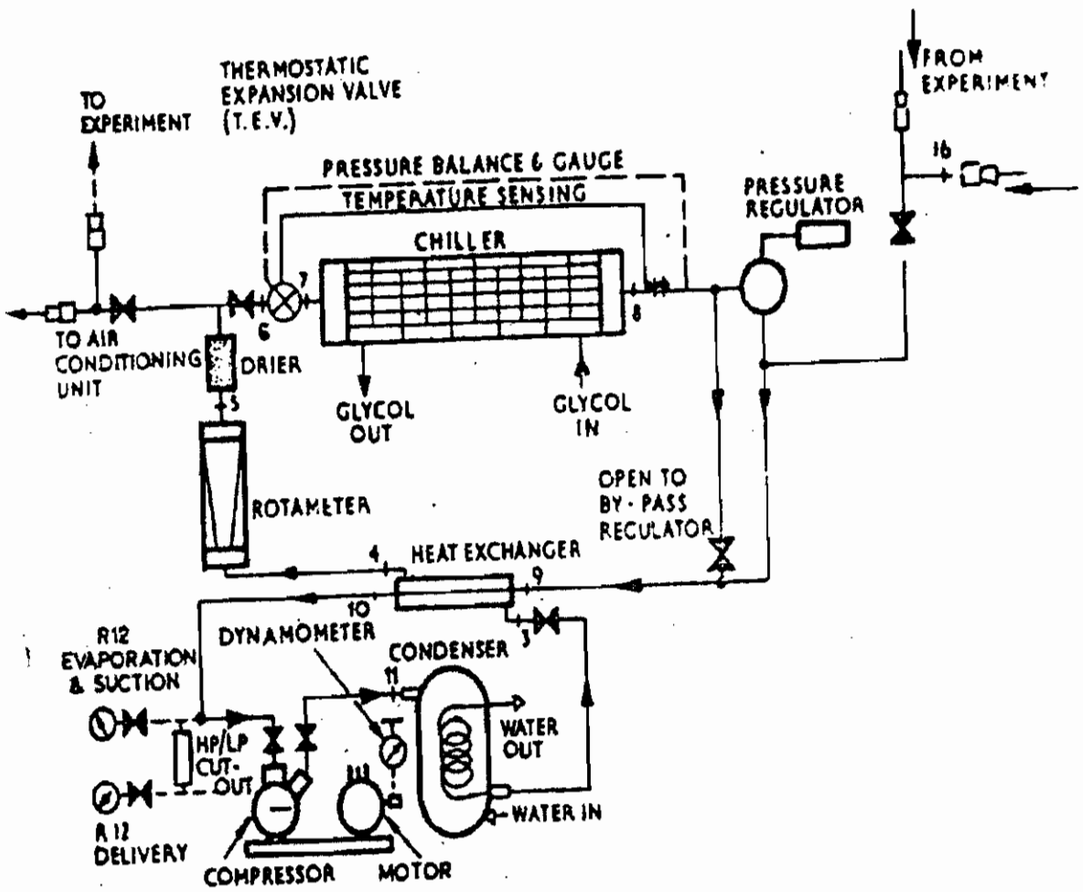

Figure A.1,Freon (R.12) cycle at the TD30 Machine

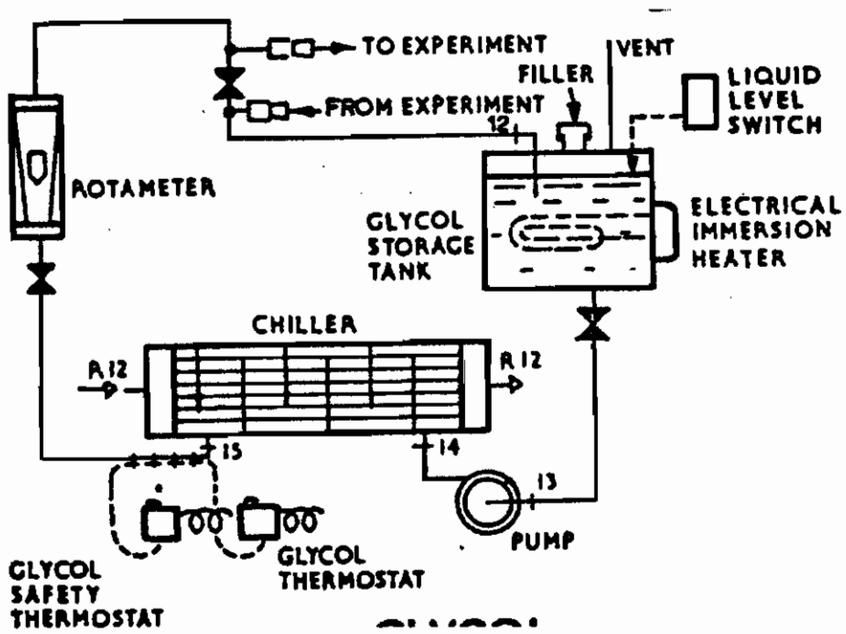

Figure A.2, Ethylene glycol cycle at the TD30 machine

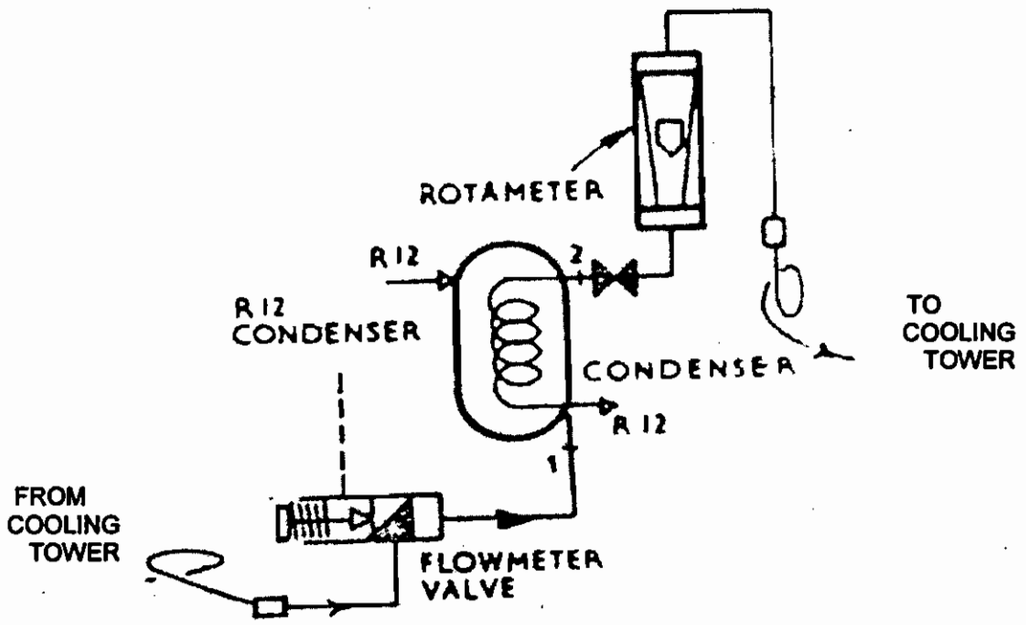

Figure A.3, Condensing water coolant cycle at the TD30 Machine.

APPENDEX-B

DATA RECORDED

Table B-1:Inlet and outlet temperature of the coolant and the falling water for m_c=0.38kg/s Parallel arrangement, Jet mode"RUN 1(P)

Time(min)	T_{ci}(C)	T_{co}(C)	T_{li}(C)	T_{lo}(C)	Δ Tc	Δ Tl	Q(W)
			5 minutes run				
0	-8.8	-8.2	0.5	0.2	0.6	0.3	763.53
1	-8.6	-8	0.5	0.1	0.6	0.4	763.53
2	-8.5	-8	0.4	0.1	0.5	0.3	636.27
3	-8.5	-8	0.4	0.1	0.5	0.3	636.27
4	-8.5	-8.1	0.3	0	0.4	0.3	509.02
5	-8.5	-8.1	0.3	0	0.4	0.3	509.02
			10 minutes run			Qc,ave(W)	636.27
0	-9	-8.4	0.5	0.1	0.6	0.4	763.53
1	-8.7	-8.1	0.5	0.2	0.6	0.3	763.53
2	-8.5	-8	0.5	0.1	0.5	0.4	636.27
3	-8.4	-7.9	0.5	0.1	0.5	0.4	636.27
4	-8.4	-7.9	0.5	0.2	0.5	0.3	636.27
5	-8.4	-7.9	0.3	0	0.5	0.3	636.27
6	-8.3	-7.9	0.3	0	0.4	0.3	509.02
7	-8.3	-7.9	0.3	0	0.4	0.3	509.02
8	-8.3	-7.9	0.3	0	0.4	0.3	509.02
9	-8.15	-7.75	0.3	0	0.4	0.3	509.02
10	-8.15	-7.75	0.3	0	0.4	0.3	509.02
			15 minutes run			Qc,ave(W)	598.10
0	-9	-8.4	0.5	0.2	0.6	0.3	763.53
1	-8.9	-8.3	0.5	0.2	0.6	0.3	763.53
2	-8.7	-8.1	0.5	0.2	0.6	0.3	763.53
3	-8.5	-8	0.4	0.1	0.5	0.3	636.27
4	-8.4	-7.9	0.5	0.1	0.5	0.4	636.27
5	-8.3	-7.9	0.3	0	0.4	0.3	509.02
6	-8.2	-7.8	0.3	0	0.4	0.3	509.02
7	-8.2	-7.8	0.3	0	0.4	0.3	509.02
8	-8.2	-7.8	0.3	0	0.4	0.3	509.02
9	-8.2	-7.8	0.3	0	0.4	0.3	509.02
10	-8.15	-7.75	0.3	0	0.4	0.3	509.02
11	-8.1	-7.7	0.3	0	0.4	0.3	509.02
12	-8.1	-7.8	0.3	0	0.3	0.3	381.76
13	-8.1	-7.8	0.3	0	0.3	0.3	381.76
14	-8.1	-7.7	0.3	0	0.4	0.3	509.02
15	-8.1	-7.8	0.3	0	0.3	0.3	381.76
			20 minutes run			Qc,ave(W)	547.19
0	-9.2	-8.6	0.5	0.1	0.6	0.4	763.53
1	-9.1	-8.4	0.5	0.2	0.7	0.3	890.78
2	-8.7	-8.1	0.5	0.1	0.6	0.4	763.53
3	-8.5	-8	0.5	0.1	0.5	0.4	636.27
4	-8.4	-7.9	0.5	0.2	0.5	0.3	636.27
5	-8.2	-7.8	0.4	0	0.4	0.4	509.02
6	-8.2	-7.8	0.4	0.1	0.4	0.3	509.02
7	-8.2	-7.8	0.4	0.1	0.4	0.3	509.02
8	-8.2	-7.8	0.4	0	0.4	0.4	509.02
9	-8.2	-7.8	0.3	0	0.4	0.3	509.02
10	-8.15	-7.75	0.3	0	0.4	0.3	509.02
11	-8.1	-7.7	0.3	0	0.4	0.3	509.02
12	-8.1	-7.7	0.3	0	0.4	0.3	509.02
13	-8.1	-7.7	0.3	0	0.4	0.3	509.02
14	-8.1	-7.7	0.4	0	0.4	0.4	509.02
15	-8.1	-7.7	0.3	0.1	0.4	0.2	509.02
16	-8.1	-7.8	0.3	0	0.3	0.3	381.76
17	-8.1	-7.8	0.3	0	0.3	0.3	381.76
18	-8.1	-7.8	0.3	0	0.3	0.3	381.76
19	-8.1	-7.8	0.3	0	0.3	0.3	381.76
20	-8.1	-7.8	0.3	0	0.3	0.3	381.76
						Qc,ave(W)	531.29

Time(min)	T_{ci}(C)	T_{co}(C)	T_{li}(C)	T_{lo}(C)	Δ Tc	Δ Tl	Qc(W)
25 minutes run							
0	-9	-8.4	0.4	0.2	0.6	0.2	763.53
1	-8.7	-8.1	0.5	0.1	0.6	0.4	763.53
2	-8.6	-8.1	0.3	0	0.5	0.3	636.27
3	-8.5	-8	0.5	0.1	0.5	0.4	636.27
4	-8.4	-7.9	0.4	0.1	0.5	0.3	636.27
5	-8.2	-7.8	0.4	0.1	0.4	0.3	509.02
6	-8.2	-7.8	0.4	0.1	0.4	0.3	509.02
7	-8.2	-7.8	0.4	0.1	0.4	0.3	509.02
8	-8.2	-7.8	0.4	0.1	0.4	0.3	509.02
9	-8.2	-7.8	0.4	0.1	0.4	0.3	509.02
10	-8.15	-7.75	0.4	0.1	0.4	0.3	509.02
11	-8.1	-7.7	0.4	-0.1	0.4	0.5	509.02
12	-8.1	-7.7	0.3	0	0.4	0.3	509.02
13	-8.1	-7.7	0.3	0	0.4	0.3	509.02
14	-8.1	-7.7	0.3	0	0.4	0.3	509.02
15	-8.1	-7.7	0.3	-0.1	0.4	0.4	509.02
16	-8.1	-7.8	0.3	0	0.3	0.3	381.76
17	-8.1	-7.8	0.3	0	0.3	0.3	381.76
18	-8.2	-7.8	0.3	0	0.4	0.3	509.02
19	-8.2	-7.8	0.3	0	0.4	0.3	509.02
20	-8.2	-7.8	0.3	0	0.4	0.3	509.02
21	-8.2	-7.8	0.3	0	0.4	0.3	509.02
22	-8.2	-7.9	0.3	0	0.3	0.3	381.76
23	-8.2	-7.9	0.3	0	0.3	0.3	381.76
24	-8.2	-7.9	0.3	0	0.3	0.3	381.76
25	-8.2	-7.9	0.3	0	0.3	0.3	381.76
		30 minutes run				Qc,ave(W)	511.56
0	-9.1	-8.5	0.5	0.1	0.6	0.4	763.53
1	-8.8	-8.2	0.5	0.2	0.6	0.3	763.53
2	-8.6	-8.1	0.4	0.1	0.5	0.3	636.27
3	-8.5	-8	0.4	0.1	0.5	0.3	636.27
4	-8.4	-7.9	0.4	0.1	0.5	0.3	636.27
5	-8.2	-7.8	0.5	0.1	0.4	0.4	509.02
6	-8.2	-7.8	0.5	0.1	0.4	0.4	509.02
7	-8.2	-7.8	0.4	0	0.4	0.4	509.02
8	-8.2	-7.8	0.4	0	0.4	0.4	509.02
9	-8.2	-7.8	0.4	0	0.4	0.4	509.02
10	-8.15	-7.75	0.4	0	0.4	0.4	509.02
11	-8.1	-7.7	0.4	0	0.4	0.4	509.02
12	-8.1	-7.7	0.4	0	0.4	0.4	509.02
13	-8.1	-7.7	0.3	0	0.4	0.3	509.02
14	-8.1	-7.8	0.3	0	0.3	0.3	381.76
15	-8.1	-7.8	0.3	0	0.3	0.3	381.76
16	-8.1	-7.8	0.3	0	0.3	0.3	381.76
17	-8.2	-7.8	0.3	0	0.4	0.3	509.02
18	-8.2	-7.8	0.3	0	0.4	0.3	509.02
19	-8.2	-7.8	0.3	0	0.4	0.3	509.02
20	-8.2	-7.9	0.3	0	0.3	0.3	381.76
21	-8.2	-7.8	0.3	0	0.4	0.3	509.02
22	-8.2	-7.8	0.3	0	0.4	0.3	509.02
23	-8.2	-7.8	0.3	0	0.4	0.3	509.02
24	-8.2	-7.8	0.3	0	0.4	0.3	509.02
25	-8.2	-7.9	0.3	0	0.3	0.3	381.76
26	-8.2	-7.9	0.3	0	0.3	0.3	381.76
27	-8.2	-7.9	0.3	0	0.3	0.3	381.76
28	-8.2	-7.9	0.3	0	0.3	0.3	381.76
29	-8.2	-7.9	0.3	0	0.3	0.3	381.76
30	-8.2	-7.9	0.3	0	0.3	0.3	381.76
						Qc,ave(W)	494.17

Time(min)	T_{ci}(C)	T_{co}(C)	T_{li}(C)	T_{lo}(C)	Δ Tc	Δ Tl	Qc(W)
45minutes run							
0	-8.8	-8.2	0.4	0	0.6	0.4	763.53
1	-8.6	-8.1	0.4	0	0.5	0.4	636.27
2	-8.5	-8	0.4	0	0.5	0.4	636.27
3	-8.4	-7.9	0.5	0.1	0.5	0.4	636.27
4	-8.2	-7.8	0.5	0.1	0.4	0.4	509.02
5	-8.2	-7.8	0.5	0.2	0.4	0.3	509.02
6	-8.2	-7.8	0.3	0	0.4	0.3	509.02
7	-8.2	-7.8	0.3	0	0.4	0.3	509.02
8	-8.2	-7.8	0.3	0	0.4	0.3	509.02
9	-8.15	-7.75	0.3	0	0.4	0.3	509.02
10	-8.1	-7.7	0.3	0	0.4	0.3	509.02
11	-8.1	-7.7	0.3	0	0.4	0.3	509.02
12	-8.1	-7.7	0.3	0	0.4	0.3	509.02
13	-8.1	-7.7	0.3	0	0.4	0.3	509.02
14	-8.1	-7.8	0.3	0	0.3	0.3	381.76
15	-8.1	-7.8	0.3	0	0.3	0.3	381.76
16	-8.1	-7.8	0.3	0	0.3	0.3	381.76
17	-8.2	-7.8	0.3	0	0.4	0.3	509.02
18	-8.2	-7.8	0.3	0	0.4	0.3	509.02
19	-8.2	-7.8	0.3	0	0.4	0.3	509.02
20	-8.2	-7.8	0.3	0	0.4	0.3	509.02
21	-8.1	-7.8	0.3	0	0.3	0.3	381.76
22	-8.2	-7.8	0.3	0	0.4	0.3	509.02
23	-8.2	-7.8	0.3	0	0.4	0.3	509.02
24	-8.2	-7.9	0.3	0	0.3	0.3	381.76
25	-8.2	-7.9	0.3	0	0.3	0.3	381.76
26	-8.3	-7.9	0.3	0	0.4	0.3	509.02
27	-8.3	-7.9	0.3	0	0.4	0.3	509.02
28	-8.3	-7.9	0.3	0	0.4	0.3	509.02
29	-8.3	-7.9	0.3	0	0.4	0.3	509.02
30	-8.4	-8.1	0.3	0	0.3	0.3	381.76
31	-8.4	-8.1	0.3	0	0.3	0.3	381.76
32	-8.4	-8.1	0.3	0	0.3	0.3	381.76
33	-8.5	-8.2	0.3	0	0.3	0.3	381.76
34	-8.5	-8.2	0.3	0	0.3	0.3	381.76
35	-8.5	-8.2	0.3	0	0.3	0.3	381.76
36	-8.6	-8.2	0.3	0	0.4	0.3	509.02
37	-8.6	-8.2	0.3	0	0.4	0.3	509.02
38	-8.8	-8.4	0.3	0	0.4	0.3	509.02
39	-8.4	-8.1	0.3	0	0.3	0.3	381.76
40	-8.3	-8	0.3	0	0.3	0.3	381.76
41	-8.2	-7.9	0.3	0	0.3	0.3	381.76
42	-8.2	-7.9	0.3	0	0.3	0.3	381.76
43	-8.2	-7.9	0.3	0	0.3	0.3	381.76
44	-8.2	-8	0.3	0	0.2	0.3	254.51
45	-8.2	-8	0.3	0	0.2	0.3	254.51
60minutes run						Qc,ave(W)	463.77
0	-8.8	-8.2	0.5	0.1	0.6	0.4	763.53
1	-8.6	-8.1	0.5	0.1	0.5	0.4	636.27
2	-8.5	-8	0.5	0.1	0.5	0.4	636.27
3	-8.4	-7.9	0.5	0.1	0.5	0.4	636.27
4	-8.2	-7.8	0.5	0.1	0.4	0.4	509.02
5	-8.2	-7.8	0.5	0.1	0.4	0.4	509.02
6	-8.2	-7.8	0.4	0.1	0.4	0.3	509.02
7	-8.2	-7.8	0.4	0.1	0.4	0.3	509.02
8	-8.2	-7.8	0.4	0.1	0.4	0.3	509.02
9	-8.15	-7.75	0.4	0	0.4	0.4	509.02
10	-8.1	-7.7	0.4	0	0.4	0.4	509.02
11	-8.1	-7.7	0.3	0	0.4	0.3	509.02
12	-8.1	-7.7	0.3	0	0.4	0.3	509.02
13	-8.1	-7.7	0.3	0	0.4	0.3	509.02
14	-8.1	-7.8	0.3	0	0.3	0.3	381.76
15	-8.1	-7.8	0.3	0	0.3	0.3	381.76
16	-8.1	-7.8	0.3	0	0.3	0.3	381.76
17	-8.2	-7.8	0.3	0	0.4	0.3	509.02
18	-8.2	-7.8	0.3	0	0.4	0.3	509.02

Time(min)	T_{ci}(C)	T_{co}(C)	T_{li}(C)	T_{lo}(C)	Δ Tc	Δ Tl	Qc(W)
21	-8.1	-7.8	0.3	0	0.3	0.3	381.76
22	-8.2	-7.8	0.3	0	0.4	0.3	509.02
23	-8.2	-7.8	0.3	0	0.4	0.3	509.02
24	-8.2	-7.9	0.3	0	0.3	0.3	381.76
25	-8.2	-7.9	0.3	0	0.3	0.3	381.76
26	-8.3	-7.9	0.3	0	0.4	0.3	509.02
27	-8.3	-7.9	0.3	0	0.4	0.3	509.02
28	-8.3	-7.9	0.3	0	0.4	0.3	509.02
29	-8.3	-7.9	0.3	0	0.4	0.3	509.02
30	-8.4	-8.1	0.3	0	0.3	0.3	381.76
31	-8.4	-8.1	0.3	0	0.3	0.3	381.76
32	-8.4	-8.1	0.3	0	0.3	0.3	381.76
33	-8.5	-8.2	0.3	0	0.3	0.3	381.76
34	-8.5	-8.2	0.3	0	0.3	0.3	381.76
35	-8.5	-8.2	0.3	0	0.3	0.3	381.76
36	-8.6	-8.2	0.3	0	0.4	0.3	509.02
37	-8.6	-8.2	0.3	0	0.4	0.3	509.02
38	-8.8	-8.4	0.3	0	0.4	0.3	509.02
39	-8.4	-8.1	0.3	0	0.3	0.3	381.76
40	-8.3	-8	0.3	0	0.3	0.3	381.76
41	-8.2	-7.9	0.3	0	0.3	0.3	381.76
42	-8.2	-7.9	0.3	0	0.3	0.3	381.76
43	-8.2	-7.9	0.3	0	0.3	0.3	381.76
44	-8.2	-8	0.3	0	0.2	0.3	254.51
45	-8.2	-8	0.3	0	0.2	0.3	254.51
46	-8.3	-8	0.3	0	0.3	0.3	381.76
47	-8.3	-8	0.3	0	0.3	0.3	381.76
48	-8.3	-8.1	0.3	0	0.2	0.3	254.51
49	-8.4	-8.1	0.3	0	0.3	0.3	381.76
50	-8.4	-8.1	0.3	0	0.3	0.3	381.76
51	-8.4	-8.2	0.3	0	0.2	0.3	254.51
52	-8.4	-8.2	0.3	0	0.2	0.3	254.51
53	-8.4	-8.2	0.3	0	0.2	0.3	254.51
54	-8.4	-8.2	0.3	0	0.2	0.3	254.51
55	-8.4	-8.2	0.3	0	0.2	0.3	254.51
56	-8.4	-8.2	0.3	0	0.2	0.3	254.51
57	-8.4	-8.2	0.3	0	0.2	0.3	254.51
58	-8.5	-8.2	0.3	0	0.3	0.3	381.76
59	-8.5	-8.3	0.3	0	0.2	0.3	254.51
60	-8.5	-8.2	0.3	0	0.3	0.3	381.76
61	-8.5	-8.2	0.3	0	0.3	0.3	381.76
62	-8.6	-8.3	0.3	0	0.3	0.3	381.76
63	-8.6	-8.4	0.3	0	0.2	0.3	254.51
64	-8.7	-8.4	0.3	0	0.3	0.3	381.76
65	-8.7	-8.4	0.3	0	0.3	0.3	381.76
66	-8.8	-8.6	0.3	0	0.2	0.3	254.51
67	-8.8	-8.6	0.3	0	0.2	0.3	254.51
68	-8.8	-8.5	0.3	0	0.3	0.3	381.76
69	-8.8	-8.6	0.3	0	0.2	0.3	254.51
70	-8.8	-8.6	0.3	0	0.2	0.3	254.51
71	-8.8	-8.6	0.3	0	0.2	0.3	254.51
72	-8.9	-8.6	0.3	0	0.3	0.3	381.76
73	-8.9	-8.7	0.3	0	0.2	0.3	254.51
74	-9	-8.8	0.3	0	0.2	0.3	254.51
75	-9	-8.8	0.3	0	0.2	0.3	254.51
76	-9.1	-8.9	0.3	0	0.2	0.3	254.51
77	-9.1	-8.9	0.3	0	0.2	0.3	254.51
78	-9.2	-9	0.3	0	0.2	0.3	254.51
79	-9.3	-9.1	0.3	0	0.2	0.3	254.51
80	-9.3	-9.1	0.3	0	0.2	0.3	254.51
						Qc,ave(W)	391.31

Table B-2 :Inlet and outlet temperature of the coolant and the falling water for $\dot{m}_c$=0.162kg/s "Parallel arrangement,jet mode"RUN 2(P)

Time(min)	T_{ci}(C)	T_{co}(C)	T_{wi}(C)	T_{wo}(C)	Δ Tc	Δ Tw	Qc(W)
80 minutes run							
0	-11	-10.3	0.9	0.3	0.7	0.6	380
1	-11	-9.9	0.7	0.1	1.1	0.6	597
2	-10.8	-9.9	0.6	0.2	0.9	0.4	488
3	-10.4	-9.6	0.5	0.1	0.8	0.4	434
4	-10.5	-9.7	0.5	0.1	0.8	0.4	434
5	-10.1	-9.3	0.4	0	0.8	0.4	434
6	-9.8	-9.3	0.4	0.1	0.5	0.3	271
7	-9.8	-9.2	0.3	0	0.6	0.3	326
8	-9.7	-9.1	0.3	0.1	0.6	0.2	326
9	-9.6	-9	0.3	0	0.6	0.3	326
10	-9.5	-8.9	0.3	0.2	0.6	0.1	326
11	-9.4	-8.8	0.3	0	0.6	0.3	326
12	-9.3	-8.8	0.3	0	0.5	0.3	271
13	-9.3	-8.7	0.3	0	0.6	0.3	326
14	-9.2	-8.6	0.3	0	0.6	0.3	326
15	-9.2	-8.6	0.3	0.1	0.6	0.2	326
16	-9.2	-8.6	0.3	0.1	0.6	0.2	326
17	-9.2	-8.6	0.3	0.1	0.6	0.2	326
18	-9.2	-8.6	0.3	0	0.6	0.3	326
19	-9.2	-8.6	0.3	0	0.6	0.3	326
20	-9.3	-8.7	0.3	0	0.6	0.3	326
21	-9.4	-8.8	0.3	0	0.6	0.3	326
22	-9.4	-8.8	0.3	0	0.6	0.3	326
23	-9.4	-8.8	0.3	0.2	0.6	0.1	326
24	-9.5	-8.9	0.3	0.1	0.6	0.2	326
25	-9.5	-8.9	0.3	0	0.6	0.3	326
26	-9.5	-8.9	0.3	0	0.6	0.3	326
27	-9.6	-9	0.3	0	0.6	0.3	326
28	-9.6	-9	0.3	0	0.6	0.3	326
29	-9.6	-9.1	0.3	0	0.5	0.3	271
30	-9.6	-9.1	0.3	0	0.5	0.3	271
31	-9.6	-9.1	0.3	0.1	0.5	0.2	271
32	-9.6	-9.1	0.3	0.2	0.5	0.1	271
33	-9.6	-9.1	0.3	0.1	0.5	0.2	271
34	-9.6	-9.1	0.3	0	0.5	0.3	271
35	-9.8	-9.2	0.3	0	0.6	0.3	326
36	-9.8	-9.2	0.3	0	0.6	0.3	326
37	-9.8	-9.2	0.3	0.1	0.6	0.2	326
38	-9.8	-9.2	0.3	0.1	0.6	0.2	326
39	-9.8	-9.2	0.3	0	0.6	0.3	326
40	-9.8	-9.2	0.3	0	0.6	0.3	326
41	-9.8	-9.2	0.3	0	0.6	0.3	326
42	-9.8	-9.2	0.3	0.2	0.6	0.1	326
43	-9.8	-9.2	0.3	0.1	0.6	0.2	326
44	-10	-9.4	0.3	0	0.6	0.3	326
45	-9.9	-9.4	0.3	0	0.5	0.3	271
46	-9.9	-9.4	0.3	0.1	0.5	0.2	271
47	-9.9	-9.4	0.3	0.1	0.5	0.2	271
48	-9.9	-9.4	0.3	0	0.5	0.3	271
49	-9.9	-9.4	0.3	0	0.5	0.3	271
50	-9.9	-9.4	0.3	0	0.5	0.3	271
51	-9.9	-9.4	0.3	0	0.5	0.3	271
52	-9.9	-9.4	0.3	0	0.5	0.3	271
53	-9.9	-9.4	0.3	0.1	0.5	0.2	271
54	-9.9	-9.4	0.3	0.1	0.5	0.2	271
55	-9.9	-9.4	0.3	0.1	0.5	0.2	271
56	-9.9	-9.4	0.3	0	0.5	0.3	271
57	-9.4	-8.8	0.3	0	0.6	0.3	326
58	-9.4	-8.8	0.3	0	0.6	0.3	326
59	-9.5	-8.9	0.3	0	0.6	0.3	326
60	-9.6	-9.1	0.3	0	0.5	0.3	271
61	-9.7	-9.2	0.3	0.1	0.5	0.2	271
62	-9.8	-9.2	0.3	0	0.6	0.3	326

63	-9.8	-9.3	0.3	0	0.5	0.3	271
64	-9.8	-9.3	0.3	0.1	0.5	0.2	271
65	-9.9	-9.4	0.3	0	0.5	0.3	271
66	-9.9	-9.4	0.3	0	0.5	0.3	271
67	-9.9	-9.4	0.3	0.2	0.5	0.1	271
68	-9.9	-9.4	0.3	0	0.5	0.3	271
69	-9.9	-9.4	0.3	0	0.5	0.3	271
70	-9.9	-9.4	0.3	0.1	0.5	0.2	271
71	-9.9	-9.5	0.3	0	0.4	0.3	217
72	-9.8	-9.4	0.3	0	0.4	0.3	217
73	-9.8	-9.4	0.3	0.1	0.4	0.2	217
74	-9.8	-9.4	0.3	0	0.4	0.3	217
75	-9.8	-9.4	0.3	0	0.4	0.3	217
76	-9.8	-9.4	0.3	0.1	0.4	0.2	217
77	-9.8	-9.4	0.3	0	0.4	0.3	217
78	-9.8	-9.4	0.3	0	0.4	0.3	217
79	-9.8	-9.4	0.3	0	0.4	0.3	217
80	-9.8	-9.4	0.3	0.1	0.4	0.2	217
						Qc,ave(W)	302.13

Table B-3:Inlet and outlet temperature of the coolant and the falling water for mc=0.023kg/s "Series arrangement, jet mode" RUN 3(S)

120 minutes run

Time(min)	T_{ci}(C)	T_{co}(C)	T_{wi}(C)	T_{wo}(C)	Δ Tc	Δ Tw	Qc(W)
0	-12.7	-10.6	0.5	0.2	2.1	0.3	161.76
1	-12.7	-8.5	0.4	0.1	4.2	0.3	323.51
2	-12.8	-6.7	0.5	0.2	6.1	0.3	469.86
3	-12.8	-6.5	0.4	0	6.3	0.4	485.27
4	-12.7	-6.7	0.4	0.1	6	0.3	462.16
5	-12.7	-7	0.4	0.2	5.7	0.2	439.05
6	-12.6	-7	0.5	0.1	5.6	0.4	431.35
7	-12.5	-7.1	0.5	0.1	5.4	0.4	415.95
8	-12.5	-7.2	0.4	0.1	5.3	0.3	408.24
9	-12.4	-7.4	0.3	0.1	5	0.2	385.14
10	-12.5	-7.5	0.4	0.1	5	0.3	385.14
11	-12.3	-7.6	0.4	0.1	4.7	0.3	362.03
12	-12.3	-7.6	0.4	0.1	4.7	0.3	362.03
13	-12.2	-7.7	0.3	0	4.5	0.3	346.62
14	-12.2	-7.7	0.3	0	4.5	0.3	346.62
15	-12.2	-7.8	0.3	0	4.4	0.3	338.92
16	-12.1	-7.8	0.3	0	4.3	0.3	331.22
17	-12.1	-7.9	0.3	0	4.2	0.3	323.51
18	-12.1	-7.9	0.3	0	4.2	0.3	323.51
19	-11.9	-7.9	0.3	0	4	0.3	308.11
20	-12	-8	0.3	0	4	0.3	308.11
21	-11.9	-7.9	0.3	0	4	0.3	308.11
22	-11.9	-7.9	0.3	0	4	0.3	308.11
23	-11.9	-8	0.3	0	3.9	0.3	300.41
24	-11.9	-7.9	0.3	0	4	0.3	308.11
25	-11.9	-8	0.3	0	3.9	0.3	300.41
26	-11.9	-8	0.3	0	3.9	0.3	300.41
27	-11.9	-8	0.3	0	3.9	0.3	300.41
28	-11.9	-8	0.3	0	3.9	0.3	300.41
29	-11.9	-8	0.3	0	3.9	0.3	300.41
30	-11.9	-8	0.3	0	3.9	0.3	300.41
31	-11.9	-8	0.3	0	3.9	0.3	300.41
32	-11.9	-8	0.3	0	3.9	0.3	300.41
33	-11.9	-8	0.3	0	3.9	0.3	300.41
34	-11.9	-8	0.3	0	3.9	0.3	300.41
35	-11.9	-8.1	0.3	0	3.8	0.3	292.70
36	-11.9	-8.1	0.3	0	3.8	0.3	292.70
37	-11.9	-8.1	0.3	0	3.8	0.3	292.70
38	-11.9	-8.1	0.3	0	3.8	0.3	292.70
39	-11.9	-8.1	0.3	0	3.8	0.3	292.70
40	-11.9	-8.1	0.3	0	3.8	0.3	292.70
41	-11.9	-8.2	0.3	0	3.7	0.3	285.00
42	-11.9	-8.2	0.3	0	3.7	0.3	285.00
43	-11.9	-8.2	0.3	0	3.7	0.3	285.00
44	-12	-8.3	0.3	0	3.7	0.3	285.00
45	-12.1	-8.3	0.3	0	3.8	0.3	292.70
46	-12.1	-8.3	0.3	0	3.8	0.3	292.70
47	-12.1	-8.3	0.3	0	3.8	0.3	292.70
48	-12.1	-8.3	0.3	0	3.8	0.3	292.70
49	-12.1	-8.4	0.3	0	3.7	0.3	285.00
50	-12.1	-8.4	0.3	0	3.7	0.3	285.00
51	-12.1	-8.4	0.3	0	3.7	0.3	285.00
52	-12.1	-8.5	0.3	0	3.6	0.3	277.30
53	-12.1	-8.5	0.3	0	3.6	0.3	277.30
54	-12.1	-8.6	0.3	0	3.5	0.3	269.59
55	-12.1	-8.6	0.3	0	3.5	0.3	269.59
56	-12.1	-8.6	0.3	0	3.5	0.3	269.59
57	-12.1	-8.6	0.3	0	3.5	0.3	269.59
58	-12.1	-8.7	0.3	0	3.4	0.3	261.89
59	-12.1	-8.7	0.3	0	3.4	0.3	261.89

Time(min)	T_{ci}(C)	T_{co}(C)	T_{wi}(C)	T_{wo}(C)	ΔTc	ΔTw	Qc(W)
60	-12.1	-8.7	0.3	0	3.4	0.3	261.89
61	-12.1	-8.7	0.3	0	3.4	0.3	261.89
62	-12.1	-8.8	0.3	0	3.3	0.3	254.19
63	-12.1	-8.8	0.3	0	3.3	0.3	254.19
64	-12.1	-8.9	0.3	0	3.2	0.3	246.49
65	-12.2	-9	0.3	0	3.2	0.3	246.49
66	-12.2	-9	0.3	0	3.2	0.3	246.49
67	-12.2	-9.1	0.3	0	3.1	0.3	238.78
68	-12.2	-9.1	0.3	0	3.1	0.3	238.78
69	-12.3	-9.2	0.3	0	3.1	0.3	238.78
70	-12.3	-9.2	0.3	0	3.1	0.3	238.78
71	-12.3	-9.2	0.3	0	3.1	0.3	238.78
72	-12.3	-9.2	0.3	0	3.1	0.3	238.78
73	-12.3	-9.2	0.3	0	3.1	0.3	238.78
74	-12.3	-9.3	0.3	0	3	0.3	231.08
75	-12.3	-9.3	0.3	0	3	0.3	231.08
76	-12.3	-9.3	0.3	0	3	0.3	231.08
77	-12.3	-9.3	0.3	0	3	0.3	231.08
78	-12.3	-9.3	0.3	0	3	0.3	231.08
79	-12.4	-9.4	0.3	0	3	0.3	231.08
80	-12.4	-9.4	0.3	0	3	0.3	231.08
81	-12.4	-9.4	0.3	0	3	0.3	231.08
82	-12.4	-9.5	0.3	0	2.9	0.3	223.38
83	-12.4	-9.6	0.3	0	2.8	0.3	215.68
84	-12.4	-9.6	0.3	0	2.8	0.3	215.68
85	-12.4	-9.6	0.3	0	2.8	0.3	215.68
86	-12.4	-9.7	0.3	0	2.7	0.3	207.97
87	-12.4	-9.7	0.3	0	2.7	0.3	207.97
88	-12.4	-9.7	0.3	0	2.7	0.3	207.97
89	-12.4	-9.8	0.3	0	2.6	0.3	200.27
90	-12.4	-9.8	0.3	0	2.6	0.3	200.27
91	-12.4	-9.8	0.3	0	2.6	0.3	200.27
92	-12.4	-9.9	0.3	0	2.5	0.3	192.57
93	-12.4	-9.9	0.3	0	2.5	0.3	192.57
94	-12.4	-9.9	0.3	0	2.5	0.3	192.57
95	-12.4	-9.9	0.3	0	2.5	0.3	192.57
96	-12.5	-10	0.3	0	2.5	0.3	192.57
97	-12.6	-10.1	0.3	0	2.5	0.3	192.57
98	-12.7	-10.2	0.3	0	2.5	0.3	192.57
99	-12.7	-10.2	0.3	0	2.5	0.3	192.57
100	-12.7	-10.2	0.3	0	2.5	0.3	192.57
101	-13	-10.5	0.3	0	2.5	0.3	192.57
102	-13	-10.5	0.3	0	2.5	0.3	192.57
103	-13	-10.5	0.3	0	2.5	0.3	192.57
104	-13	-10.6	0.3	0	2.4	0.3	184.86
105	-13	-10.6	0.3	0	2.4	0.3	184.86
106	-13.2	-10.7	0.3	0	2.5	0.3	192.57
107	-13.2	-10.7	0.3	0	2.5	0.3	192.57
108	-13.1	-10.8	0.3	0	2.3	0.3	177.16
109	-13.2	-10.8	0.3	0	2.4	0.3	184.86
110	-13.1	-10.8	0.3	0	2.3	0.3	177.16
111	-13.3	-10.9	0.3	0	2.4	0.3	184.86
112	-13.3	-10.9	0.3	0	2.4	0.3	184.86
113	-13.4	-10.9	0.3	0	2.5	0.3	192.57
114	-13.4	-11	0.3	0	2.4	0.3	184.86
115	-13.4	-11	0.3	0	2.4	0.3	184.86
116	-13.4	-11	0.3	0	2.4	0.3	184.86
117	-13.4	-11	0.3	0	2.4	0.3	184.86
118	-13.5	-11.1	0.3	0	2.4	0.3	184.86
119	-13.5	-11.1	0.3	0	2.4	0.3	184.86
120	-13.5	-11.1	0.3	0	2.4	0.3	184.86
						Qc,ave	264.17

Table B-4 :Inlet and outlet temperature of the coolant and the falling water for mc=0.08 kg/s "Series arrangement, jet mode"RUN 4(S)

70 minutes run

Time(min)	Tgi(C)	Tgo(C)	Twi(C)	Two(C)	delta Tg	delta Tw	Qc(W)
1	-13.2	-9.5	0.6	0.1	3.7	0.5	743.4336
2	-13	-9.6	0.6	0.1	3.4	0.5	683.1552
3	-12.9	-9.8	0.5	0	3.1	0.5	622.8768
4	-12.6	-9.9	0.5	0.1	2.7	0.4	542.5056
5	-12.6	-10	0.4	0	2.6	0.4	522.4128
6	-12.5	-10	0.4	0	2.5	0.4	502.32
7	-12.4	-10.1	0.3	0	2.3	0.3	462.1344
8	-12.3	-10.2	0.3	0	2.1	0.3	421.9488
9	-12.3	-10.2	0.3	0	2.1	0.3	421.9488
10	-12.1	-10.2	0.3	0.1	1.9	0.2	381.7632
11	-12.1	-10.2	0.3	0	1.9	0.3	381.7632
12	-12	-10.2	0.3	0	1.8	0.3	361.6704
13	-12.1	-10.3	0.3	0	1.8	0.3	361.6704
14	-12.1	-10.4	0.3	0	1.7	0.3	341.5776
15	-12.1	-10.3	0.3	0	1.8	0.3	361.6704
16	-12.1	-10.4	0.3	0	1.7	0.3	341.5776
17	-12.1	-10.4	0.3	0	1.7	0.3	341.5776
18	-12.1	-10.5	0.3	0	1.6	0.3	321.4848
19	-12	-10.4	0.3	0	1.6	0.3	321.4848
20	-12.1	-10.5	0.3	0.1	1.6	0.2	321.4848
21	-12	-10.5	0.3	0	1.5	0.3	301.392
22	-12	-10.5	0.3	0	1.5	0.3	301.392
23	-12	-10.5	0.3	0	1.5	0.3	301.392
24	-12	-10.5	0.3	0	1.5	0.3	301.392
25	-12	-10.6	0.3	0	1.4	0.3	281.2992
26	-12.1	-10.6	0.3	0	1.5	0.3	301.392
27	-12.1	-10.6	0.3	0	1.5	0.3	301.392
28	-12.1	-10.6	0.3	0	1.5	0.3	301.392
29	-12.1	-10.6	0.3	0	1.5	0.3	301.392
30	-12.1	-10.6	0.3	0	1.5	0.3	301.392
31	-12.2	-10.7	0.3	0	1.5	0.3	301.392
32	-12.2	-10.7	0.3	0	1.5	0.3	301.392
33	-12.2	-10.8	0.3	0	1.4	0.3	281.2992
34	-12.2	-10.8	0.3	0	1.4	0.3	281.2992
35	-12.3	-10.8	0.3	0	1.5	0.3	301.392
36	-12.3	-10.8	0.3	0	1.5	0.3	301.392
37	-12.3	-10.9	0.3	0	1.4	0.3	281.2992
38	-12.4	-10.9	0.3	0	1.5	0.3	301.392
39	-12.4	-11	0.3	0	1.4	0.3	281.2992
40	-12.4	-11	0.3	0	1.4	0.3	281.2992
41	-12.5	-11	0.3	0	1.5	0.3	301.392
42	-12.5	-11	0.3	0	1.5	0.3	301.392
43	-12.5	-11.1	0.3	0	1.4	0.3	281.2992
44	-12.5	-11.1	0.3	0	1.4	0.3	281.2992
45	-12.5	-11.1	0.3	0	1.4	0.3	281.2992
46	-12.5	-11.1	0.3	0	1.4	0.3	281.2992
47	-12.5	-11.1	0.3	0	1.4	0.3	281.2992
48	-12.6	-11.2	0.3	0	1.4	0.3	281.2992
49	-12.6	-11.2	0.3	0	1.4	0.3	281.2992
50	-12.7	-11.3	0.3	0	1.4	0.3	281.2992
51	-12.7	-11.3	0.3	0	1.4	0.3	281.2992
52	-12.7	-11.3	0.3	0	1.4	0.3	281.2992
53	-12.8	-11.5	0.3	0	1.3	0.3	261.2064
54	-12.8	-11.5	0.3	0	1.3	0.3	261.2064
55	-12.8	-11.5	0.3	0	1.3	0.3	261.2064
56	-12.8	-11.5	0.3	0	1.3	0.3	261.2064
57	-12.8	-11.5	0.3	0	1.3	0.3	261.2064
58	-12.8	-11.6	0.3	0	1.2	0.3	241.1136
59	-12.9	-11.7	0.3	0	1.2	0.3	241.1136
60	-12.9	-11.7	0.3	0	1.2	0.3	241.1136
61	-12.9	-11.7	0.3	0	1.2	0.3	241.1136
62	-12.9	-11.7	0.3	0	1.2	0.3	241.1136
63	-13	-11.8	0.3	0	1.2	0.3	241.1136
64	-13	-11.8	0.3	0	1.2	0.3	241.1136
65	-13	-11.8	0.3	0	1.2	0.3	241.1136
66	-13.1	-11.9	0.3	0	1.2	0.3	241.1136
67	-13.1	-11.9	0.3	0	1.2	0.3	241.1136
68	-13.1	-11.9	0.3	0	1.2	0.3	241.1136
69	-13.2	-12	0.3	0	1.2	0.3	241.1136
70	-13.2	-12	0.3	0	1.2	0.3	241.1136
						Qc,ave(W)	314.7394

Table B-5 :Inlet and outlet temperature of the coolant and the falling water for $\dot{m}_w$=0.128kg/s "Series arrangement, jet mode"RUN 5(S)

60 minutes run

Time(min)	T_{ci}(C)	T_{co}(C)	T_{wi}(C)	T_{wo}(C)	Δ Tc	Δ Tw	Qc(W)
0	-13	-11.6	0.7	0.2	1.4	0.5	600.10
1	-12.7	-10.4	0.6	0.1	2.3	0.5	985.89
2	-12.4	-10.4	0.5	0	2	0.5	857.29
3	-12.2	-10.4	0.4	0.1	1.8	0.3	771.56
4	-12	-10.4	0.4	0	1.6	0.4	685.83
5	-11.9	-10.4	0.3	0.1	1.5	0.2	642.97
6	-11.7	-10.3	0.3	0	1.4	0.3	600.10
7	-11.5	-10.3	0.3	0.1	1.2	0.2	514.38
8	-11.5	-10.3	0.3	0	1.2	0.3	514.38
9	-11.5	-10.4	0.3	0.1	1.1	0.2	471.51
10	-11.5	-10.4	0.3	0	1.1	0.3	471.51
11	-11.5	-10.5	0.3	0.1	1	0.2	428.65
12	-11.5	-10.5	0.3	0	1	0.3	428.65
13	-11.5	-10.5	0.3	0	1	0.3	428.65
14	-11.5	-10.5	0.3	0	1	0.3	428.65
15	-11.5	-10.5	0.3	0.1	1	0.2	428.65
16	-11.5	-10.6	0.3	0	0.9	0.3	385.78
17	-11.5	-10.6	0.3	0	0.9	0.3	385.78
18	-11.5	-10.6	0.3	0	0.9	0.3	385.78
19	-11.7	-10.8	0.3	0	0.9	0.3	385.78
20	-11.7	-10.8	0.3	0	0.9	0.3	385.78
21	-11.8	-10.9	0.3	0	0.9	0.3	385.78
22	-11.8	-11	0.3	0	0.8	0.3	342.92
23	-11.9	-11	0.3	0	0.9	0.3	385.78
24	-12	-11.1	0.3	0	0.9	0.3	385.78
25	-12	-11.1	0.3	0	0.9	0.3	385.78
26	-12	-11.1	0.3	0	0.9	0.3	385.78
27	-12	-11.2	0.3	0	0.8	0.3	342.92
28	-12.1	-11.2	0.3	0	0.9	0.3	385.78
29	-12.1	-11.3	0.3	0	0.8	0.3	342.92
30	-12.2	-11.4	0.3	0	0.8	0.3	342.92
31	-12.3	-11.4	0.3	0	0.9	0.3	385.78
32	-12.3	-11.5	0.3	0	0.8	0.3	342.92
33	-12.3	-11.5	0.3	0	0.8	0.3	342.92
34	-12.3	-11.5	0.3	0	0.8	0.3	342.92
35	-12.4	-11.6	0.3	0	0.8	0.3	342.92
36	-12.4	-11.6	0.3	0	0.8	0.3	342.92
37	-12.5	-11.7	0.3	0	0.8	0.3	342.92
38	-12.5	-11.7	0.3	0	0.8	0.3	342.92
39	-12.5	-11.7	0.3	0	0.8	0.3	342.92
40	-12.5	-11.8	0.3	0	0.7	0.3	300.05
41	-12.5	-11.8	0.3	0	0.7	0.3	300.05
42	-12.5	-11.8	0.3	0	0.7	0.3	300.05
43	-12.5	-11.8	0.3	0	0.7	0.3	300.05
44	-12.6	-11.9	0.3	0	0.7	0.3	300.05
45	-12.6	-11.9	0.3	0	0.7	0.3	300.05
46	-12.6	-11.9	0.3	0	0.7	0.3	300.05
47	-12.7	-12	0.3	0	0.7	0.3	300.05
48	-12.7	-12	0.3	0	0.7	0.3	300.05
49	-12.7	-12	0.3	0	0.7	0.3	300.05
50	-12.7	-12	0.3	0	0.6	0.3	257.19
51	-12.8	-12	0.3	0	0.8	0.3	342.92
52	-12.8	-12.1	0.3	0	0.7	0.3	300.05
53	-12.8	-12.1	0.3	0	0.7	0.3	300.05
54	-12.9	-12.3	0.3	0	0.6	0.3	257.19
55	-12.9	-12.3	0.3	0	0.6	0.3	257.19
56	-12.9	-12.3	0.3	0	0.6	0.3	257.19
57	-12.9	-12.3	0.3	0	0.6	0.3	257.19
58	-13	-12.4	0.3	0	0.6	0.3	257.19
59	-13	-12.4	0.3	0	0.6	0.3	257.19
60	-13	-12.4	0.3	0	0.6	0.3	257.19
						Qc,ave(W)	393.51

Table B-6:Inlet and outlet temperature of the coolant and the falling water for $\dot{m}c$=0.162 kg/s "Series arrangement, jet mode" RUN 6(S)

60minutes run

Time(min)	Tci(C)	Tco(C)	Twi(C)	Two(C)	Δ Tc	Δ Tw	Qc(W)
0	-10	-7.9	0.5	0.1	2.1	0.4	1139.26
1	-10	-8.2	0.6	0.2	1.8	0.4	976.51
2	-10	-8.3	0.5	0.1	1.7	0.4	922.26
3	-9.5	-8.4	0.4	0	1.1	0.4	596.76
4	-9.3	-8.3	0.4	0.1	1	0.3	542.51
5	-9.2	-8.3	0.4	0.1	0.9	0.3	488.26
6	-9.2	-8.3	0.3	0.1	0.9	0.2	488.26
7	-9.2	-8.3	0.3	0	0.9	0.3	488.26
8	-9.2	-8.4	0.3	0	0.8	0.3	434.00
9	-9.1	-8.4	0.3	0	0.7	0.3	379.75
10	-9.1	-8.5	0.3	0	0.6	0.3	325.50
11	-9.2	-8.5	0.3	0	0.7	0.3	379.75
12	-9.3	-8.6	0.3	0	0.7	0.3	379.75
13	-9.4	-8.7	0.3	0	0.7	0.3	379.75
14	-9.5	-8.8	0.3	0	0.7	0.3	379.75
15	-9.6	-8.9	0.3	0	0.7	0.3	379.75
16	-9.7	-9	0.3	0	0.7	0.3	379.75
17	-9.7	-9	0.3	0	0.7	0.3	379.75
18	-9.7	-9	0.3	0	0.7	0.3	379.75
19	-9.7	-9	0.3	0	0.7	0.3	379.75
20	-9.8	-9.1	0.3	0	0.7	0.3	379.75
21	-9.8	-9.1	0.3	0	0.7	0.3	379.75
22	-9.9	-9.2	0.3	0	0.7	0.3	379.75
23	-10	-9.4	0.3	0	0.6	0.3	325.50
24	-10	-9.4	0.3	0	0.6	0.3	325.50
25	-10.1	-9.5	0.3	0	0.6	0.3	325.50
26	-10.2	-9.6	0.3	0	0.6	0.3	325.50
27	-10.2	-9.6	0.3	0	0.6	0.3	325.50
28	-10.3	-9.7	0.3	0	0.6	0.3	325.50
29	-10.3	-9.7	0.3	0	0.6	0.3	325.50
30	-10.4	-9.8	0.3	0	0.6	0.3	325.50
31	-10.4	-9.8	0.3	0	0.6	0.3	325.50
32	-10.4	-9.8	0.3	0	0.6	0.3	325.50
33	-10.4	-9.8	0.3	0	0.6	0.3	325.50
34	-10.4	-9.8	0.3	0	0.6	0.3	325.50
35	-10.4	-9.8	0.3	0	0.6	0.3	325.50
36	-10.4	-9.8	0.3	0	0.6	0.3	325.50
37	-10.4	-9.8	0.3	0	0.6	0.3	325.50
38	-10.4	-9.8	0.3	0	0.6	0.3	325.50
39	-10.4	-9.8	0.3	0	0.6	0.3	325.50
40	-10.4	-9.8	0.3	0	0.6	0.3	325.50
41	-10.4	-9.8	0.3	0	0.6	0.3	325.50
42	-10.4	-9.9	0.3	0	0.5	0.3	271.25
43	-10.4	-9.9	0.3	0	0.5	0.3	271.25
44	-10.4	-9.9	0.3	0	0.5	0.3	271.25
45	-10.4	-9.9	0.3	0	0.5	0.3	271.25
46	-10.4	-9.9	0.3	0	0.5	0.3	271.25
47	-10.4	-9.9	0.3	0	0.5	0.3	271.25
48	-10.4	-9.9	0.3	0	0.5	0.3	271.25
49	-10.4	-9.9	0.3	0	0.5	0.3	271.25
50	-10.4	-9.9	0.3	0	0.5	0.3	271.25
51	-10.4	-9.9	0.3	0	0.5	0.3	271.25
52	-10.4	-9.9	0.3	0	0.5	0.3	271.25
53	-10.4	-9.9	0.3	0	0.5	0.3	271.25
54	-10.4	-9.9	0.3	0	0.5	0.3	271.25
55	-10.4	-9.9	0.3	0	0.5	0.3	271.25
56	-10.4	-9.9	0.3	0	0.5	0.3	271.25
57	-10.4	-9.9	0.3	0	0.5	0.3	271.25
58	-10.4	-9.9	0.3	0	0.5	0.3	271.25
59	-10.4	-9.9	0.3	0	0.5	0.3	271.25
60	-10.4	-9.9	0.3	0	0.5	0.3	271.25
						Qc,ave(W)	366.19

Table B-7:Inlet and outlet temperature of the coolant and the falling water for mc=0.162 kg/s "Series arrangement, sheet mode" RUN 7(S)

60 minutes run

Time(min)	Tci(C)	Tco(C)	Twi(C)	Two(C)	Δ Tc	Δ Tw	Qc(W)
0	-10.7	-8.5	0.5	0.2	2.2	0.3	1193.58
1	-10.5	-8.2	0.5	0.1	2.3	0.4	1247.84
2	-10.4	-8.3	0.4	0.1	2.1	0.3	1139.33
3	-10.3	-8.6	0.3	0.1	1.7	0.2	922.31
4	-10.2	-8.7	0.3	0	1.5	0.3	813.81
5	-10.1	-8.8	0.3	0	1.3	0.3	705.30
6	-9.9	-8.8	0.3	0	1.1	0.3	596.79
7	-9.9	-8.8	0.3	0	1.1	0.3	596.79
8	-9.9	-8.8	0.3	0	1.1	0.3	596.79
9	-9.9	-8.8	0.3	0	1.1	0.3	596.79
10	-10	-9.1	0.3	0	0.9	0.3	488.28
11	-10	-9.2	0.3	0	0.8	0.3	434.03
12	-10	-9.2	0.3	0	0.8	0.3	434.03
13	-10	-9.2	0.3	0	0.8	0.3	434.03
14	-10	-9.2	0.3	0	0.8	0.3	434.03
15	-10.1	-9.3	0.3	0	0.8	0.3	434.03
16	-10.1	-9.3	0.3	0	0.8	0.3	434.03
17	-10.1	-9.3	0.3	0	0.8	0.3	434.03
18	-10.2	-9.4	0.3	0	0.8	0.3	434.03
19	-10.2	-9.4	0.3	0	0.8	0.3	434.03
20	-10.2	-9.4	0.3	0	0.8	0.3	434.03
21	-10.4	-9.7	0.3	0	0.7	0.3	379.78
22	-10.4	-9.7	0.3	0	0.7	0.3	379.78
23	-10.4	-9.7	0.3	0	0.7	0.3	379.78
24	-10.5	-9.8	0.3	0	0.7	0.3	379.78
25	-10.5	-9.8	0.3	0	0.7	0.3	379.78
26	-10.6	-9.9	0.3	0	0.7	0.3	379.78
27	-10.7	-10.1	0.3	0	0.6	0.3	325.52
28	-10.7	-10.1	0.3	0	0.6	0.3	325.52
29	-10.7	-10.1	0.3	0	0.6	0.3	325.52
30	-10.7	-10.1	0.3	0	0.6	0.3	325.52
31	-10.4	-9.8	0.3	0	0.6	0.3	325.52
32	-10.4	-9.8	0.3	0	0.6	0.3	325.52
33	-10.4	-9.8	0.3	0	0.6	0.3	325.52
34	-10.4	-9.8	0.3	0	0.6	0.3	325.52
35	-10.4	-9.8	0.3	0	0.6	0.3	325.52
36	-10.4	-9.8	0.3	0	0.6	0.3	325.52
37	-10.4	-9.8	0.3	0	0.6	0.3	325.52
38	-10.4	-9.8	0.3	0	0.6	0.3	325.52
39	-10.4	-9.8	0.3	0	0.6	0.3	325.52
40	-10.4	-9.8	0.3	0	0.6	0.3	325.52
41	-10.4	-9.8	0.3	0	0.6	0.3	325.52
42	-10.4	-9.8	0.3	0	0.6	0.3	325.52
43	-10.4	-9.9	0.3	0	0.5	0.3	271.27
44	-10.4	-9.9	0.3	0	0.5	0.3	271.27
45	-10.4	-9.9	0.3	0	0.5	0.3	271.27
46	-10.4	-9.9	0.3	0	0.5	0.3	271.27
47	-10.4	-9.9	0.3	0	0.5	0.3	271.27
48	-10.4	-9.9	0.3	0	0.5	0.3	271.27
49	-10.4	-9.9	0.3	0	0.5	0.3	271.27
50	-10.4	-9.9	0.3	0	0.5	0.3	271.27
51	-10.4	-9.9	0.3	0	0.5	0.3	271.27
52	-10.4	-9.9	0.3	0	0.5	0.3	271.27
53	-10.4	-9.9	0.3	0	0.5	0.3	271.27
54	-10.4	-9.9	0.3	0	0.5	0.3	271.27
55	-10.4	-9.9	0.3	0	0.5	0.3	271.27
56	-10.4	-9.9	0.3	0	0.5	0.3	271.27
57	-10.4	-9.9	0.3	0	0.5	0.3	271.27
58	-10.4	-9.9	0.3	0	0.5	0.3	271.27
59	-10.4	-9.9	0.3	0	0.5	0.3	271.27
60	-10.4	-9.9	0.3	0	0.5	0.3	271.27
						Q· c,ave(W)	414.59

Table B-8:Inlet and outlet temperature of the coolant and the falling water for $\dot{m}_c$=0.162 kg/s "Series arrangement, droplet mode" RUN 8(S)

60 minutes run

Time(min)	Tci(C)	Tco(C)	Twi(C)	Two(C)	Δ Tc	Δ Tw	Qc(W)
0	-10.7	-8.9	0.7	0.2	1.8	0.5	976.51
1	-10.5	-8.6	0.5	0.1	1.9	0.4	1030.76
2	-10.4	-8.7	0.5	0.1	1.7	0.4	922.26
3	-10.1	-8.9	0.3	0.1	1.2	0.2	651.01
4	-10	-8.9	0.4	0	1.1	0.4	596.76
5	-10	-8.9	0.3	0.1	1.1	0.2	596.76
6	-9.9	-8.9	0.3	0	1	0.3	542.51
7	-9.9	-9	0.4	0.1	0.9	0.3	488.26
8	-9.9	-9	0.4	0.1	0.9	0.3	488.26
9	-9.9	-9.1	0.3	0	0.8	0.3	434.00
10	-10	-9.2	0.3	0.1	0.8	0.2	434.00
11	-10	-9.2	0.3	0	0.8	0.3	434.00
12	-10	-9.2	0.3	0	0.8	0.3	434.00
13	-10	-9.2	0.3	0	0.8	0.3	434.00
14	-10	-9.2	0.3	0	0.8	0.3	434.00
15	-10	-9.3	0.3	0	0.7	0.3	379.75
16	-10	-9.3	0.3	0	0.7	0.3	379.75
17	-10	-9.3	0.3	0	0.7	0.3	379.75
18	-10.2	-9.5	0.3	0	0.7	0.3	379.75
19	-10.2	-9.5	0.3	0	0.7	0.3	379.75
20	-10.2	-9.5	0.3	0	0.7	0.3	379.75
21	-10.4	-9.8	0.3	0	0.6	0.3	325.50
22	-10.4	-9.8	0.3	0	0.6	0.3	325.50
23	-10.4	-9.8	0.3	0	0.6	0.3	325.50
24	-10.5	-9.9	0.3	0	0.6	0.3	325.50
25	-10.5	-9.9	0.3	0	0.6	0.3	325.50
26	-10.6	-9.9	0.3	0	0.7	0.3	379.75
27	-10.7	-10.1	0.3	0	0.6	0.3	325.50
28	-10.7	-10.1	0.3	0	0.6	0.3	325.50
29	-10.7	-10.1	0.3	0	0.6	0.3	325.50
30	-10.7	-10.1	0.3	0	0.6	0.3	325.50
31	-10.4	-9.9	0.3	0	0.5	0.3	271.25
32	-10.4	-9.9	0.3	0	0.5	0.3	271.25
33	-10.4	-9.9	0.3	0	0.5	0.3	271.25
34	-10.4	-9.9	0.3	0	0.5	0.3	271.25
35	-10.4	-9.9	0.3	0	0.5	0.3	271.25
36	-10.4	-9.9	0.3	0	0.5	0.3	271.25
37	-10.4	-9.9	0.3	0	0.5	0.3	271.25
38	-10.4	-9.9	0.3	0	0.5	0.3	271.25
39	-10.4	-9.9	0.3	0	0.5	0.3	271.25
40	-10.4	-9.9	0.3	0	0.5	0.3	271.25
41	-10.4	-9.9	0.3	0	0.5	0.3	271.25
42	-10.4	-9.9	0.3	0	0.5	0.3	271.25
43	-10.4	-9.9	0.3	0	0.5	0.3	271.25
44	-10.4	-9.9	0.3	0	0.5	0.3	271.25
45	-10.4	-9.9	0.3	0	0.5	0.3	271.25
46	-10.4	-9.9	0.3	0	0.5	0.3	271.25
47	-10.4	-9.9	0.3	0	0.5	0.3	271.25
48	-10.4	-9.9	0.3	0	0.5	0.3	271.25
49	-10.4	-9.9	0.3	0	0.5	0.3	271.25
50	-10.4	-9.9	0.3	0	0.5	0.3	271.25
51	-10.4	-9.9	0.3	0	0.5	0.3	271.25
52	-10.4	-9.9	0.3	0	0.5	0.3	271.25
53	-10.4	-9.9	0.3	0	0.5	0.3	271.25
54	-10.4	-9.9	0.3	0	0.5	0.3	271.25
55	-10.4	-9.9	0.3	0	0.5	0.3	271.25
56	-10.4	-9.9	0.3	0	0.5	0.3	271.25
57	-10.4	-9.9	0.3	0	0.5	0.3	271.25
58	-10.4	-9.9	0.3	0	0.5	0.3	271.25
59	-10.4	-9.9	0.3	0	0.5	0.3	271.25
60	-10.4	-9.9	0.3	0	0.5	0.3	271.25
						Qc,ave(W)	366.64

Table B-9 :Inlet and outlet temperature of the coolant and the falling liquid for $\dot{m}_w$=0.023kg/s
"Series arrangement, jetmode"RUN 6(S)(2% aceton in water)
120 minutes run

Time(min)	T_{ci}(C)	T_{co}(C)	T_{wi}(C)	T_{wo}(C)	Δ Tc	Δ Tw	Qc(W)
0	-12.8	-9.5	1.1	-0.5	3.3	1.6	254.17
1	-12.7	-7.7	0.4	-0.5	5	0.9	385.11
2	-12.7	-7.2	0.3	-0.5	5.5	0.8	423.62
3	-12.7	-6.8	0.4	-0.5	5.9	0.9	454.43
4	-12.5	-6.7	0.3	-0.5	5.5	0.8	423.62
5	-12.5	-6.9	0.3	-0.5	5.5	0.8	423.62
6	-12.5	-7.1	0.3	-0.5	5.3	0.8	408.22
7	-12.5	-7.3	0.3	-0.5	5.2	0.8	400.52
8	-12.4	-7.5	0.3	-0.5	4.9	0.8	377.41
9	-12.4	-7.7	0.3	-0.5	4.7	0.8	362.01
10	-12.4	-7.8	0.3	-0.5	4.6	0.8	354.30
11	-12.4	-7.9	0.3	-0.5	4.5	0.8	346.60
12	-12.4	-7.9	0.4	-0.5	4.5	0.9	346.60
13	-12.4	-7.9	0.4	-0.5	4.5	0.9	346.60
14	-12.4	-7.9	0.5	-0.5	4.5	1	346.60
15	-12.4	-8	0.5	-0.5	4.4	1	338.90
16	-12.3	-8	0.5	-0.5	4.3	1	331.20
17	-12.4	-8.2	0.5	-0.5	4.2	1	323.49
18	-12.4	-8.2	0.5	-0.5	4.2	1	323.49
19	-12.4	-8.2	0.5	-0.5	4.2	1	323.49
20	-12.4	-8.1	0.5	-0.5	4.3	1	331.20
21	-12.4	-8.2	0.5	-0.5	4.2	1	323.49
22	-12.4	-8.1	0.5	-0.5	4.3	1	331.20
23	-12.4	-8.1	0.5	-0.5	4.3	1	331.20
24	-12.4	-8.1	0.5	-0.5	4.3	1	331.20
25	-12.4	-8.1	0.5	-0.5	4.3	1	331.20
26	-12.4	-8.2	0.5	-0.5	4.2	1	323.49
27	-12.4	-8.3	0.5	-0.5	4.1	1	315.79
28	-12.5	-8.4	0.5	-0.5	4.1	1	315.79
29	-12.5	-8.4	0.5	-0.5	4.1	1	315.79
30	-12.7	-8.6	0.5	-0.5	4.1	1	315.79
31	-12.6	-8.7	0.5	-0.5	3.9	1	300.39
32	-12.6	-8.8	0.5	-0.5	3.8	1	292.69
33	-12.7	-8.7	0.5	-0.5	4	1	308.09
34	-12.7	-8.8	0.5	-0.5	3.9	1	300.39
35	-12.7	-8.8	0.5	-0.5	3.9	1	300.39
36	-12.8	-8.9	0.5	-0.5	3.9	1	300.39
37	-12.7	-8.9	0.5	-0.5	3.8	1	292.69
38	-12.8	-9	0.5	-0.5	3.8	1	292.69
39	-12.8	-9	0.5	-0.5	3.8	1	292.69
40	-12.8	-9.1	0.5	-0.5	3.7	1	284.98
41	-12.9	-9.1	0.5	-0.5	3.8	1	292.69
42	-12.9	-9.1	0.5	-0.5	3.8	1	292.69
43	-12.9	-9.1	0.5	-0.5	3.8	1	292.69
44	-12.9	-9.1	0.5	-0.5	3.8	1	292.69
45	-12.9	-9.1	0.5	-0.5	3.8	1	292.69
46	-12.9	-9.1	0.5	-0.5	3.8	1	292.69
47	-12.9	-9.1	0.5	-0.5	3.8	1	292.69
48	-12.9	-9.2	0.5	-0.5	3.7	1	284.98
49	-13	-9.3	0.5	-0.5	3.7	1	284.98
50	-13	-9.3	0.5	-0.5	3.7	1	284.98
51	-13	-9.3	0.5	-0.5	3.7	1	284.98
52	-13	-9.3	0.5	-0.5	3.7	1	284.98
53	-13	-9.3	0.5	-0.5	3.7	1	284.98
54	-13	-9.4	0.5	-0.5	3.6	1	277.28
55	-13	-9.4	0.5	-0.5	3.6	1	277.28
56	-13	-9.4	0.5	-0.5	3.6	1	277.28
57	-13	-9.4	0.5	-0.5	3.6	1	277.28
58	-13.1	-9.6	0.5	-0.5	3.5	1	269.58
59	-13.1	-9.6	0.5	-0.5	3.5	1	269.58
60	-13.1	-9.6	0.5	-0.5	3.5	1	269.58
61	-13.1	-9.6	0.5	-0.5	3.5	1	269.58
62	-13.1	-9.6	0.5	-0.5	3.5	1	269.58
63	-13.1	-9.7	0.5	-0.5	3.4	1	261.88
64	-13.1	-9.7	0.5	-0.5	3.4	1	261.88

65	-13.1	-9.7	0.5	-0.5	3.4	1	261.88
66	-13.1	-9.7	0.5	-0.5	3.4	1	261.88
67	-13.1	-9.7	0.5	-0.5	3.4	1	261.88
68	-13.1	-9.7	0.5	-0.5	3.4	1	261.88
69	-13	-9.7	0.5	-0.5	3.3	1	254.17
70	-13	-9.7	0.5	-0.5	3.3	1	254.17
71	-13	-9.7	0.5	-0.5	3.3	1	254.17
72	-13	-9.7	0.5	-0.5	3.3	1	254.17
73	-13	-9.7	0.5	-0.5	3.3	1	254.17
74	-13	-9.7	0.5	-0.5	3.3	1	254.17
75	-13	-9.7	0.5	-0.5	3.3	1	254.17
76	-13	-9.7	0.5	-0.5	3.3	1	254.17
77	-13	-9.7	0.5	-0.5	3.3	1	254.17
78	-13	-9.7	0.5	-0.5	3.3	1	254.17
79	-13	-9.7	0.5	-0.5	3.3	1	254.17
80	-13	-9.7	0.5	-0.5	3.3	1	254.17
81	-13	-9.7	0.5	-0.5	3.3	1	254.17
82	-13	-9.7	0.5	-0.5	3.3	1	254.17
83	-13	-9.7	0.5	-0.5	3.3	1	254.17
84	-13	-9.7	0.5	-0.5	3.3	1	254.17
85	-13	-9.7	0.5	-0.5	3.3	1	254.17
86	-13	-9.7	0.5	-0.5	3.3	1	254.17
87	-13	-9.7	0.5	-0.5	3.3	1	254.17
88	-13	-9.7	0.5	-0.5	3.3	1	254.17
89	-13.1	-9.9	0.5	-0.5	3.2	1	246.47
90	-13.1	-9.9	0.5	-0.5	3.2	1	246.47
91	-13.1	-9.9	0.5	-0.5	3.2	1	246.47
92	-13.1	-9.9	0.5	-0.5	3.2	1	246.47
93	-13.1	-9.9	0.5	-0.5	3.2	1	246.47
94	-13.1	-9.9	0.5	-0.5	3.2	1	246.47
95	-13.1	-9.9	0.5	-0.5	3.2	1	246.47
96	-13.1	-9.9	0.5	-0.5	3.2	1	246.47
97	-13.1	-9.9	0.5	-0.5	3.2	1	246.47
98	-13.1	-9.9	0.5	-0.5	3.2	1	246.47
99	-13.2	-10	0.5	-0.5	3.2	1	246.47
100	-13.2	-10	0.5	-0.5	3.2	1	246.47
101	-13.2	-10	0.5	-0.5	3.2	1	246.47
102	-13.2	-10	0.5	-0.5	3.2	1	246.47
103	-13.2	-10	0.5	-0.5	3.2	1	246.47
104	-13.2	-10	0.5	-0.5	3.2	1	246.47
105	-13.2	-10	0.5	-0.5	3.2	1	246.47
106	-13.2	-10	0.5	-0.5	3.2	1	246.47
107	-13.2	-10	0.5	-0.5	3.2	1	246.47
108	-13.2	-10	0.5	-0.5	3.2	1	246.47
109	-13.2	-10	0.5	-0.5	3.2	1	246.47
110	-13.3	-10.1	0.5	-0.5	3.2	1	246.47
111	-13.3	-10.1	0.5	-0.5	3.2	1	246.47
112	-13.3	-10.1	0.5	-0.5	3.2	1	246.47
113	-13.3	-10.1	0.5	-0.5	3.2	1	246.47
114	-13.3	-10.1	0.5	-0.5	3.2	1	246.47
115	-13.3	-10.1	0.5	-0.5	3.2	1	246.47
116	-13.3	-10.1	0.5	-0.5	3.2	1	246.47
117	-13.3	-10.1	0.5	-0.5	3.2	1	246.47
118	-13.3	-10.1	0.5	-0.5	3.2	1	246.47
119	-13.3	-10.1	0.5	-0.5	3.2	1	246.47
120	-13.3	-10.1	0.5	-0.5	3.2	1	246.47
						Qc,ave(W)	286.11

Table B-10 :Surface temperature of the test tube for water, $\dot{m}c$=0.023 kg/s "Series arrangement,jet mode"

t(min)	T1	T2	T3	T4	T5	T6
1	-0.6	-0.7	-0.7	-0.7	-0.6	-0.5
3	-1.6	-1.5	-1.5	-1.5	-1.6	-1.8
6	-2.8	-2.8	-2.8	-2.8	-2.8	-2.9
9	-3.6	-3.4	-3.4	-3.4	-3.6	-3.8
12	-4.4	-4.2	-4.1	-4.2	-4.4	-4.5
15	-4.7	-4.6	-4.6	-4.6	-4.7	-4.9
18	-5.3	-5	-5	-5.1	-5.3	-5.4
21	-5.6	-5.4	-5.4	-5.4	-5.7	-5.8
24	-5.9	-5.7	-5.7	-5.7	-5.9	-6
27	-6.1	-5.9	-5.9	-5.9	-6.1	-6.3
30	-6.4	-6.2	-6.2	-6.2	-6.4	-6.6
33	-6.6	-6.5	-6.4	-6.4	-6.6	-6.8
36	-6.8	-6.6	-6.6	-6.6	-6.8	-7
39	-7.1	-7	-7	-7	-7.1	-7.3
42	-7.1	-7	-7	-7	-7.1	-7.3
45	-7.1	-7.1	-7.1	-7.1	-7.1	-7.3
48	-7.2	-7.2	-7.1	-7.1	-7.2	-7.4
51	-7.3	-7.3	-7.2	-7.3	-7.3	-7.5
54	-7.4	-7.3	-7.2	-7.3	-7.4	-7.6
57	-7.5	-7.4	-7.3	-7.4	-7.5	-7.7
60	-7.7	-7.6	-7.5	-7.6	-7.7	-7.8
78	-8.8	-8.5	-8.6	-8.6	-8.8	-9
81	-8.9	-8.7	-8.7	-8.8	-8.9	-9.2
90	-9.4	-9.1	-9.2	-9.2	-9.4	-9.6
93	-9.6	-9.3	-9.4	-9.4	-9.6	-9.7
110	-10	-9.8	-9.8	-9.8	-10	-10.2
120	-10.4	-10	-10	-10.1	-10.3	-10.6

Table B-11 :Surface temperature of the test tube for 2%aceton, $\dot{m}c$=0.023 kg/s "Series arrangement,jet mode"

t(min)	T1	T2	T3	T4	T5	T6
1	-0.6	-0.7	-0.7	-0.7	-0.6	-0.5
3	-1.8	-1.6	-1.6	-1.6	-1.8	-2
6	-2.8	-2.6	-2.6	-2.6	-2.8	-2.9
9	-3.6	-3.4	-3.4	-3.5	-3.6	-3.7
12	-4.1	-4	-3.9	-3.9	-4.1	-4.2
15	-4.6	-4.5	-4.4	-4.4	-4.6	-4.8
18	-4.9	-4.8	-4.7	-4.8	-4.9	-5
21	-5.1	-5	-5	-5.1	-5.1	-5.3
24	-5.4	-5.4	-5.4	-5.4	-5.5	-5.6
27	-5.7	-5.7	-5.6	-5.6	-5.8	-6
30	-6	-6.1	-6	-6	-6.1	-6.4
33	-6.4	-6.3	-6.2	-6.3	-6.4	-6.6
36	-6.6	-6.5	-6.4	-6.5	-6.6	-6.7
39	-6.7	-6.6	-6.6	-6.7	-6.8	-6.8
42	-6.9	-6.8	-6.7	-6.8	-6.9	-7
45	-7	-6.9	-6.9	-6.9	-7	-7.2
48	-7.1	-7	-7	-7	-7.1	-7.2
51	-7.2	-7.1	-7	-7.1	-7.2	-7.3
54	-7.3	-7.2	-7.2	-7.2	-7.2	-7.4
57	-7.4	-7.3	-7.2	-7.3	-7.4	-7.5
60	-7.6	-7.5	-7.4	-7.5	-7.6	-7.7
64	-7.8	-7.6	-7.5	-7.6	-7.8	-7.9
69	-7.9	-7.8	-7.8	-7.8	-7.9	-8
74	-8.3	-8.2	-8.1	-8.2	-8.3	-8.4
79	-8.6	-8.5	-8.5	-8.5	-8.6	-8.8
84	-8.8	-8.7	-8.7	-8.7	-8.8	-9.1
114	-9.7	-9.5	-9.5	-9.5	-9.7	-9.9

بحث تجريبي على تجمد غشاء ساقط

إعداد

هاني حسين ولي سيت

رسالة مقدمة لإستكمال متطلبات درجة الماجستير

في الهندسة الميكانيكية(هندسة حرارية وتقنية تحلية المياه)

كلية الهندسة

جامعة الملك عبد العزيز

جدة-المملكة العربية السعودية

ذوالقعدة١٤١٩هـ-فبراير١٩٩٩ م

شكر وتقدير

الحمد لله رب العالمين والصلاة والسلام على أشرف المرسلين سيدنا محمد وعلى آله وصحبه أجمعين،أحمده سبحانه الذي وفقني وأعانني على إتمام هذه الرسالة للحصول على درجة الماجستير ، والتي أرجو من الله أن تكون من العلم النافع الذي يؤجر عليه صاحبه في الدنيا والآخرة. وأتقدم بالشكر الجزيل إلى معلمي الفاضل الدكتور قدري فتح الله لما بذله من جهد وافر في الإشراف والتوجيه.كما أتقدم بالشكر الجزيل إلى المعلمين الفاضلين الدكتور رمزي جوده والدكتور عبد الظاهر سليم على جهودهما في إكمال البحث وملاحظاتهم المفيدة . كما أتقدم بالشكر الجزيل إلى جميع أساتذتي في قسم الهندسة الحرارية وتقنية تحلية المياه لما أضافوه إلى محصلتي في العلم.ولا يفوتني أن أتقدم بالشكر الجزيل إلى والدي الحبيبين الذين صبرا على تقصيري أثناء فترة البحث، وإلى زوجتي الحبيبة التي أعانتني وشدت من أزري وإلى أبنائي سلمى وحمزة وسحر وإلى جميع إخواني وأخواتي وأصدقائي وزملائي الذين لم يبخلوا علي بالعون والتشجيع فلهم مني جزيل الشكر والعرفان.

بحث تجريبي على تجمد غشاء ساقط

إعداد

هاني حسين ولي سيت

المستخلص

هناك طريقتان لتجميد الثلج على الأنابيب :الأولى باستعمال الأنابيب المغمورة والثانية بتجميد الغشـــاء الساقط على الأنابيب.المبادلات الحرارية ذات الأغشية الساقطة لها إســـتعمالات كثـــيرة في الصناعـــة والتبريد وتحلية المياه وغيرها لأنها تتميز بمعامل انتقال حرارة كبير وتعمل بكمية مياه أقل مـــن المبـــادل الحراري ذي الأنابيب المغمورة.المبادل الحراري تحت البحث هو مبادل حراري ذي غشاء ساقط علـــى أنابيب أفقية.ويمكن أن يأخذ الغشاء الساقط شكل قطرات منفصلة أو شكل نافث أو شـــكل غشـــاء مستمر حسب إختلاف معدل السريان.

في هذا البحث يسقط السائل المبرد على مجموعة من سبعة أنابيب منظومة علـــى التـــوازي أو علـــى التوالي.حيث يتجمد السائل الساقط على أنابيب الإختبار من الخارج، والتي تبرد داخليا بواسطة جـــهاز تبريد ذو درجة محكومة للحرارة. السائل الساقط إما ماء أو ماء مضافا إليه٢% من مادة الأسيتون.أمـــا مائع التبريد داخل الأنابيب فهو محلولا من مادة الايثيلين جليكول بتركيز ٤٠%.وسوف تقاس كميـــة الثلج المتكونة على عدة فترات وكذلك معامل إنتقال الحرارة.

تم التعامل مع متغيرين رئيسيين لدراسة تأثير كل واحد منهما على كمية الثلج المتكون ومعامل إنتقـــال الحرارة.وهما:معدل سريان مائع التبريد داخل الأنابيب ومعدل السريان للسائل الساقط .وقـــد تمـــت دراسة تسع حالات مختلفة حسب تنظيم الأنابيب واختلافات ومعدل السريان.وقد وجد أنـــه بزيـــادة معدل السريان لمائع التبريد يزيد تكون الثلج على الأنابيب نتيجة لزيادة معامل إنتقال الحرارة الداخلـــي. وعند زيادة معدل السريان للسائل الساقط فإنه يتحول من قطرات منفصلة إلى نافث وأخيرا إلى شـــكل

غشاء مستمر ،والذي أنتج أكبر كمية من الثلج .منظومة التوالي أعطت كمية أكبر من الثلج من منظومة التوازي عند تثبيت معدل السريان لكلا المائعين ،وذلك بسبب زيادة سرعة مائع التبريد داخل الأنابيب.

وقد وجد أن زيادة تراكم الثلج على سطح الأنابيب يؤثر سلبيا على معدل إنتقال الحرارة بين السائل الساقط وبين مائع التبريد.وهذا يؤدي إلى تقليل الفرق في درجة الحرارة بين الداخل والخارج لمجموعة الأنابيب بزيادة تراكم الثلج. إن طبقة الثلج تعمل كعازل لانتقال الحرارة بين السائلين.إضافة مادة الأسيتون للماء يقلل تراكم الثلج على الأنابيب ولكن لم نحصل على مستحلب من حبيبات من الثلج كما كان متوقعا.يؤمل أن تكون نتائج النموذج تطبيقا تقنيا لدراسات المقارنة للمخازن الحرارية المبردة.

بحث تجريبي على تجمد غشاء ساقط

إعداد

هاني حسين ولي سيت

ملخص الرسالة

تكاليف إنتاج الطاقة الكهربائية وإستهلاكها يتزايد بسرعة في مدن المملكة العربية السعودية وقد يصل الجزء المستهلك في تبريد الهواء إلى حوالي ٧٥ % من هذا الاستهلاك وخصوصا في فصل الصيف حيث وصلت الزيادة السنوية إلى ٢١% في الفترة ١٩٧٧-١٩٨٨.ويلاحظ أن التبريد يحتل فترة ذروة لساعات قليلة في اليوم أو لأشهر خلال السنة مما يمثل ضغطا إضافيا على شركات الكهرباء خلال هذه الفترة.

ومن الطرق الفعالة للتغلب على مشكلة الذروة ،إستعمال الخزن الحراري للبرودة. تطورت تقنية خزن البرودة بشكل ملحوظ منذ بداية الثمانينات عندما أدركت شركات توليد الكهرباء الحاجة لخفض فترة الذروة في أنظمة التوليد والتوزيع لديهم.وتستفيد أنظمة خزن البرودة من الفترة التي يقل فيها الاحتياج للبرودة (خلال الليل) وتعمل على خزن البرودة في وسط معين.ومن ثم يستفاد من البرودة المخزنة لتكييف الهواء خلال فترة الذروة.

ويمكن تقسيم أوساط خزن البرودة بشكل عام إلى ثلاثة أنواع رئيسية وهم: ماء مبرد، ثلج أو مادة متصلبة متغيرة الطور.ولأن الطاقة الكامنة للثلج عالية (٣٣٥ كجول/كغ) فإنه يعتبر من أفضل الأنواع المستخدمة لخزن البرودة.ومن الطرق المناسبة الشائعة الإستخدام تكوين الثلج على الأنابيب.

هناك طريقتان لتجميد الثلج على الأنابيب :الأولى باستعمال الأنابيب المغمورة والثانية بتجميد الغشاء الساقط على الأنابيب.وللمبادل الحراري ذي الغشاء الساقط إستعمالات كثيرة في الصناعة والتبريد وتحلية المياه وغيرها لأنه يتميز بمعامل انتقال حرارة كبير ويعمل بمحتوى مائي أقل من المبادل الحراري ذي الأنابيب المغمورة.والمبادل الحراري تحت البحث هو مبادل حراري ذي غشاء ساقط على أنابيب

أفقية.ويمكن أن يأخذ الغشاء الساقط شكل قطرات منفصلة أو شكل نافث أو شكل غشـــاء مســـتمر حسب إختلاف معدل السريان.

الهدف الأساسي من هذا البحث هو العمل على تخفيض الحمل الحراري على شركات الكهرباء خـــلال فترة الذروة وذلك بتحسين طرق خزن الطاقة المعروفة عن طريق تكوين الثلج ،للإستفادة منه خـــلال وقت الذروة. والفكرة الأساسية في البحث تقوم على عمل تجربة عملية لنموذج مبـــادل حـــراري ذي غشاء ساقط على أنابيب أفقية والاستفادة منه في تكوين الثلج عل السطح الخارجي للأنابيب . وقـــد تم عمل تنظيمين للأنابيب أحدهما على التوازي والآخر على التوالي حيث يدخل مائع التـــبريد (محلـــول الايثيلين جليكول المبرد عن طريق مكنة تبريد) من أسفل المبادل عبر أنبوبة داخلية إلى الأنبوبة الخارجيـــة حيث يتجمد عليها الغشاء الساقط من الخارج ومغادراً المبادل من الأعلى للتأكد من مرور المائع علـــى جميع أنابيب المبادل وطرد الهواء الداخلي. وللإسراع في عملية تكوين الثلج خلال التجربة فإن الغشـــاء الساقط يبرد أولا في خزان معزول مثبت على إرتفاع معين إلى درجة حرارة جزئية أعلى مـــن الصفـــر المئوي وبالتالي يسهل تجميده. عند نزول الغشاء الساقط على الأنابيب فإن جزءًا منه يتجمـــد ويضـــخ الجزء المتبقي منه إلى خزان التبريد الأولي مرة أخرى.ولحساب كمية الثلج المتكونة فإنه يضخ مائع مـــن نفس نوع مائع التبريد بدرجة حرارة عالية من خزان آخر إلى داخل منظومة أنابيب الاختبار،حيث يـــدأ الثلج في الانصهار إلى أن يسقط في بركة السائل أسفل وعاء المبادل.وبالتالي يمكن حساب كمية الثلـــج عن طريق قياس فرق الارتفاع في السائل قبل وبعد ضخ الماء الساخن.خلال مراحل التجربة كان يتـــم تسجيل درجات الحرارة قبل وبعد دخول كلا من المائعين بالإضافة إلى قياس معـــدل التدفـــق لكـــلا المائعين.وفي بعض التجارب تم قياس درجة الحرارة على سطح إحدى أنابيب الاختبار.

الجزء الأول من هذا البحث يشتمل على مقدمة عن أهمية إستخدام خزن البرودة للاســـتفادة منـــها في أوقات الذروة كما يركز على الأبحاث السابقة التي تطرقت إلى هذا الموضوع وبشكل خـــاص علـــى الأبحاث التي تركزت حول تجميد الثلج حول الأنابيب ، وقد تم توضيح الفوارق التي استدعت القيـــام بهذا البحث والتي كان أهمها إستخدام المبادل الحراري ذي الأغشية الساقطة في التجميد.كما يعطي هـــذا الجزء خلفية حسابية عن كيفية حساب معامل إنتقال الحرارة للأنابيب الإسطوانية متعددة الطبقات.

يشتمل الجزء الثاني على شرح تفصيلي لمكونات وأجزاء التجربة العملية والتي تشمل :

١) وعاء المبادل الحراري الحامل للأنابيب.

٢) أنبوبة التغذية للغشاء الساقط.

٣) تنظيم الأنابيب على التوازي.

٤) تنظيم الأنابيب على التوالي.

٥) خزان التبريد الأولي.

٦) طريقة تثبيت الازدواجات الحرارية على الأنابيب،وطريقة قياسها.

٧) جهاز التبريد المتحكم في درجة حرارة مائع التبريد(الايثيلين جليكول)

وفي هذا الجزء تم شرح كل جزء من أجزاء التجربة على حدة مع رسم توضيحي يوضح كيفية تكوين هذا الجزء وأبعاده .كما يشمل على رسومات توضح كيفية عمل التجربة بشكل عام.

يتكون الجزء الثالث من هذا البحث من قسمين رئيسيين وهما:

- شرح مفصل عن طريقة عمل الحسابات المختلفة والقوانين المستخدمة لعمل الإتزان الحراري، ولإثبات صحة مسار التجربة والقراءات بمقارنتها بالقيم والحسابات النظرية.
- شرح مفصل عن الحالات المختلفة لهذه التجربة وخطوات إجراء التجربة والملاحظات العامة،كما يشمل إجراء تسع حالات دراسة مختلفة بحيث تختلف كل حالة عن الأخرى إما في تصميم الأنابيب أو في معدل سريان كلاً من مائع التبريد أو الغشاء الساقط أو في نوعية السائل المستخدم في الغشاء الساقط.ويشمل هذا الجزء أيضا حسابات كمية الثلج المتكونة وحسابات الإنتقال الحراري لحساب كمية الحرارة المنتقلة من الغشاء الساقط(البارد) إلى مائع التبريد(الأقل برودة). وتم توضيح نتائج هذه الحالات برسومات بيانية عن معدل تكون الثلج وعن معامل إنتقال الحرارة الكلي وعن الإتزان الحراري وغيرها من المقارنات بين نتائج الدراسة.

تركز البحث على دراسة ثلاثة أنظمة مختلفة حيث يحتوي كل نظام على متغيرات تميزه عن النظام الآخر.

هدف المنظومة الأولى هو دراسة تأثير وضع أنابيب الإختبار على التوازي على كمية الثلج المتكونة ومعامل إنتقال الحرارة وتشتمل الدراسة على حالتين كالتالي:

أ) معدل سريان مائع التبريد عالي جداً = ٠,٣٨ كغ/ث.و شكل النافث للغشاء الساقط.

ب) خفض معدل السريان إلى ٠,١٦٢ كغ/ث ، لزيادة الدقة في الحسابات، مع تثبيت شكل الغشاء الساقط على وضع النافث.

ولأخذ دقة أكبر في الحسابات وللحصول على معامل إنتقال حرارة أكبر تم عمل المنظومة الثانية وهي ترتيب الأنابيب على التوالي وتم دراسة الحالات التالية:

أ) معدل سريان مائع التبريد = ٠,٠٢٣ كغ/ث.و شكل النافث للغشاء الساقط.

ب)معدل سريان مائع التبريد = ٠,٠٦٠ كغ/ث.و شكل النافث للغشاء الساقط.لدراسة تأثير زيادة معدل سريان مائع التبريد على المبادل الحراري.

ج) معدل سريان مائع التبريد = ٠,١٢٨ كغ/ث.و شكل النافث للغشاء الساقط. لدراسة تأثير زيادة معدل سريان مائع التبريد على المبادل الحراري.

د) معدل سريان مائع التبريد = ٠,١٦٢ كغ/ث.و شكل النافث للغشاء الساقط.لمقارنة أداء منظومة التوالي بمنظومة التوازي عند نفس الظروف.

هـ) معدل سريان مائع التبريد = ٠,١٦٢ كغ/ث.و شكل اللوح الكامل للغشاء الساقط. لدراسة تأثير زيادة معدل سريان الغشاء الساقط على المبادل الحراري.

و) معدل سريان مائع التبريد = ٠,١٦٢ كغ/ث.و شكل القطرات للغشاء الساقط. لدراسة تأثير تقليل معدل سريان الغشاء الساقط على المبادل الحراري.

وقد لوحظ مما سبق دراسته أن تكون الثلج على الأنابيب يقلل من معدل إنتقال الحرارة بين المائعين، حيث يعمل الثلج كمادة عازلة لانتقال الحرارة ، وكان أحد الحلول لهذه الظاهرة هو العمل على إقلال تراكم الثلج على الأنابيب وجعله يتكون على شكل حبيبات عائمة في السائل يمكن تجميعها في وعاء المبادل.وكان من المواد المقترحة الأسيتون حيث عملت به المنظومة الثالثة للتجربة.

أ) معدل سريان مائع التبريد = ٠,٠٢٣ كغ/ث.و شكل النافث للغشاء الساقط.والمادة المتجمدة هي محلول مائي به٢% أسيتون.

وقد اتضح من نتائج دراسة المنظومة الأولى أنه تكونت لدينا كمية كبيرة من الثلج،إلا أن الفرق في درجة الحرارة بين الداخل والخارج لمائع التبريد صغيرة جدا وبالتالي فإن نسبة الخطأ في القراءة تكاد تكون كبيرة جداً.وعند محاولة زيادة الفرق بتقليل معدل السريان انخفضت كمية الثلج بشكل ملحوظ نتيجة لانخفاض معامل إنتقال الحرارة الداخلي.

وبدراسة نتائج المنظومة الثانية وجد أنه بزيادة معدل السريان لمائع التبريد يزيد تكون الثلج على الأنابيب نتيجة لزيادة معامل إنتقال الحرارة الداخلي. وعند زيادة معدل السريان للسائل الساقط فإنه يتحول من قطرات منفصلة إلى نافث وأخيرا إلى شكل غشاء مستمر ،والذي أنتج أكبر كمية من الثلج.كما أن الفرق في درجة الحرارة كان مناسباً وأقل تأثرا بالخطأ المحتمل .منظومة التوالي أعطت كمية أكبر من الثلج من منظومة التوازي عند تثبيت معدل السريان لكلا المائعين ،وذلك بسبب زيادة سرعة مائع التبريد داخل الأنابيب.

وقد بينت المنظومة الثالثة أن إضافة أسيتون للماء يقلل تراكم الثلج على الأنابيب ولكن لم نحصل على حبيبات من الثلج كما كان متوقعا.لذا فإنه يوصى بدراسة مستقبلية لهذه المادة أو مواداً أخرى يحتمل أنها تعطي نتائج أفضل.